Vol. 32, Issue 2, June 2023 pp 65–142

pISSN: 0853-1773 eISSN: 2252-8083

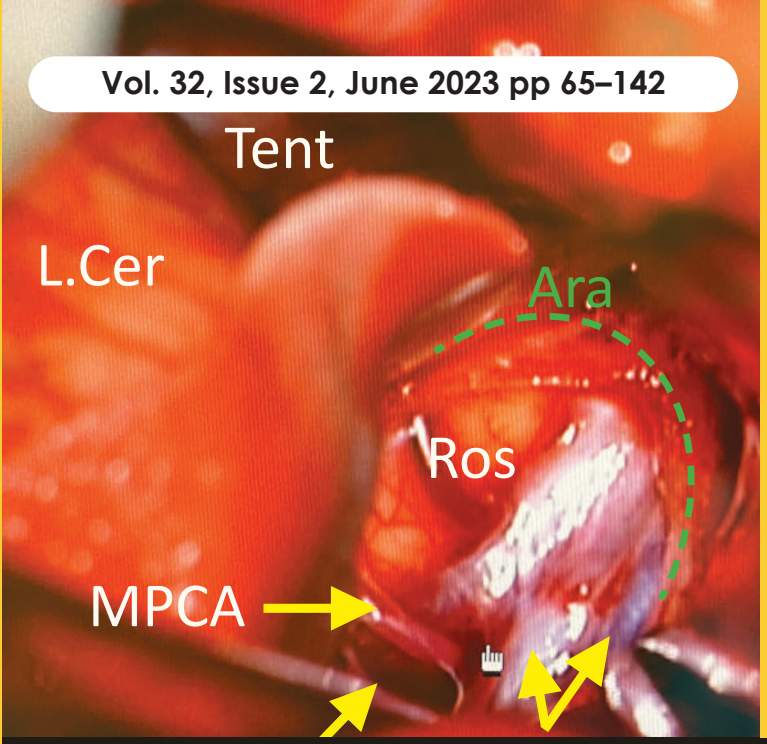

Medical Journal of Indonesia

- √ Journal's role in doctoral dissertation
- √ Metaverse in medical education
- √ Diversity of *Spa* types among *S. aureus*
- √ Seizure recurrence with afebrile seizure
- √ Prognostic role in ovarian cancer
- √ Food-induced brain activity in obesity
- √ Coagulation factors in COVID-19
- √ Machine learning and prostate cancer
- √ Behavioral change in obese adolescents
- √ Rare case of quadrigeminal arachnoid cyst
- √ Gene mutations in WS1

mji

http://mji.ui.ac.id

Published by the Faculty of Medicine Universitas Indonesia
Official Scientific Journal of the Faculty of Medicine Universitas Indonesia
in collaboration with German-Indonesia Medical Association (DIGM)
Jl. Salemba Raya No. 6 Jakarta 10430
Telp. +62-21-29189160 ext. 201605

pISSN: 0853-1773 • eISSN: 2252-8083

Medical Journal of Indonesia

The **Medical Journal of Indonesia** (abbr: Med J Indones) was founded in 1991 as the Medical Journal of the University of Indonesia (abbr: Med J Univ Indon). Since the first issue in 1992, it has been published quarterly, consistently, and continuously, covering a wide range of medical subject and issues from every medical specialist aspect. In 1995 the name was changed to Medical Journal of Indonesia which reflected the widening of its coverage beyond Universitas Indonesia. The mission of our journal is to provide biomedical scientist, clinical, and public health researchers as well as other health care professionals with the media to published their research works. Starting from 2011, Deutsch-Indonesische Gesellschaft für Medizin (DIGM) Medical Journal has been merged into Medical Journal of Indonesia. This also means that DIGM is officially collaborating with Medical Journal of Indonesia and Faculty of Medicine Universitas Indonesia as the owner and publisher. The mission of the Medical Journal of Indonesia is to improve health care management by providing high-quality articles from Indonesia and worldwide.

Focus and Scope

Medical Journal of Indonesia focuses on promoting medical sciences generated from **basic sciences**, **clinical**, and **community or public health research** to integrate researches in all aspects of human health.

This journal publishes **original articles**, **reviews**, and also interesting **case reports**.

Brief communications containing short features of medicine, latest developments in diagnostic procedures, treatment, or other health issues that is important for the development of health care system are also acceptable.

Correspondence articles of our own published articles are welcome.

Abstracting and Indexing

ACI; BASE; CAB Abstracts; CiteFactor; CNKI; Dimensions; DOAJ; EBSCO; Electronic Journals Library; Embase; ESCI; GARUDA; Global Health; Google Scholar; Hinari; IMSEAR; ISC; JournalTOCs; Microsoft Academics; PKP Index; Proquest; Scilit; Scopus; SINTA; Ulrichsweb Global Serial Directory; WorldCat.

Open Access Policy

Medical Journal of Indonesia is an open-access journal which provides immediate, worldwide, and barrier-free access to the full text of all published articles without charge readers or their institutions for access. Readers have right to read, download, copy, distribute, print, search, or link to the full texts of all articles in Medical Journal of Indonesia.

Preprint Policy

A preprint refers to the author's version of a research manuscript shared publicly on an online preprint platform before undergoing a formal peer-review process in a journal. Medical Journal of Indonesia allows the submission of preprint manuscripts with prior notice in the cover letter by providing a link to the preprint and a description of any revisions or changes made in the submitted manuscript. Preprints will not be regarded as prior publications and will not adversely affect the review process.

Subscription

The price per volume (four printed issues): international USD 160 (surface postage included), for ASEAN countries USD 100 (surface postage included), for Indonesia IDR 400,000 (surface postage excluded).

Advertising Policy

Editorial materials will not be influenced by advertisement. Readers can criticize the advertisement by sending it to the office. Advertisement will appear in the print or online version depending on request. For all inquiries, contact the Medical Journal of Indonesia editorial office at Medical Journal of Indonesia, Education Tower 6th floor, IMERI building, Faculty of Medicine Universitas Indonesia, Jalan Salemba Raya 6, Jakarta Pusat 10430, Indonesia; tel. +6221-29189160 ext. 201605; e-mail mji@ui.ac.id.

Copyright Notice

Editorial Office
Medical Journal of Indonesia
Jl. Salemba Raya 6, Jakarta Pusat 10430, Indonesia
Tel: +6221-29189160 ext. 201605
Mobile: +628111400115
E-mail: mji@ui.ac.id

Published by
Faculty of Medicine Universitas Indonesia
Jl. Salemba Raya 6, Jakarta Pusat 10430, Indonesia
Tel/fax: +62 21-3912477
E-mail: humas@fk.ui.ac.id

Printed by
UI Publishing
Komplek ILRC Gedung B Lt.1 & 2, Perpustakaan Lama Universitas Indonesia, Kampus UI, Depok, Jawa Barat 16424
Tel: +6221-78888199/78888278
Jl. Salemba Raya 4, Jakarta Pusat 10430
Tel: +6221-31935373/31930172/31930252
E-mail: uipublishing@ui.ac.id

Official Scientific Journal of the Faculty of Medicine, Universitas Indonesia
in Collaboration with German-Indonesian Medical Association (DIGM)
Accredited journal (2020-2024) based on Ministerial Decree of the Minister of Research and Technology /Head of National Research and Innovation Agency of the Republic of Indonesia No. 148/M/KPT/2020.

The paper meets the requirements for acid free paper.

Editorial Board

Medical Journal of **Indonesia**

Volume 32 • Number 2 • June 2023 • page 65–142 • pISSN: 0853-1773 • eISSN: 2252-8083

Contents

Case Report/Series

***Front Page*:** Preoperative non-contrast brain MRI showed a hypointense lesion in the supracerebellar area confirming a type II quadrigeminal arachnoid cyst, and intraoperative finding showed the quadrigeminal supracerebellar area after some cyst walls removal with a microscope tilting; the remaining thick arachoid cyst (green dashed line) was still visible, as reported by Graciela et al. These are published in this issue.

mji | Medical Journal of Indonesia

Contents

See the journal website for contents.

Medical Journal of Indonesia
Instructions for Authors

Submission

The submitted manuscript should be addressed to Editor-in-chief of the Medical Journal of Indonesia. Manuscript must be submitted through online submission (https://mji.ui.ac.id/journal/index.php/mji/about/submissions) by registered users. You can easily register in the journal system. For further questions contact us at mji@ui.ac.id.

General Principles

As a basic requirement, all articles submitted to the Medical Journal of Indonesia must be original work, which has never been published previously and is submitted exclusively to the Medical Journal of Indonesia. They must follow the latest version of "Recommendations for the Conduct, Reporting, Editing and Publication of Scholarly Work in Medical Journals" (http://www.icmje.org/), which was established by the International Committee of Medical Journal Editors (ICMJE). The Editorial Board reserves the right to edit all articles in aspects of style, format, and clarity. Authors may be required to revise their manuscripts for reasons of any aspect. Manuscripts with excessive errors in any aspect may be returned to authors for retyping or may be rejected. All manuscripts will be subjected to peer and editorial review.

We accept four types of articles: (1) original articles: **basic medical research, clinical research,** or **community research;** (2) **case report;** (3) **review article;** (4) **brief communication;** (5) **correspondence.** Authors must also supply:

ICMJE conflicts of interest statement form (http: mji.ui.ac.id/journal/public/journals/1/coi_disclosure.pdf) (if there is any difficulties in accessing the form, you can directly visit http://www.icmje.org/conflicts-of-interest/); copy of ethical approval (for all researches involving human and animal); and final checklist (http://mji.ui.ac.id/journal/public/journals/1/FinalChecklist.pdf) signed by all author(s).

A cover letter should be provided along with the submission addressed to the Editor-in-chief of Medical Journal of Indonesia which should include a statement about all previous submissions of the manuscript and previous reports that might be regarded as redundant publication of the work. If the manuscript has been submitted previously to another journal, authors are encouraged to provide previous comments along with the responses to accelerate the review process. Author(s) also have to mention the work whether it has been presented in a congress/conference/seminar.

The template is provided for cover letter (https://mji.ui.ac.id/journal/public/journals/1/template/Template-for-Cover-Letter.dotx), original articles (https://mji.ui.ac.id/journal/public/journals/1/template/Template-for-Original-Article.dotx), and case report (https://mji.ui.ac.id/journal/public/journals/1/template/Template-for-Case-Report.dotx).

Study Ethics

All submitted papers containing animal experiments and/or involving human subjects should have obtained approval from an independent ethics committee. The copy of approval should be provided to the editorial office as mentioned above.

Informed Consent

For each article published in the Medical Journal of Indonesia (MJI) an informed consent should be obtained from each participant. Informed consent consists of written permission granted by a patient or a patient's relative on his/her behalf to publish any information, image, or case report associated with the patient's clinical condition on the MJI. The informed consent and patient confidentiality policies are in compliance with all relevant regulations regarding data/privacy protection and the Fourth Amendment 1945 Constitution of the Republic of Indonesia, Article 28(G).

The contents of patient consent form should be adjusted to the local regulations in which the study was conducted. The author must indicate, in the main text of the manuscript, whether informed consent was obtained, including consent to publish the study a patient enrolled in. The author may be requested by the journal's editor to submit the consent form. In some circumstances, informed consent requirements may be exempted from studies. The decision to require or waive informed consent must come from the ethics committee that reviewed and approved the study. For studies in which informed consent is waived, the author must submit the official approval letter from the ethics committee that indicates the waiver.

All identifiers, including but not limited to names, initials, dates of birth, medical record numbers, must be removed from the patient's data or information published on the manuscript.

On the submitted and published manuscripts, the patient's face must be blurred or, when applicable, the patient's eyes are concealed with black bars. Images, including from ultrasound results, conventional radiography, computed tomography images, pathology images, or images taken during a surgery, must be de-identified.

Absence of a patient consent form for an appropriate study will result in the submission rejection.

Publication Ethics

The publisher of this journal is a member of Committee on Publication Ethics (COPE). This journal follows guidelines

from COPE in facing all aspects of publication ethics and, in particular, how to handle cases of research and publication misconduct. All articles in this journal involving human subjects should respect principles of research ethics as described in the Declaration of Helsinki and studies involving animals should obey the International Guiding Principles for Biomedical Research as developed by the Council for International Organization of Medical Sciences (CIOMS).

Medical Journal of Indonesia adapts COPE principle to meet high quality standard of ethics for publisher, editors, authors, and reviewers. As an essential issue, publication ethics need to be explained clearly to improve the quality of research worldwide. In this part, we explain the standard for editors, authors, and reviewers. In addition, publisher does not have the right to interfere with the integrity of the contents and only support to publish in timely manner.

Clinical Trial Registration

The authors have to register all clinical trials to the publicly accessible registration in any registry as recommended by the ICMJE or integrated to the WHO International Clinical Trials Registry Platform (ICTRP) (https://www.who.int/clinical-trials-registry-platform/network) or in ClinicalTrials.gov, which is a data provider to the WHO ICTRP. The ICMJE defines a clinical trial as any research project that prospectively assigns people or a group of people to an intervention, with or without concurrent comparison or control groups, to study the relationship between a health-related intervention and a health outcome. The registration should be done prior to the conduct of the trial. The trial registration number should be provided at the end of the abstract.

Systematic Review and Meta-Analysis Registration

The authors are encouraged to register their systematic review and meta-analysis to the PROSPERO (https://www.crd.york.ac.uk/prospero/), an open-access database of prospectively registered systematic reviews in health. The registration should be done prior to the data extraction. The authors who submit unregistered systemstic review/meta-analysis should provide the reasons along with the cover letter for editorial consideration.

Structure and Language

Articles will be published in US English, following American spelling. Articles in English that are linguistically inadequate may be rejected. Manuscripts should be written double-spaced in all parts of the manuscript using Times New Roman 12, with margin of 2.54 cm of all sides. Articles must be submitted in the following structural order: title page and authorship, abstract, keywords, text, conflicts of interest, acknowledgments (if any), funding disclosure, references, tables, figures, and legends (if any).

Title Page and Authorship

The **Title Page** should contain: title of the article (concise, no abbreviations, maximum 16 words); full names of authors (without academic titles); authors' affiliations [name(s) of department(s) and institution(s)]; corresponding author's name, mailing address, telephone and fax numbers, and e-mail address (institution specific address and e-mail address of the corresponding author will be published along with the article); conflict of interest declaration for each author; short running title [maximum 40 characters (letters and spaces)]; source(s) of support in the form of funding, equipment, drugs, or all of these (if any); disclaimers (if any); acknowledgement (if any); word counts [A word count for the text only (excluding abstract, acknowledgments, tables, figure legends, and references)]; and number of figures and tables. To ensure the process of double blind peer-review, the authors should provide the file of title page in separate file. The template for title page is provided on https://mji.ui.ac.id/journal/public/journals/1/template/template-for-cover-letter.docx.

Authorship of articles should be limited to those who have contributed sufficiently to take public responsibility for the contents. This includes (a) conception and design, or analysis and interpretation of data, or both; (b) drafting the article or revising it critically for important intellectual content; (c) final approval of the version to be published; (d) and agreement to be accountable for all aspects of the work in ensuring that questions related to the accuracy or integrity of any part of the work are appropriately investigated and resolved. Contributors who meet fewer than all four criteria above should be listed in acknowledgments and the contributions should be specified. Corresponding authors should assure the permission of acknowledged individuals to be mentioned in the acknowledgment.

Abstract and Keywords

The **abstract** should be formally structured and prepared in English with a maximum of 250 words for biomedical, clinical, and community research articles and systematic review or meta analysis; for case reports, brief communications, and narrative reviews, the **abstract** should not be structured formally and should not exceed a maximum of 150 words. Abstracts should be concise and precise with enough information, highlighting the points and importance of the article. It should contain: **background** and purpose of the study; **methods** (basic procedures, study subject selection, observational or analytical methods); main findings or **results**; and principal **conclusion**. **Keywords** are limited to 3–6 words or short phrases that will allow proper and convenient indexing. They should be obtained from Medical Subject Headings (MeSH®) (https://meshb.nlm.nih.gov/search) thesaurus produced by National Library of Medicine.

Main Text

The main **text** should be structured as **introduction**, **methods**, **results**, and **discussion** (IMRAD). Methods

should provide clarity about how, why, and when the study was done. The methods section should include the statement of approval by local, regional, or national review board. It should also clearly describe the selection of the study's participants. Materials and equipment used should be identified in **methods** section by specifically giving the manufacturer's name and address in parentheses. References to all established methods must be given. All **statistical methods** used should be described in detail in the **methods** section of the manuscript. Relying solely on statistical hypothesis testing, such as *p* values should be avoided; instead, important information about effect size and precision of estimates should be provided. Statistical terms, abbreviations, and symbols should be defined. Computer software and version used should be specified. In the **results** section, data should be presented in a concise and precise way, either in figures or tables, but not the same finding in a figure and a table. Unnecessary figures and tables, as well as footnotes should be avoided and their contents incorporated into the text. In the end of the **discussion**, a conclusion should be stated.

Statistical Methods

All **statistical methods** used should be described in detail in the methods section of the manuscript. Avoid relying solely on statistical hypothesis testing, such as p values, which fail to convey important information about effect size and precision of estimates. Define statistical terms, abbreviations, and most symbols. Specify the computer software and version used.

Conflicts of Interest

Conflicts of interest should be transparent as detail as possible as provided in the ICMJE form as a standardized authors' disclosures. Financial and personal relationships are easily identifiable that might bias or be seen to bias the work. Funding sources for the work should be described specifically with explanations of the role of those sources and the authors should declare that the supporting sources had no involvement in specific role. The authors should declare that the authors had access to all the study and the sponsors did not intervene the data or the work. Each author should submit a separate form from ICMJE.

Acknowledgments

Personal acknowledgments should be limited to appropriate professionals who contributed to the paper, including technical help and financial or material support, also general support by a department chairperson.

Funding Sources

Funding sources for the work should be described specifically with explanations of the role of those sources and the authors should declare that the supporting sources had no involvement into nor influence on the content of the manuscript. This statement should be written separately and limited to the funding for the work. If funder(s) had any impact into or influence on the design; data collection, management, analysis and interpretation of the data, the preparation, review, or approval of the manuscript or the decision to submit the manuscript for publication, their role must be disclosed in detail.

Tables and Figures

Total of tables and figures are advisable not to exceed 6 in number. **Tables** and its title should be presented in separate sheets. Tables should be numbered in Arabic numerals with brief captions clearly indicating the purpose or content of each table. Provide a footnote to each table, identifying in alphabetical order all abbreviations used. Number tables consecutively in the order of their first citation in the text and supply a brief title for each. Do not use internal horizontal or vertical lines. Give each column a short or an abbreviated heading. Explain all nonstandard abbreviations and explanatory matters in footnotes, and for explanatory matters use the following symbols, in sequence: *, †, ‡, §, ¶, **, ††, ‡‡, §§, ¶¶, etc. Identify statistical measures of variations, such as standard deviation and standard error of the mean. Be sure that each table is cited in the text. If you use data from another published source, obtain permission and fully acknowledge that source.

Figures should be either professionally drawn or photographed, and submitted in a format (JPEG or TIFF) in the following resolutions [gray-scale or color in RGB (red, green, blue mode) at least 300 dpi (dots per inch). For x-ray films, scans, and other diagnostic images, as well as pictures of pathology specimens or photomicrographs, send sharp, glossy, black-and-white or color photographic prints, usually 127 × 173 mm (5 × 7 inches). Write the word "top" on the back of each figure at the appropriate place. Figures should be made as self-explanatory as possible; titles and detailed explanations belong in the legends-not on the figures themselves. Photomicrographs should have internal scale markers. Symbols, arrows, or letters used in photomicrographs should contrast with the background. When symbols, arrows, numbers, or letters are used to identify parts of the illustrations, identify and explain each one clearly in the legend. Explain the internal scale and identify the method of staining in photomicrographs. Photographs of potentially identifiable people must be accompanied by written permission to use the photograph.

Tables and figures should be numbered consecutively according to the order in which they have been cited in the text. If a table or figure has been published previously, acknowledge the original source and submit written permission from the copyright holder to reproduce it. Permission is required irrespective of authorship or publisher except for documents in the public domain using license of CC BY SA (https://creativecommons.org/licenses/by-sa/4.0/legalcode). Color figures are allowed in special circumstances, provided that the author is willing to cover the cost of reproduction. If the original size of the figures is too large, you can provide us lower quality figures on submission and ensure the availability of good quality figures after the acceptance of the manuscript.

Units of Measurement

For measurements use both local and S.I. (System International) units. Measurements should be abbreviated (e.g. mm, kcal, etc.) in accordance with the Style Manual for Biological Sciences and using the metric system. Measurements of length, height, weight, and volume should be reported in appropriate scientific units. Temperatures should be in degrees Celsius. Blood pressures should be in millimeters of mercury (mmHg). Drug concentrations may be reported in either SI or mass units, but the alternative should be provided in parentheses where appropriate.

Abbreviation

Use only standard abbreviations; use of nonstandard abbreviations can be confusing to readers. Avoid abbreviations in the title of the manuscript. When first mentioned, all abbreviations must be spelled out followed by the abbreviation in parenthesis, unless the abbreviation is a standard unit of measurement. Abbreviations must be spelled out when first mentioned in the abstract and main text. If a sentence begins with a number, it should be spelled out except in abstract.

Supplementary File

A supplementary file is an additional document to provide further details related to the main text but is excluded due to space constraints or formatting limitations. It can include tables, figures, questionnaires, or other supporting materials that were referenced in the main text but not fully presented. The file is typically submitted along with the main manuscript and undergoes a peer-review process. The publication of a supplementary file would depend upon its importance in supporting the main text, decided solely by the Editor-in-Chief. Copyright regulations for a supplementary file refer to the copyright regulations for Tables and Figures. The authors are fully responsible for ensuring the accuracy and functionality of the file.

References

Use Arabic numerals in superscript to cite **references** in National of Medicine style. **References** are advisably not to exceed 25 in number but not less than 10, and should in general be limited to the last decade, except for references to methods used: they must be cited no matter how old they are. More than 25 references may be accepted when it is necessary. References must be numbered in the order in which they are mentioned in the text. Use the style of the examples below, which are based on the International Committee of Medical Journal Editors (ICMJE) Recommendations for the Conduct, Reporting, Editing and Publication of Scholarly Work in Medical Journals: Sample References (http://www.nlm.nih.gov/bsd/uniform_requirements.html). The titles of journals should be abbreviated according to the style used for MEDLINE (http://www.ncbi.nlm.nih.gov/nlmcatalog/journals). Avoid using abstracts as references. Information from manuscripts submitted but not yet accepted should be cited in the text as "unpublished observations" with written permission from the source. Papers accepted but not yet published may be included as references; designate the journal and add "Forthcoming". Avoid citing "personal communication" unless it provides essential information not available publicly, name the person and date of communication, obtain written permission and confirmation of accuracy from the source of personal communication. Authors are recommended to use reference management software, in writing the citations and references such as: Mendeley®, Zotero®, EndNote®, and Reference Manager®.

Here are some examples of the references:

1. ***Standard journal article***

   Up to six authors, list all the authors.

   - Halpern SD, Ubel PA, Caplan AL. Solid-organ transplantation in HIV-infected patients. N Engl J Med. 2002 Jul 25;347(4):284–7.

   More than six authors, list the first six authors, followed by et al.

   - Rose ME, Huerbin MB, Melick J, Marion DW, Palmer AM, Schiding JK, et al. Regulation of interstitial excitatory amino acid concentrations after cortical contusion injury. Brain Res. 2002;935(1-2):40–6.

   Optional addition of a database's unique identifier for the citation: [Edited 12 May 2009]

   - Halpern SD, Ubel PA, Caplan AL. Solid-organ transplantation in HIV-infected patients. N Engl J Med. 2002 Jul 25;347(4):284–7. PubMed PMID: 12140307.
   - Forooghian F, Yeh S, Faia LJ, Nussenblatt RB. Uveitic foveal atrophy: clinical features and associations. Arch Ophthalmol. 2009 Feb;127(2):179–86. PubMed PMID: 19204236; PubMed Central PMCID: PMC2653214.

   Optional addition of a clinical trial registration number: [Added 12 May 2009]

   - Trachtenberg F, Maserejian NN, Soncini JA, Hayes C, Tavares M. Does fluoride in compomers prevent future caries in children? J Dent Res. 2009 Mar;88(3):276–9. PubMed PMID: 19329464. ClinicalTrials.gov registration number: NCT00065988.

   As an option, if a journal carries continuous pagination throughout a volume (as many medical journals do) the month and issue number may be omitted.

   - Halpern SD, Ubel PA, Caplan AL. Solid-organ transplantation in HIV-infected patients. N Engl J Med. 2002;347:284–7.

2. ***Chapter in a book***

   Meltzer PS, Kallioniemi A, Trent JM. Chromosome alterations in human solid tumors. In: Vogelstein B, Kinzler KW, editors. The genetic basis of human cancer. New York: McGraw-Hill; 2002. p. 93–113.

3. ***Homepage/Web site*** **[Edited 12 May 2009]**

   Cancer-Pain.org [Internet]. New York: Association of Cancer Online Resources, Inc.; c2000-01 [updated 2002 May 16; cited 2002 Jul 9]. Available from: http://www.cancer-pain.org/.

Editorial Process

The submitted manuscript will be checked by an editor for its suitability with Medical Journal of Indonesia's

focus and scope and for major methodological flaws within two weeks. Staff will work with the author to fulfill all the requirements within two weeks. Every submitted manuscript which passes this step will then be checked for plagiarism by Similarity Check. The manuscript needs to be re-worked if indicated for minor plagiarism and will be rejected if indicated for major plagiarism. Then, an editor-in-charge and an editorial assistant will be assigned for the manuscript. In this stage, the manuscript will be assessed based on novelty and adherence to reporting guidelines. Subsequently, the manuscript will go through peer-review process. The revisions may be required and will be re-evaluated by the editor-in-charge after the authors providing sufficient responses. The manuscript will be passed to the editor-in-chief for any further revision and ultimately will take an editorial decision. The accepted manuscript will be sent to copyediting stage for correction of grammar and spelling errors, standardizing the journal in-house style, improving table, figure, and writing quality. The incomplete revision of this stage will result in pending scheduled publication. Then, the manuscript will enter production stage for typesetting. A pdf file is sent to the author for review and there should be no more scientific revision. A failure to comply will result in a delay of the publication since it needs editor confirmation for the changes. It will be scheduled for publication after the payment has been received. The final approval is needed from the corresponding author before it is published. The manuscript submitted by one of the editorial team of the Medical Journal of Indonesia will be processed by other editorial board members who do not have any conflict of interest with the manuscript and follow the same editorial process.

Peer Review

All submitted manuscripts (except editorial, commentary, and correspondence) in Medical Journal of Indonesia undergo double blind peer review by at least two reviewers. All manuscripts are sent to the reviewers anonymously. Reviewers' comments are also sent anonymously to the corresponding author to take the necessary actions and responses. All the reviewers are subjected to submit their evaluation not more than six weeks. Medical Journal of Indonesia staff ensure that the referee reports are complete. In some occasions, the review process needs more time to seek the appropriate reviewers.

Correction and Retraction Policies

Medical Journal of Indonesia is committed to publish Correction (Errata and Corrigenda) or Retraction dependent on the situation and in accordance with the COPE Retraction Guidelines. In all cases, these notices are linked to the original article.

Correction consist of errata and corrigenda. **Errata** provide a means of correcting errors that occurred after proofreading process. This includes writing, typing, editing, or publication (e.g., a misspelling, a dropped word or line, or mislabeling in a figure) of a published article. The authors need to send direct email to the editorial office (mji@ui.ac.id) to ask for an erratum and the correction will be taken based on the last proofread provided. **Corrigenda** provides a means of correcting errors that are made by the authors but the errors should not alter the overall basic results or conclusions of a published article. Note that the addition of new data is not permitted. For corrections of a scientific nature or issues involving authorship, all disputing parties must agree, in writing, to publication of the Correction. For omission of an author's name, letters must be signed by the authors of the article and the author whose name was omitted. The editor who handled the article will be consulted if necessary. Medical Journal of Indonesia followed COPE Retraction Guidelines for **Retraction**.

Publication Fee

This journal only charges the article publication fee for all manuscript types, without any submission fee. The publication fee is USD 300 for foreign authors and IDR 3,000,000,- for Indonesian authors. For each printed page that contains colored figure, you will be asked to pay USD 50 (IDR 500,000,-) more of each printed page. Authors who want to publish Corrigenda need to pay an additional charge of USD 50 (IDR 500,000) per each printed page. After the manuscript has been proofread by the corresponding author, Medical Journal of Indonesia office will send the invoice and the payment needs to be completed before being appeared online.

To enhance the research in health program, Medical Journal of Indonesia will cover the publication fee of authors from the countries that are included in group A and group B countries of HINARI by WHO. Waiver of payment is not only limited to those countries. All authors may ask a waive, and they need to send letter of waiver to editor-in-chief explaining the importance of the study and why author(s) need to be waived. The decision is made prior to the process of the review and it is the editors' privilege to approve or reject the request.

Copyright Notice

the purposes of these terms, commercial use means use in any manner that is primarily intended for or directed toward commercial advantage or monetary compensation, including but not limited to provision or distribution of any article or part of any article (including any abstract, figures or tables) in any format: to support marketing activities; in response to medical information requests; to support activities at a conference, exhibition or trade show; as resource material on a company or product-specific website. You may contact to our office at mji@ui.ac.id.

Updated - August 2023

Medical Journal of **Indonesia**

Final Checklist & Submission Form

Title of article: _____

_____

1. **Manuscript Preparation**
   The author(s) hereby affirm that I do substantial contributions to the conception or design of the work; or the acquisition, analysis, or interpretation of data for the work; AND drafting the work or revising it critically for important intellectual content; AND final approval of the version to be published; AND agreement to be accountable for all aspects of the work in ensuring that questions related to the accuracy or integrity of any part of the work are appropriately investigated and resolved. The author(s) affirm that the material has not been previously published and that the author(s) have not transferred elsewhere any rights to the article. The author(s) have checked the manuscript to comply with the instructions for authors of Medical Journal of Indonesia and agreed to contribute for publication fee.
2. **Informed Consent**
   The author(s) haven't suggested any personal information that may make the identity of the patient recognizable in any forms of description part, photograph or pedigree. When the photographs of the patient were essential and indispensable as scientific information, the author(s) have received the consent in writing form and have clearly stated it.
3. **Human and Animal Right**
   In case of experimenting on human, the author(s) have certified that the process of the research is in accordance with ethical standards of Helsinki declaration, domestic and foreign committees that preside over human experiment. If any doubts is raised whether the research was proceeded in accordance with the declaration, the author(s) would explain it. In case of experimenting on animals, the author(s) have certified that the author(s) had followed the domestic and foreign guideline related to experiment of animals in a laboratory.
4. **Permission Approvals**
   The author(s) have received consent from the author or editor the picture or the table that was quoted from other journals or books. A portion or entire of the article hasn't been published on other journals nor contributed to other journals and under review.
5. **Copyright Notice**
   The author(s) retain copyright and grant Faculty of Medicine Universitas Indonesia rights to publish the work licensed under a Creative Commons Attribution-Non Commercial License (http://creativecommons.org/licenses/by-nc/4.0/). Further information of this topic is available on http://mji.ui.ac.id/journal/index.php/mji/copyright.
6. **Disclosure of Conflict of Interest**
   The author(s) of the journal have clarified everything that interest may arise such as work, research expenses, consultant expenses, and intellectual property on the document of ICMJE form disclosure of conflicts of interest.

Author's Name:	Signature:	E-mail:	Date:

Notes: This form must be signed by all authors in order as appeared in the article.

Community Research

Behavioral change readiness among obese adolescents in Jakarta, Indonesia

Dewi Friska[1], Aria Kekalih[1,2], Muhammad Erlangga Putra Harimurti[3], Deviena Nabila[3]

pISSN: 0853-1773 • eISSN: 2252-8083
https://doi.org/10.13181/mji.oa.236543
Med J Indones. 2023;32:122–8

Received: November 09, 2022
Accepted: August 30, 2023
Published online: September 14, 2023

Authors' affiliations:
[1]Department of Community Medicine, Faculty of Medicine, Universitas Indonesia, Jakarta, Indonesia,
[2]Southeast Asian Ministers of Education Organization Regional Center of Food and Nutrition (SEAMEO RECFON)/ Pusat Kajian Gizi Regional Universitas Indonesia (PKGR UI), Jakarta, Indonesia,
[3]International Class Undergraduate Program, Faculty of Medicine, Universitas Indonesia, Jakarta, Indonesia

Corresponding author:
Muhammad Erlangga Putra Harimurti
International Class Undergraduate Program, Faculty of Medicine, Universitas Indonesia, Jalan Pegangsaan Timur No. 16, Menteng, Central Jakarta 10310, DKI Jakarta, Indonesia
Tel/Fax: +62-21-31905502
E-mail: harimurtierlangg@gmail.com

ABSTRACT

BACKGROUND Prochaska's transtheoretical model of behavioral change process, consisting of stages and processes of change, should be monitored to evaluate obesity management, particularly in adolescents. Two of four processes of change are supporting relationships, which promote behavioral change, and weight management actions, which are activities that push individuals to a particular direction in patients' weight loss progress. This study aimed to determine the participants' current stages of change, nutritional status, and their relationship with the processes of change.

METHODS This cross-sectional study used secondary data collected in 2018 from 115 obese adolescents aged 15–21 years in Jakarta, Indonesia, using an Indonesian-translated and validated questionnaire adapted from Andrés et al's study. The questionnaire evaluated participants' processes of change, focusing on scores of supporting relationships (5 items) and weight management actions (10 items).

RESULTS Of the participants, 71.3% were classified as obese grade I, and 28.7% were obese grade II. Most participants were in the contemplation (31.3%) and action (31.3%) stages. The mean supporting relationships and weight management actions scores were different between participants with obese I and obese II (66.67 *versus* 80, p = 0.004; 64.17 *versus* 70, p = 0.008, respectively). Meanwhile, no differences were identified in supporting relationships and weight management actions scores in all stages of change.

CONCLUSIONS Adolescents with obesity and higher BMI (based on the obesity grading of the WHO Asia Pacific) tended to have significantly higher scores for supporting relationships and weight management actions, indicating that external reinforcement and immediate weight loss actions played pivotal roles in readiness for behavioral change.

KEYWORDS adolescent, obesity, stages of change, transtheoretical model

The World Health Organization (WHO) defines obesity as a condition characterized by abnormal or excessive accumulation of body fat.[1,2] From 2013 to 2018, the prevalence of adult obesity in Indonesia sharply increased. Additionally, approximately 30% of Jakarta's population is experiencing obesity, with an increasing trend observed in adolescents.[3,4] Childhood obesity is a common phenomenon with numerous repercussions, including type II diabetes, hypertension, coronary artery disease, and stroke, which are twice as likely in children with obesity compared to children with normal body weight.[5–7] During adolescence (i.e., 15–24 years), puberty causes significant physical, cognitive, social, and emotional changes. Moreover, external factors, such as social support from peers and family members, influence behavioral development.[8,9] A lack of support and negative perceptions from peers may lead adolescents with obesity to become

hostile and resentful toward others; therefore, having supportive peers and family members is important in addressing obesity.[9] Considering the potential long-term effects and complications associated with obesity, particularly concerning age and behavioral characteristics, immediate action must be taken to reduce its prevalence among adolescents.[10]

The "gold standard" for obesity management includes behavioral treatment, dietary guidance, and physical activity.[10] Prior studies have suggested that behavioral change is a crucial driving factor for weight loss. Subsequently, one method for assessing behavioral change is to determine individuals' current stages and processes of change. In 1997, Prochaska and Wayne introduced the transtheoretical model of behavioral change, consisting of five stages: precontemplation (no intention to change in the foreseeable future), contemplation (intention to change in the next 6 months), preparation (intention to change in 30 days), action (action taken to change ≤6 months), and maintenance (action taken to change ≥6 months). These stages demonstrate a temporal dimension and continuity of the behavioral change process for the processes of change: emotional reevaluation, weight consequences evaluation, weight management actions, and environmental restructuring (including supporting relationships).[11–13]

Both the stages and processes of change are closely related to the behavioral change continuum, showing that the two components co-exist.[13] By determining an individual's stage of change, correlated processes, and their relevance, interventions can be tailored to that stage, which increases the success rate.[12,13] Based on the transtheoretical model, Andrés et al[11,12] developed a questionnaire to assess the five stages and four processes of change. This study aimed to determine the stages of behavioral change in adolescents with obesity, evaluate the processes of change using their supporting relationships and weight management actions scores, and identify any significant mean differences in behavioral change process scores among participants at different stages of change and with varying nutritional statuses.

METHODS

Study design

This cross-sectional study used secondary data previously collected by a research team from the Southeast Asian Ministers of Education Organization Regional Center of Food and Nutrition in Jakarta, Indonesia. The study participants were high school students from SMAN 21 Jakarta and first-year university students from Universitas Indonesia. Participants were recruited using a consecutive (non-probabilistic) sampling method to determine their stages of change and assess their behavioral change processes based on supporting relationships and weight management actions scores. Various educational settings were used for data collection to recruit participants within a diverse age range covering all phases of adolescence according to Sawyer et al,[8] who classified adolescence into three stages: early adolescence (10–14 years old), late adolescence (15–19 years old), and young adulthood (20–24 years old). This study was approved by the Ethics Committee of the Faculty of Medicine, Universitas Indonesia (No: 0525/UN2. F1/ETIK/2018).

Sampling techniques

The number of samples needed was determined using a mean comparison formula for unpaired numeric data analysis ($n1 = n2 = 2 \times [(Za + Zb) \times s/(x1 - x2)]^2$), with $Za = 1.96$, $Zb = 0.84$, $s = 16.59$, $X1 = 48.72$, $X2 = 42.54$. Based on this calculation, the minimum number of samples required was 113; thus, 115 participants were recruited for the original study. The inclusion criteria were high school and first-year university students, aged 15–21 years, had a body mass index (BMI) of ≥25 kg/m^2 (classified as obese according to the WHO Asia Pacific at the time of data collection). All participants provided their informed consent. The independent variables in this study were BMI and the stages of change. The dependent variables were the processes of change as determined by participants' supporting relationships and weight management actions scores.

Data collection and statistical analysis

The research data were collected in both settings using an integrated form. The first questionnaire collected informed consent and sociodemographic data. Furthermore, the processes of change were assessed using an Indonesian-validated questionnaire containing 34 questions adapted from Andrés et al's study[11] on the application of behavioral change processes for managing adult obesity in the United Kingdom (Cronbach's alpha

for supporting relationships: 0.861 [0.595–0.815], weight management actions: 0.878 [0.547–0.657]). However, only 32 out of 34 questions were analyzed, in accordance with a prior study by Andrés et al.[11] The questionnaire included five items related to supporting relationships and 10 related to weight management actions; possible scores ranged from 1 to 5. The scores for each process were later accumulated and rounded to the nearest hundredth.[11,12]

Following data collection, statistical analyses were performed using SPSS software version 20 (IBM Corp., USA). We first conducted univariate analysis to assess participants' sociodemographic data, which are presented as descriptive statistics of frequencies (and percentages), means (standard deviation), and medians (interquartile ranges). We assessed continuous variables for normality using the Kolmogorov–Smirnov test (n>50). The variable data were not normally distributed; therefore, Mann–Whitney and Kruskal–Wallis tests were used for bivariate analysis to determine the relationships among BMI, the five stages of change, and the processes of change (as measured by supporting relationships and weight management actions scores). *p*-values of <0.05 indicated statistical significance.

RESULTS

Of the 115 adolescents, 71.3% were grade I obese (BMI 25–30 kg/m^2), and 28.7% were grade II obese (BMI ≥30 kg/m^2). Most participants were in the contemplation and action stages (both 31.3%), suggesting that most had already advanced into the middle to later stages of change with moderate to high scores for supporting relationships and weight management actions (Table 1).

We individually assessed each questionnaire items related to supporting relationships and weight management actions. The average scores of individual supporting relationships items ranged from 2.99 (1.009) to 3.58 (0.943). Item 32, "people around me support me in trying to lose weight," had the highest average score among participants; item 33, "I have someone who listens to me when I need to talk about me being overweight," had the lowest average score (Table 2).

A similar trend was observed in weight management actions scores, ranging from 2.59 to 3.59. Item 15, "I avoid places where I eat a lot," had the lowest average score among the participants. Item 18, "I have learned skills that reduce my desire to eat (i.e., distracting

Table 1. Sociodemographic characteristic proportions of the study participants

Characteristics	n (%) (N = 115)	Mean (SD)	Median (IQR)
Male sex	58 (50.4)	-	-
Education	-	-	-
High school	59 (51.3)		
University (first-year)	56 (48.7)		
Age (years)		17.32 (1.61)	16.29 (3)
15–19	109 (94.8)		
20–21	6 (5.2)		
BMI (kg/m^2)	-	28.64 (3.87)	27.31 (5)
Nutritional status	-	-	-
Obese grade I	82 (71.3)		
Obese grade II	33 (28.7)		
Stages of change		-	-
Precontemplation	9 (7.8)		
Contemplation	36 (31.3)		
Preparation	20 (17.4)		
Action	36 (31.3)		
Maintenance	14 (12.2)		
Process of change scores			
SR	-	69.97 (14.84)	73.33 (20)
WMA	-	64.75 (11.53)	65 (15)

BMI=body mass index; IQR=interquartile range; SD=standard deviation; SR=supporting relationships; WMA=weight management actions

Table 2. Score for questionnaire about supporting relationships

Questionnaire item	Mean (SD)	Median (IQR)
I am aware that there are more and more people who encourage me to lose weight	3.46 (1.033)	3 (1)
My family and friends praise me for not overeating	3.02 (0.951)	3 (0)
My family and friends congratulate me when I manage to lose weight	3.25 (1.037)	3 (1)
People around me support me in trying to lose weight	3.58 (0.943)	4 (1)
I have someone who listens to me when I need to talk about me being overweight	2.99 (1.009)	3 (2)

IQR=interquartile range; SD=standard deviation

Table 3. Score for questionnaire about weight management actions

Questionnaire item	Mean (SD)	Median (IQR)
I look for information about the types of food that could help me lose weight	3.59 (0.996)	4 (1)
I try to put food away to avoid nibbling	3.28 (1.086)	3 (2)
I tell myself positive things to avoid overeating	3.44 (0.847)	3 (1)
I try not to have food in sight	2.95 (1.020)	3 (2)
When I really want to eat, I do activities to avoid it	2.78 (0.905)	3 (1)
I avoid places where people eat a lot	2.59 (0.932)	3 (1)
I have learned skills that reduce my desire to eat (e.g., distracting myself)	3.58 (1.023)	4 (1)
When I am on a diet, I avoid eating with people who I overeat with	2.96 (1.066)	3 (2)
I avoid buying high-calorie food	3.28 (1.001)	3 (1)
To avoid overeating, I prefer eating at home or cooking my own food	3.41 (0.996)	3 (1)

IQR=interquartile range; SD=standard deviation

Table 4. Analysis of obesity grading and behavioral change process with SR and WMA scores

	SR score, median (IQR)	*p*	WMA score, median (IQR)	*p*
BMI		**0.004***		**0.008***
Obese grade I	66.67 (20)		64.17 (14.17)	
Obese grade II	80 (20)		70 (10)	
Stages of change		0.215†		0.192†
Precontemplation	60 (23.33)		60 (11.67)	
Contemplation	73.33 (18.33)		64.17 (12.92)	
Preparation	73.33 (20)		65 (14.58)	
Action	73.33 (26.67)		68.33 (11.67)	
Maintenance	70 (8.33)		69.17 (13.75)	

IQR=interquartile range; SR=supporting relationships; WMA=weight management actions
*Mann–Whitney test, significant if $p<0.05$; †Kruskal–Wallis test, significant if $p<0.05$

myself)," and item 2, "I look for information about the types of food that could help me lose weight," had the highest average scores (Table 3).

Participants with higher BMIs had significantly higher average supporting relationships and weight management actions scores ($p<0.05$). In contrast, the differences in mean scores for supporting relationships and weight management actions between the stages of change were not statistically significant (Table 4).

DISCUSSION

This study indicated that the participants were already in the middle stages of behavioral change,

as they were willing to embark on their weight loss journey. On average, most participants had sufficient support systems and took action to manage their weight; this is further strengthened by the questionnaire items found to have the highest average scores. Furthermore, the findings showed that social support and data accessibility are two crucial aspects of supporting relationships and weight management actions for adolescents to further motivate themselves to transition toward the later stages of change, suggesting that external reinforcements and direct action are important for obesity management.

No significant differences were found across the stages of change for supporting relationships and weight management actions scores. However, BMI was statistically significantly related to the scores for both (supporting relationships and weight management actions), indicating that participants with higher BMIs had better support and took more action to lose weight.

This study was based on prior research by Andrés et al,[11,12] who evaluated the transtheoretical theory model for managing obesity in adult populations (with an average age of 32.03 ± 12.88 years) in the United Kingdom. Following Andrés et al,[11,12] the present study only assessed supporting relationships and weight management actions scores because, compared to those with low scores in these categories, most participants with higher scores were in more advanced stages of change, which ranged from preparation to maintenance. These findings support those of the original study, which reported that emotional reevaluation and weight consequences evaluation (in the form of self-reevaluation) tended to occur in the earlier stages of change (from precontemplation to contemplation), while environmental restructuring (supporting relationships) and weight management actions tended to occur in the later stages (from action to maintenance).[13]

Andrés et al[11] found that most participants were in the action (38.27%) and maintenance (34.50%) stages. Similarly, we identified contemplation and action as the most prevalent stages (each 31.3%). Moreover, their findings revealed that the highest average supporting relationships and weight management actions scores were found in the action stage. In contrast, the present study found that the contemplation, preparation, and action stages had the highest average supporting relationships scores, while the maintenance stage exhibited the highest weight management actions score.

In 2017, Karintrakul et al[14] assessed the behavioral change readiness of women with obesity in Thailand based on the transtheoretical model as an intervention for obesity. They found that BMI was a statistically significant factor in participants at different stages of change in the control and intervention groups ($p<0.001$). In addition, they assessed other parameters of obesity such as body weight, body impedance analysis (consisting of percent body fat, fat mass, and muscle mass), and weight circumference, which also mostly showed significant results, except for muscle mass. However, other studies reported contradictory findings to our results. For example, one previous study found that adolescents with obesity received significant support from parents and close friends, but no data were available on the relationship between BMI and familial support.[15] However, they found a relationship between BMI and teacher support, suggesting that the higher one's BMI, the lower the perceived support. Another study on social support and obesity in adult African-American women found that a lower BMI was related to higher support from friends in exercising because they perceived a higher possibility of weight loss; meanwhile, older populations living in rural areas had significantly more encouragement from family and friends to eat a healthy diet.[16] Similarly, a study of African-American university students showed that having a BMI above the threshold for overweight and obesity had no statistically significant relationship with social support.[17] This phenomenon might occur because students typically seek independence from their parents while receiving support from their peers; therefore, obesity would not be related to the amount of social support they gain from others. In addition, a study of medical students in Sudan found that weight management actions were associated with BMI.[18] Although physical activity did not show any statistically significant results, significant differences in BMI were observed between students with varying eating behaviors, including uncontrolled, conscious restraint, and emotional eaters.[18]

This study focused on participants from late adolescents to young adults, including high school and first-year university students.[8] High school students in late adolescence tend to have a stronger sense of self-identity than younger adolescents while adjusting to physical changes.[8] They begin to develop

independence and the desire to connect with their peers.[8] Social support from peers can facilitate positive lifestyle changes in students at this age.[8] In contrast, first-year university students are young adults with higher emotional stability and a firmer sense of identity and independence; nevertheless, they still highly value friendships while beginning to develop romantic interests.[8] Transitioning from high school to university involves several lifestyle changes, including new living arrangements, academic surroundings, peer relationships, and greater independence and responsibilities.[19,20] During this period, social support from teachers and friends is crucial in helping first-year university students develop a sense of belonging and engage in group activities. The presence of social support is significantly related to higher quality friendships, leading to better adaptation for students during their first academic year.[20] Therefore, first-year university students have distinctive living circumstances compared to high school students, with numerous new methods for gaining reinforcement and support while navigating the next stage of personal and academic life.

Regardless of the diverse findings in previous research, the current study's findings indicate the potential role of the processes of change in weight management. One study reported that supporting relationships and weight management actions are associated with weight management.[21] High school adolescents who were overweight or obese and had more support from their family and friends showed greater diet and physical activity improvements in a follow-up model. Weight management should be a crucial component of adolescents' lives as they start to gain independence, receive less parental supervision, and be more influenced by their peers. Furthermore, social support could further facilitate behavioral change in weight management, leading people to take action toward weight loss. In the present study, the scores and analysis results could reflect the lack of supporting relationships and weight management actions, along with lower levels of awareness about obesity and its management among participants.

This study had some limitations. First, we used secondary data obtained through convenience sampling during the initial data collection period, and we did not perform randomization to sort the participants. Although the number of participants was sufficient, the lack of randomization might have led to biases that compromised the reliability of the statistical analyses of the results. Second, no follow-up was performed to further assess participants' stages and processes of change after the initial encounter, thereby limiting the scope of the results and strength of the analysis. Finally, the processes of change, as part of the transtheoretical model established by Prochaska et al,[13] have not been frequently studied, especially by Indonesian researchers, despite the strong potential to enhance behavioral interventions related to obesity in adolescents. Therefore, finding relevant prior studies and relating the findings to the general Indonesian population was challenging. Although the authors are optimistic that interest in this specific topic will increase over time, the concept of the transtheoretical model itself is beneficial for behavioral change in multiple studies, regardless of the intervention or examined health problem.

In conclusion, adolescents with obesity and higher BMI (based on the obesity grading of the WHO Asia-Pacific) tended to have significantly higher scores for supporting relationships and weight management actions, indicating that external reinforcement and immediate weight loss actions play pivotal roles in readiness for behavioral change. No significant differences were found between participants' current stages of change and their scores for supporting relationships or weight management actions; however, increasing trends in average scores in each consecutive stage of change were observed for each category. Further research with better methodologies is recommended to diversify the target populations, prevent biases, and increase the quality of the findings. These findings can be incorporated into other observational studies and applied in interventional programs based on the transtheoretical model and behavioral change process to manage obesity in adolescents.

Conflict of Interest

The authors affirm no conflict of interest in this study.

Acknowledgment

We would like to thank the Southeast Asian Ministers of Education Organization Regional Center for Food and Nutrition (SEAMEO RECFON) for funding this research. We would also like to thank SMAN 21 Jakarta and Klinik Makara Universitas Indonesia for providing researchers, whose resources were very beneficial for the completion of this study.

Funding Sources

This study was funded by Southeast Asian Ministers of Education Organization Regional Center of Food and Nutrition (SEAMEO RECFON), as a part of an umbrella study titled "Assessment on Process and Stage of Behavioural Change Readiness Level for

Weight Management based on the Trans-Theoretical Model in Overweight-Obese Adolescence in Jakarta, Indonesia" by Kekalih et al.

REFERENCES

1. World Health Organization (WHO). Obesity and overweight [Internet]. World Health Organization (WHO); 2020 [cited 2022 Oct 11]. Available from: https://www.who.int/news-room/fact-sheets/detail/obesity-and-overweight.
2. Ng M, Fleming T, Robinson M, Thomson B, Graetz N, Margono C, et al. Global, regional, and national prevalence of overweight and obesity in children and adults during 1980-2013: a systematic analysis for the Global Burden of Disease Study 2013. Lancet. 2014;384(9945):766–81.
3. Indonesian National Institute of Health Research and Development. Basic Health Research 2013. Jakarta: Indonesian Ministry of Health; 2013. p. 223–5.
4. Indonesian National Institute of Health Research and Development. Basic Health Research 2018. Jakarta: Indonesian Ministry of Health; 2013. p. 95–8.
5. Rachmi CN, Li M, Alison Baur L. Overweight and obesity in Indonesia: prevalence and risk factors-a literature review. Public Health. 2017;147:20–29.
6. Hruby A, Hu FB. The epidemiology of obesity: a big picture. Pharmacoeconomics. 2015;33(7):673–89.
7. Abdelaal M, le Roux CW, Docherty NG. Morbidity and mortality associated with obesity. Ann Transl Med. 2017;5(7):161.
8. Sawyer SM, Afifi RA, Bearinger LH, Blakemore SJ, Dick B, Ezeh AC, et al. Adolescence: a foundation for future health. Lancet. 2012;379(9826):1630–40.
9. Salvy SJ, Bowker JC. Peers and obesity during childhood and adolescence: a review of the empirical research on peers, eating, and physical activity. J Obes Weight Loss Ther. 2014;4(1):207.
10. Raj M, Kumar RK. Obesity in children & adolescents. Indian J Med Res. 2010;132(5):598–607.
11. Andrés A, Saldaña C, Beeken RJ. Assessment of processes of change for weight management in a UK sample. Obes Facts. 2015;8(1):43–53.
12. Andrés A, Saldaña C, Gómez-Benito J. Establishing the stages and processes of change for weight loss by consensus of experts. Obesity (Silver Spring). 2009;17(9):1717–23.
13. Prochaska JO, Velicer WF. The transtheoretical model of health behavior change. Am J Health Promot. 1997;12(1):38–48.
14. Karintrakul S, Angkatavanich J. A randomized controlled trial of an individualized nutrition counseling program matched with a transtheoretical model for overweight and obese females in Thailand. Nutr Res Pract. 2017;11(4):319–26.
15. Herzer M, Zeller MH, Rausch JR, Modi AC. Perceived social support and its association with obesity-specific health-related quality of life. J Dev Behav Pediatr. 2011;32(3):188–95.
16. Johnson ER, Carson TL, Affuso O, Hardy CM, Baskin ML. Relationship between social support and body mass index among overweight and obese African American women in the rural deep South, 2011-2013. Prev Chronic Dis. 2014;11:E224.
17. So WY, Swearingin B, Robbins J, Lynch P, Ahmedna M. Relationships between body mass index and social support, physical activity, and eating habits in African American university students. Asian Nurs Res (Korean Soc Nurs Sci). 2012;6(4):152–7.
18. Yousif MM, Kaddam LA, Humeda HS. Correlation between physical activity, eating behavior and obesity among Sudanese medical students Sudan. BMC Nutr. 2019;5:6.
19. Lerner RM, Steinberg L. Individual bases of adolescent development. In: Lerner RM, Steinberg L, editors. Handbook of adolescent psychology: individual bases of adolescent development. 3rd ed. John Wiley & Sons Inc.; Hoboken: 2009.
20. Pittman LD, Richmond A. University belonging, friendship quality, and psychological adjustment during the transition to college. J Exp Educ. 2008;76(4):343–61.
21. Wang M, Druker S, Gapinski MA, Gellar L, Schneider K, Osganian S, et al. The role of social support vs. modeling on adolescents' diet and physical activity: findings from a school-based weight management trial. J Child Adolesc Behav. 2014;2(2):132.

Clinical Research

Accuracy of machine learning models using ultrasound images in prostate cancer diagnosis: a systematic review

Retta Catherina Sihotang[1], Claudio Agustino[1], Ficky Huang[1], Dyandra Parikesit[2], Fakhri Rahman[1], Agus Rizal Ardy Hariandy Hamid[1]

pISSN: 0853-1773 • eISSN: 2252-8083
https://doi.org/10.13181/mji.oa.236765
Med J Indones. 2023;32:112–21

Received: January 31, 2023
Accepted: September 11, 2023

Authors' affiliations:
[1]Department of Urology, Faculty of Medicine, Universitas Indonesia, Cipto Mangunkusumo Hospital, Jakarta, Indonesia, [2]Urology Medical Staff Group, Universitas Indonesia, Universitas Indonesia Hospital, Depok, Indonesia

Corresponding author:
Agus Rizal Ardy Hariandy Hamid
Department of Urology, Faculty of Medicine, Universitas Indonesia, Cipto Mangunkusumo Hospital, Jalan Salemba Raya No. 6, Central Jakarta 10430, DKI Jakarta, Indonesia
Tel/Fax: +62-21-3912477
E-mail: rizalhamid.urology@gmail.com

ABSTRACT

BACKGROUND In prostate cancer (PCa) diagnosis, many developed machine learning (ML) models using ultrasound images show good accuracy. This study aimed to analyze the accuracy of neural network ML models in PCa diagnosis using ultrasound images.

METHODS The protocol was registered with PROSPERO registration number CRD42021277309. Three reviewers independently conducted a literature search in 5 online databases (PubMed, EBSCO, Proquest, ScienceDirect, and Scopus). We included all cohort, case-control, and cross-sectional studies in English, that used neural networks ML models for PCa diagnosis in humans. Conference/review articles and studies with combination examination with magnetic resonance imaging or had no diagnostic parameters were excluded.

RESULTS Of 391 titles and abstracts screened, 9 articles relevant to the study were included. Risk of bias analysis was conducted using the QUADAS-2 tool. Of the 9 articles, 5 used artificial neural networks, 1 used deep learning, 1 used recurrent neural networks, and 2 used convolutional neural networks. The included articles showed a varied area under the curve (AUC) of 0.76–0.98. Factors affecting the accuracy of artificial intelligence (AI) were the AI model, mode and type of transrectal sonography, Gleason grading, and prostate-specific antigen level.

CONCLUSIONS The accuracy of neural network ML models in PCa diagnosis using ultrasound images was relatively high, with an AUC value above 0.7. Thus, this modality is promising for PCa diagnosis that can provide instant information for further workup and help doctors decide whether to perform a prostate biopsy.

KEYWORDS artificial intelligence, machine learning, neural network model, prostate cancer, ultrasonography

Prostate cancer (PCa) is the third most common cancer globally and the second most common in men.[1] It significantly affects male health, and early detection facilitates curative treatment and reduces disease morbidity and mortality.[2,3]

Ultrasonography has a potential for PCa imaging because it is cost-effective, practical, and widely available.[4] However, standard transrectal ultrasound (TRUS) alone is not reliable due to its low sensitivity and specificity in detecting PCa.[5] The current gold standard for PCa detection is a prostate biopsy performed under TRUS guidance.[2,3,6,7] While ultrasonography is widely available, TRUS can be less comfortable for patients than the transabdominal approach. The best instruments currently available yield inaccurate results. More accurate diagnostic instruments are required to effectively detect disorders. Technological advancements, such as artificial intelligence (AI), may help overcome these challenges.[8,9]

AI is a revolutionary technology in the healthcare field that is gaining interest. Neural networks, such as artificial neural networks (ANNs), convolutional neural networks (CNNs), and recurrent neural networks (RNNs), are machine learning (ML) models that mimic human biological neurons. For PCa, AI has been shown to aid in standardized pathological grading to guide cancer stratification and treatment. Nitta et al[10] and Djavan et al[11] applied ML models to predict PCa based on prostate-specific antigen (PSA) concentrations. ML tended to be superior to conventional methods, with a region-wise area under the receiver operating characteristic curve (ROC-AUC) value ranging from 0.63 to 0.91.

The accuracy of ML based on data from ultrasonography as the primary modality has been debated. Thus, this review aimed to analyze the accuracy of neural networks trained on ultrasound images for PCa diagnosis.

METHODS

Protocol registration

The protocol for this systematic review was registered with PROSPERO registration number CRD42021277309.

Search strategy

Three reviewers (RCS, CA, and FH) independently conducted a literature search of five online databases on January 13, 2023. The databases were PubMed, EBSCO, ProQuest, ScienceDirect, and Scopus. The following keywords with various combinations were used: "Prostate Cancer," "Machine Learning OR Neural Network," "Diagnosis," and "Ultrasonography" (Figure 1). The reference lists of the articles retrieved from the literature search were also reviewed to identify other relevant studies.

Study selection and data extraction

All articles that used ultrasound images to demonstrate the application of ML to the diagnosis of PCa were included. The literature search was limited to publications in English without regard to the publication date. A study was considered significant if it met the inclusion criteria, including using human participants, neural networks, ML models, and prostate biopsy as the criterion for diagnosis. Cohort, case-control, and cross-sectional studies were included. Conference or review articles and studies that involved a combined examination with magnetic resonance imaging (MRI) or had no diagnostic parameters were excluded. Three reviewers (RCS, CA, and FH) individually reviewed

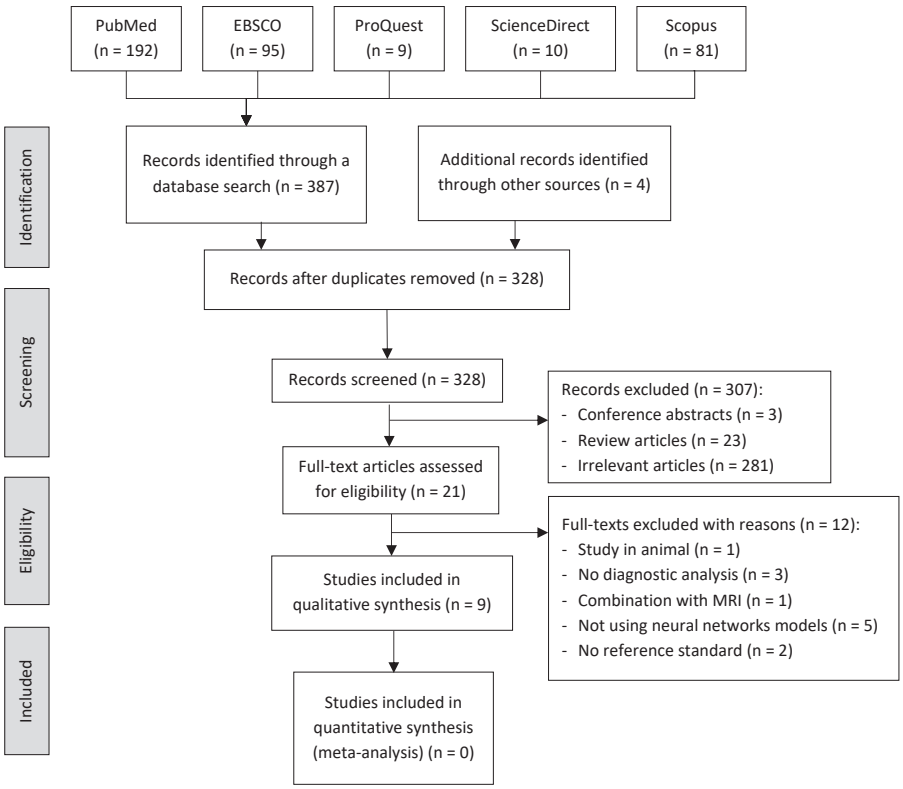

Figure 1. PRISMA flow diagram for the current study (a total of 391 articles obtained). MRI=magnetic resonance imaging; PRISMA=Preferred Reporting Items for Systematic Reviews and Meta-Analyses

the titles and abstracts of the selected studies. Disagreements were resolved through discussions with senior reviewers until a consensus was reached. All authors agreed with the final list of papers selected for extraction. The Preferred Reporting Items for Systematic Reviews and Meta-Analyses flow diagram was used to assist in selecting the articles.

The data extracted from the included articles were tabulated to summarize the outcomes. The data collection points included the number of samples and participants, ultrasound modes, ML methods, system specifications, software tools, programming languages, ML input data, ML outcomes, and diagnostic performance. The primary outcome was the accuracy of neural network ML models for PCa diagnosis. Additionally, the neural network models were compared with other ML models; we compared their available diagnostic performance data, including sensitivity, specificity, positive predictive value (PPV), negative predictive value (NPV), and ROC-AUC. The receiver operating characteristic is a graph showing the performance of a classification model at all classification thresholds to determine its accuracy. The area under the curve (AUC) is the probability that a classifier ranks a randomly selected positive example more highly than a randomly selected negative example. Based on the test, an AUC of 0.5 indicates the inability to distinguish between patients with and without disease or condition, 0.7–0.8 is acceptable, 0.8–0.9 is considered excellent, and >0.9 is outstanding.

Risk of bias assessment

The methodological quality of the research was independently evaluated by three reviewers (RCS, CA, and FH) using the QUADAS-2 tool in the Review Manager software version 5.4 (Cochrane, United Kingdom) for Mac. The reviewers were not blinded to the identities of the authors of the articles, journals, and publishers. Based on the questions in the QUADAS-2 tool, the risks of bias were categorized as high, unclear, and low.

RESULTS

Of the 391 retrieved articles, only 9 met the inclusion criteria (Figure 1). The quality assessment of the included articles is shown in Table 1 using the QUADAS-2 tool. Several articles included in the analysis had an unclear or high risk of bias. Unclear risk of bias was common for the index test parameters due to the unclear threshold of the index test. Meanwhile, a high risk of bias was also common because the interpretation was limited to standard results in several articles.[12–14]

The characteristics of each study are presented in Table 2.[12–20] Five studies used an ANN, one used deep learning (DL), one used an RNN, and two used a CNN. Nine of the included studies had a cross-sectional design. All studies examined adult males with an unknown age range owing to unclear data. The sample sizes ranged from 48 to 1,151 patients; however, the studies by Ronco and Fernandez[12] and Akatsuka et al[13] only provided the number of cases. Five studies used TRUS data only for the input parameters, whereas the others used a combination of input data from clinical findings. All studies showed various accuracy analysis parameters, including

Table 1. Risk of bias assessment using the QUADAS-2 tool

First author, year	Risk of bias				Applicability concerns		
	Patient selection	Index test	Reference standard	Flow and timing	Patient selection	Index test	Reference standard
Akatsuka,[13] 2022	Low	High	Low	Low	Low	Unclear	Low
Azizi,[17] 2018	Unclear	Unclear	Low	Low	Low	Unclear	Low
Hassan,[19] 2022	High	High	Low	Low	Unclear	Unclear	Low
Lee,[15] 2006	Low	Unclear	Low	Low	Low	Low	Low
Lee,[16] 2010	Low	Unclear	Low	Low	Low	Unclear	Low
Loch,[14] 1999	Unclear	Low	Low	Low	Low	Low	Low
Lorusso,[20] 2023	Unclear	Low	Low	Low	Unclear	Low	Low
Ronco and Fernandez,[12] 1999	Unclear	High	Low	Low	Unclear	High	Low
Wildeboer,[18] 2020	Low	Unclear	Low	Low	Low	Unclear	Low

Table 2. Characteristics and performance result of included studies

First author, year	Country	Samples	Imaging	ML method	System specifications, software tools, and programming language	Input data	Outcome	Performance results
Ronco and Fernandez,[12] 1999	Uruguay	442 cancer and benign cases	TRUS	ANN	1. System specifications: NA 2. Software tools: NeuroGenetic Optimizer version 2.5 for Windows 1995 3. Programming language: NA	1. Ultrasonographic variables (transverse axis, anteroposterior axis, longitudinal axis, prostatic volume, central zone, echoic level, volume of the pathological area, major diameter of the pathological area, minor diameter of the pathological area, presence/absence of calcifications, degree of bladder impression, PSA density [PSA/volume], and ultrasonographic diagnosis) 2. Non-ultrasonographic variables (age, previous clinical diagnosis, PSA level, and number of biopsies)	Accuracy for detecting PCa	1. PPV: 0.82 2. NPV: 0.97
Loch,[14] 1999	USA	553 specimens from 61 patients with confirmed PCa	TRUS	ANN	1. System specifications: NA 2. Software tools: Neuro-shell 2, Ward Systems Group, Inc., Frederick, MD 3. Programming language: NA	TRUS findings	Accuracy for detecting PCa	1. Benign pathology: 99% classified correctly 2. Cancer: 71% classified correctly
Lee,[15] 2006	Korea	684 patients who had undergone TRUS-guided prostate biopsy	TRUS and Doppler ultrasonography	ANN	1. System specifications: NA 2. Software tools: NeuroSolutions version 4.0, NeuroDimension Inc., Gainesville, FL 3. Programming language: NA	1. Model 1 (age, DRE findings, PSA level, PSA density, transitional zone volume, and PSA density in the transitional zone) 2. Model 2 (age, DRE findings, PSA level, PSA density, transitional zone volume, PSA density in the transitional zone, and TRUS findings [positive, suspicious, or negative])	Diagnostic performance of 2 ANN models	1. Model 2 showed better accuracy than Model 1. 2. Accuracy Model 1 (AUC PSA 0–4: 0.738, PSA 4–10: 0.753, and PSA>10: 0.774) 3. Accuracy Model 2 (AUC PSA 0–4: 0.859, PSA 4–10: 0.797, and PSA>10: 0.894)

Table continued on next page

Table 2. (continued)

First author, year	Country	Samples	Imaging	ML method	System specifications, software tools, and programming language	Input data	Outcome	Performance results
Lee,[16] 2010	Korea	1,077 patients who had undergone TRUS-guided prostate biopsy	TRUS and Doppler ultrasonography	MLRA, ANN, and SVM	1. System specifications: NA 2. Software tools and models: (MLRA: SPSS version 15, SVM: LIBSVM for multiclass classification, and ANN: detailed model of three-layer perceptron architecture, consisting of one input layer, one hidden layer, and one output layer) 3. Programming language: NA	Age, DRE findings, PSA level, PSA density, transitional zone volume, PSA density in the transitional zone, and TRUS findings (class I–V based on lesion location, outline, shape, and vascularity)	Accuracy of each model	1. ROC MLRA: 0.768 2. ROC ANN: 0.778 3. ROC SVM: 0.847
Azizi,[17] 2018	Canada	157 patients who had undergone prostate biopsy	TeUS	RNN comparing LSTM, GRU, vanilla RNN, and spectral	1. System specifications: GeForce GTX 980 Ti GPU with 6 GB of memory, hosted by a machine running Ubuntu 16.04 operating system on a 3.4 GHz Intel Core™ i7 CPU with 16 GB of memory 2. Software tools: NA 3. Programming language: Python 2.7	TeUS findings	Accuracy for detecting PCa	1. LTSM (specificity: 0.98, sensitivity: 0.76, accuracy: 0.93, and AUC: 0.96) 2. GRU (specificity: 0.95, sensitivity: 0.70, accuracy: 0.86, and AUC: 0.92) 3. Vanilla RNN (specificity: 0.72, sensitivity: 0.69, accuracy: 0.75, and AUC: 0.76) 4. Spectral (specificity: 0.73, sensitivity: 0.63, accuracy: 0.78, and AUC: 0.76)
Wildeboer,[18] 2020	Netherland	48 men with confirmed PCa	B-mode US, SWE, and DCE-US	DL	NA	TRUS findings	Accuracy of each model to localize PCa using ultrasound images	1. ROC-AUC for PCa: 0.75 2. ROC-AUC for Gleason >3+4: 0.90

Table continued on next page

Table 2. (continued)

First author, year	Country	Samples	Imaging	ML method	System specifications, software tools, and programming language	Input data	Outcome	Performance results
Hassan,[19] 2022	USA	61,119 images from 1,151 patients in open-source databases	TRUS	CNN compared to Nearest Neighbor, Gradient Boosting, SVM, and Random Forest	1. System specifications: PC with Core i7 11th generation intel processor, 16GB DDR RAM 2. Software tools: not mentioned (NN Models VGG-16) 3. Programming language: Python version 3.7 with Tensorflow 2.x and scikit learn 0.242 version	TRUS images	Accuracy of each model to efficiently classify PCa	Accuracy (VGG-16): (CNN: 0.99, Nearest Neighbor: 0.869, Gradient Boosting: 0.871, SVM: 0.872, and Random Forest: 0.875)
Akatsuka,[13] 2022	Japan	2,676 images from 691 cases	TRUS	SVM and CNN + SVM	1. System specifications: NA 2. Software tools and models (SVM: the e1071 package [version 1.7.0] and CNN: Grad-CAM) 3. Programming language: NA	1. Still ultrasound image data 2. Clinical data (age and PSA) 3. Integrated data (ultrasound image, total prostate volume, PSA density, age, and PSA)	Accuracy to detect high-grade PCa	1. ROC-AUC clinical data only (SVM): 0.691 2. ROC-AUC integrated data (CNN + SVM): 0.835
Lorusso,[20] 2023	German	64 patients with PCa	TRUS	ANN	NA	TRUS images	Diagnostic performances of the ANNA/C-TRUS system	1. Overall (sensitivity: 0.62, specificity: 0.81, NPV: 0.80, PPV: 0.64, and accuracy: 0.78) 2. PCa index lesion (sensitivity: 0.60, specificity: 0.87, NPV: 0.88, PPV: 0.58, and accuracy: 0.81) 3. ISUP grade >2 (sensitivity: 0.69, specificity: 0.77, NPV: 0.88, PPV: 0.50, and accuracy: 0.75) 4. Gleason 4 or 5 (sensitivity: 0.70, specificity: 0.74, NPV: 0.91, PPV: 0.41, and accuracy: 0.74)

ANN=artificial neural network; ANNA/C-TRUS=computerized artificial neural network analysis; AUC=area under the curve; CNN=convolutional neural network; DCE-US=dynamic contrast-enhanced ultrasound; DL=deep learning; DRE=digital rectal examination; Grad-CAM=gradient-weighted class activation mapping; GPU=graphic processing unit; GRU=gated recurrent units; LSTM=long short-term memory; ML=machine learning; MLRA=multiple logistic regression analysis; NA=not available; NPV=negative predictive value; PCa=prostate cancer; PPV=positive predictive value; PSA=prostate-specific antigen; RNN=recurrent neural network; ROC=receiver operating characteristic; ROC-AUC=a region-wise area under the receiver operating characteristics curve; SVM=support vector machine; SWE=shear-wave elastography; TeUS=temporal enhanced ultrasound; TRUS=transrectal ultrasonography

AUC, PPV, NPV, sensitivity, and specificity (Table 2). However, Loch et al[14] only used percentages. The performance results are presented in Table 2. Due to the varied parameters, a quantitative analysis could not be performed. Most of the studies used the AUC as an accuracy parameter. The AUC values of all the studies were greater than 0.7, ranging from 0.75 to 0.98.

DISCUSSION

Based on the included studies, the overall accuracy of ML showed promising results. The AUC values of nine studies were greater than 0.7, ranging from 0.75 to 0.98. Wildeboer et al[18] assessed a potential DL model based on TRUS B-mode US, shear-wave elastography (SWE), and dynamic contrast-enhanced ultrasound (DCE-US). The multiparametric classifier showed an AUC of 0.90 compared with 0.75 for the best-performing individual parameters for PCa and Gleason scores >3+4 significant PCa. This study revealed that combinations of the available modes were favored over a single mode. Lee et al[15] evaluated the accuracies of multiple logistic regression, ANN, and support vector machine (SVM) models in predicting the prostate biopsy outcomes of 684 patients (214 were confirmed to have PCa). The models were developed using the following input data: age, digital rectal examination (DRE) findings, PSA parameters, and TRUS findings. This study showed that image-based clinical decision support systems (ANN and SVM) were more accurate than multiple logistic

Table 3. Comparison of advantages and disadvantages of several ML models

ML models	Advantages	Disadvantages
ANN[26]	1. Stores data over an entire network 2. Capacity to operate with little information 3. Can overlook errors 4. Possesses a distributed memory system	1. Hardware reliant 2. Unexplained the network's behavior 3. Establishment of an appropriate network structure
CNN[26]	1. Extremely high accuracy when it comes to picture recognition challenges 2. Detects critical traits automatically and without human intervention 3. Weight distribution	1. Does not encode an object's location or orientation 2. Inability to be spatially invariant with respect to the supplied data 3. Requires numerous training data sets
RNN[27]	1. Retains all information over time and beneficial for time series prediction 2. Utilizes convolutional layers with RNNs to broaden the effective pixel neighborhood	1. Gradient difficulties of disappearing and exploding 2. Quite difficult to train 3. Incapable of processing extremely lengthy sequences
Linear regression[26]	1. Works exceptionally well in small data sets 2. Easy to build and comprehend 3. Analyzes model parameters in a statistical sense	1. Can only work in data sets that have linear relation 2. Overconfidence in the logic models 3. Can only classify dichotomous variables except multinomial linear regression
SVM[28,29]	1. Can handle several feature spaces with less risk of overfitting 2. Capable of classifying semi-structured and unstructured data well, such as texts or images	1. Results, weights, and impacts of variables are harder to comprehend and interpret. 2. Data's noise significantly impacts the classification results. 3. Expansive to build in a large data set environment
DT[28,29,30]	1. Results are simpler to comprehend and interpret. 2. Less time consuming data preparation 3. Can produce reliable classifiers that can be confirmed with statistical tests	1. Mutually exclusive classes 2. If any attribute or variable value for a non-leaf node is absent, the algorithm will not branch. 3. Less superior compared to ANN
RF[28,29]	1. A lower possibility of variance and overfitting of training data, compared to DT 2. Performs well in large data sets 3. Can calculate which variables or qualities are most significant in the categorization	1. Far more complex and expansive to build 2. When estimating variable significance, it favors variables or qualities that may take a large number of alternative values. 3. Commonly overfitting

ANN=artificial neural network; CNN=convulotional neural network; DT=decision tree; ML=machine learning; RF=Random Forest; RNN=recurrent neural network; SVM=support vector machine

regression models. They evaluated the diagnostic performance of the ANN model with and without TRUS data. The ANN model used the primary input data of age, PSA levels, and DRE findings. However, with additional TRUS data, the ANN model showed better accuracy and a higher AUC value than without TRUS data. Azizi et al[17] proposed the temporal modeling of temporal enhanced ultrasound (TeUS) using an RNN to improve cancer detection accuracy. The TeUS data were acquired from 157 patients during fusion prostate biopsy. The model achieved an AUC value of 0.96. Hassan et al[19] demonstrated a higher accuracy (0.99) with a CNN (VGG-16) than with other algorithms (Gradient Boosting, SVM, and Random Forest). Akatsuka et al[13] reported an AUC of 0.835 for CNN combined with an SVM built on clinical data and TRUS images. This was higher than the AUC for the SVM based on only clinical data. A recent study by Lorusso et al[20] demonstrated increasing sensitivity and NPV of the ANN method using TRUS images for higher grades of PCa.

Several factors influence the accuracies of models, including the AI model, TRUS modes, amount of input data, Gleason grading, and PSA concentrations. Based on the analysis of each AI model (Table 4), two included studies highlighted the superior diagnostic performance of the neural network model to those of other models.[13,20] ANN and CNN outperformed the other neural network models in terms of diagnostic performance.[14,15,19] TRUS modes are substantially related to the accuracy, with DCE-US/SWE/TeUS improving the visualization and distinction of prostate tissues over the B-mode. The amount of input data is also important for reliable predictions by ANN models. More complicated data will result in a more accurate diagnosis.[21,22] According to Lee et al,[16] Wildeboer et al,[18] and Akatsuka et al,[13] adding more complicated data increases the AUC, corresponding to better accuracy. Wildeboer et al[18] discovered a significant association between Gleason scores of >3+4 and accuracy of DL, but not in Gleason scores of 3+3 or 3+4. This could be due to a bias in patient selection; tumors with scores of 3+3 were disproportionately large for the doctors and were excluded from the study. According to Lee et al,[16] the AUC of ANN models was consistently higher for PSA concentrations greater than 10 ng/ml. This could be related to the serum PSA concentrations, corresponding to cancer extent and histological grade.[23] As a result, TRUS alone is insufficient for detecting PCa. However, TRUS data and its combinations with other pertinent input data can be used for ML. Despite its benefits, neural networks utilizing ultrasonic images have drawbacks that can be improved, such as the need for a large dataset for training.[24] Furthermore, the quality of scans, sample collection procedures, and human interpretation errors differ with datasets, making it impossible to create a gold standard.[24,25]

Reading ultrasound images requires several years of experience and training. ML has been introduced to medical imaging to address these constraints, speed up ultrasound picture analysis, and generate objective disease classification.[21] ML applications have advanced rapidly, thus reducing the time required to interpret a large amount of data and draw conclusions.[26] ML is an AI subfield in which computer algorithms learn connections between data instances for predictions.[22] As previously noted, ultrasound images are analyzed using various techniques such as classification, regression, registration, and segmentation. However, neural network techniques have been found to outperform other classifiers.[23] Neural networks function similarly to the human brain and can solve the limitations of regular ML. They can combine additional variables and produce outcomes for more complex scenarios.[23] A neural network can create input data from many variables to classify patients with PCa.

As shown in Table 3, the algorithms used to build ML have several advantages and disadvantages. Regardless of their differences, CNNs and ANNs are important in the ML field.[26,27] ANNs comprise multiple layers of interconnected artificial neurons activated by activation functions. Like traditional machine algorithms, the neural network learns specific values during training.[28] Other prominent ML models, such as SVM, work by adding a higher dimension to the input to differentiate the classes.[29] To assess whether the data meet the criteria, the decision tree (DT) employs several decision logics that act similarly to flowcharts. When numerous DTs are joined, a Random Forest method is used to reduce the overfitting tendency of the DT.[30]

The ML field is advancing rapidly, with corresponding hardware and software advancements. DL has advanced significantly in recent years, owing to data overflow and support from graphic processing unit hardware acceleration. Various DL libraries, including PyTorch, Keras, TensorFlow, Theano, and

Caffe, are currently available. Neural network fusion was recently developed to increase accuracy.[31] The utilization of ML with TRUS data could have a potential role as a diagnostic modality, especially when MRI is unavailable. Based on current guidelines, T2-weighted imaging remains the most useful method for local MRI.[32] However, a meta-analysis by de Rooij et al[33] showed that MRI had high specificity but poor sensitivity for local PCa staging. Its sensitivities and specificities for extracapsular extension, seminal vesicle invasion, and overall stage T3 detection were 0.57 (95% confidence interval [CI] = 0.49–0.64) and 0.91 (95% CI = 0.88–0.93), 0.58 (95% CI = 0.47–0.68) and 0.96 (95% CI = 0.95–0.97), and 0.61 (95% CI = 0.54–0.67) and 0.88 (95% CI = 0.85–0.91), respectively. Our findings showed that ML based on TRUS and other relevant data can improve diagnostic performance. Thus, it will become more affordable and easier to diagnose PCa without MRI. Furthermore, ML based on TRUS data can be implemented in combination with MRI for prostate biopsy and intraoperative mapping before robotic surgery. This will allow the surgeon to visualize suspected lesions on the instrument display during the procedure.

To date, no study has analyzed the cost-effectiveness of ML for PCa diagnosis. For severe cases of PCa, AI is used to reduce the processing time and facilitate early detection, resulting in a superior prognosis. Additionally, reducing the quantity of human labor enables the service to be provided at a reduced price compared with multiparametric MRI.[34] A systematic review by Khanna et al[35] reported that AI models demonstrated significant cost savings for medical diagnosis and treatment, and this is applicable to PCa diagnosis.

The present study had some limitations. The major limitations were the low to moderate quality of the included studies and the small sample of articles. The literature search was restricted to studies written in English, and some articles in other languages might have been missed. None of the studies used the same output parameters to generate a quantitative analysis. Additionally, most studies did not blind the diagnosis when testing the ML models, which might have resulted in bias. The approximate AUC and sensitivity values of the ML models in this study were not high and might have led to missed PCa cases among the patients. Further advancements in ML will continue to improve diagnostic accuracy.

In conclusion, the accuracy of the neural network models for PCa diagnosis using ultrasound images was relatively high, with AUCs greater than 0.7. Neural network models are promising for PCa diagnosis and can provide instant information for further workup with relatively high accuracy. Image-based ML models can help doctors decide on proceeding with or deferring a prostate biopsy. Further development of AI will be beneficial for diagnosis, treatment evaluation, and predicting patient prognosis. Future studies should investigate and compare the diagnostic performance of neural networks based on ultrasound images and MRI for PCa.

A preprint of this manuscript has previously been published (https://www.medrxiv.org/content/10.1101/2022.02.03.22270377v1).

Conflict of Interest

Agus Rizal Ardy Hariandy Hamid is the editor-in-chief of this journal but was not involved in the review or decision making process of the article.

Acknowledgment

Technical assistance and critical advice are provided by the staff of the Department of Urology, Cipto Mangunkusumo Hospital.

Funding Sources

None.

REFERENCES

1. Sung H, Ferlay J, Siegel RL, Laversanne M, Soerjomataram I, Jemal A, et al. Global cancer statistic 2020: GLOBOCAN estimates of incidence and mortality worldwide for 36 cancers in 185 countries. CA Cancer J Clin. 2021;71(3):209–49.
2. Hayes JH, Barry MJ. Screening for prostate cancer with the prostate-specific antigen test: a review of current evidence. JAMA. 2014;311(11):1143–9.
3. Naji L, Randhawa H, Sohani Z, Dennis B, Lautenbach D, Kavanagh O, et al. Digital rectal examination for prostate cancer screening in primary care: a systematic review and meta-analysis. Ann Fam Med. 2018;16(2):149–54.
4. Ganie FA, Wanie MS, Ganie SA, Lone H, Gani M, Mir MF, et al. Correlation of transrectal ultrasonographic findings with histopathology in prostatic cancer. J Educ Health Promot. 2014;3:38.
5. Harvey CJ, Pilcher J, Richenberg J, Patel U, Frauscher F. Applications of transrectal ultrasound in prostate cancer. The British Journal of Radiology. 2012;85 Spec No 1(Spec Iss 1):S3–17.
6. Kretschmer A, Tilki D. Biomarkers in prostate cancer - Current clinical utility and future perspectives. Crit Rev Oncol Hematol. 2017;120:180–93.
7. Bratan F, Niaf E, Melodelima C, Chesnais AL, Souchon R, Mège-Lechevallier F, et al. Influence of imaging and histological factors on prostate cancer detection and localization on multiparametric MRI: a prospective study. Eur Radiol. 2013;23(7):2019–29.
8. Loeb S, Vellekoop A, Ahmed HU, Catto J, Emberton M, Nam R, et al. Systematic review of complications of prostate biopsy. Eur Urol. 2013;64:876–92.
9. Ukimura O, Coleman JA, de la Taille A, Emberton M, Epstein JI, Freedland SJ, et al. Contemporary role of systematic prostate biopsies: indications, techniques, and implications for patient care. Eur Urol. 2013;63(2):214–30.
10. Nitta S, Tsutsumi M, Sakka S, Endo T, Hashimoto K, Hasegawa

M, et al. Machine learning methods can more efficiently predict prostate cancer compared with prostate-specific antigen density and prostate-specific antigen velocity. Prostate Int. 2019;7(3):114–8.
11. Djavan B, Remzi M, Zlotta A, Seitz C, Snow P, Marberger M. Novel artificial neural network for early detection of prostate cancer. J Clin Oncol. 2002;20(4):921–9.
12. Ronco AL, Fernandez R. Improving ultrasonographic diagnosis of prostate cancer with neural networks. Ultrasound Med Biol. 1999;25(5):729–33.
13. Akatsuka J, Numata Y, Morikawa H, Sekine T, Kayama S, Mikami H, et al. A data-driven ultrasound approach discriminates pathological high grade prostate cancer. Sci Rep. 2022;12(860).
14. Loch T, Leuschner I, Genberg C, Weichert-Jacobsen K, Küppers F, Yfantis E, et al. Artificial neural network analysis (ANNA) of prostatic transrectal ultrasound. Prostate. 1999;39(3):198–204.
15. Lee HJ, Kim KG, Lee SE, Byun SS, Hwang SI, Jung SI, et al. Role of transrectal ultrasonography in the prediction of prostate cancer: artificial neural network analysis. J Ultrasound Med. 2006;25(7):815–21.
16. Lee HJ, Hwang SI, Han SM, Park SH, Kim SH, Cho JY, et al. Image-based clinical decision support for transrectal ultrasound in the diagnosis of prostate cancer: comparison of multiple logistic regression, artificial neural network, and support vector machine. Eur Radiol. 2010;20(6):1476–84.
17. Azizi S, Bayat S, Yan P, Tahmasebi A, Kwak JT, Xu S, et al. Deep recurrent neural networks for prostate cancer detection: analysis of temporal enhanced ultrasound. IEEE Trans Med Imaging. 2018;37(12):2695–703.
18. Wildeboer RR, Mannaerts CK, van Sloun RJG, Budäus L, Tilki D, Wijkstra H, et al. Automated multiparametric localization of prostate cancer based on B-mode, shear-wave elastography, and contrast-enhanced ultrasound radiomics. Eur Radiol. 2020;30(2):806–15.
19. Hassan R, Islam F, Uddin Z, Ghoshal G, Hassan MM, Huda S, et al. Prostate cancer classification from ultrasound and MRI images using deep learning based explainable artificial intelligence. Future Gener Comput Syst. 2022;127:462–72.
20. Lorusso V, Kabre B, Pignot G, Branger N, Pacchetti A, Thomassin-Piana J, et al. External validation of the computerized analysis of TRUS of the prostate with the ANNA/C-TRUS system: a potential role of artificial intelligence for improving prostate cancer detection. World J Urol. 2023;41(3):619–25.
21. Noorbakhsh-Sabet N, Zand R, Zhang Y, Abedi V. Artificial Intelligence Transforms the Future Healthcare. Am J Med. 2019;132(7):795–801.
22. Alaloul WS, Qureshi AH. Data processing using artificial neural networks. Dynamic data assimilation - beating the uncertainties. IntechOpen; 2020.
23. Carter HB. Differentiation of lethal and non-lethal prostate cancer: PSA and PSA isoforms and kinetics. Asian J Androl. 2012;14(3):355–60.
24. Pai RK, Van Booven DJ, Parmar M, Lokeshwar SD, Shah K, Ramasamy R, et al. A review of current advancements and limitations of artificial intelligence in genitourinary cancers. Am J Clin Exp Urol. 2020;8(5):152–62.
25. Shahid N, Rappon T, Berta W. Application of artificial neural networks in health care organizational decision-making: a scoping review. PLos One. 2019;14(2):e0212356.
26. Brattain LJ, Telfer BA, Dhyani M, Grajo JR, Samir AE. Machine learning for medical ultrasound: status, method, and future opportunities. Abdom Radiol (NY). 2018;43(4):786–99.
27. Alzubaidi L, Zhang J, Humaidi AJ, Al-Dujaili A, Duan Y, Al-Shamma O, et al. Review of deep learning: concepts, CNN architectures, challenges, applications, future directions. J Big Data. 2021;8(1):53.
28. Li B, He Y. An attention mechanism oriented hybrid CNN-RNN deep learning architecture of container terminal liner handling conditions prediction. Comput Intell Neurosci. 2021;2021: 3846078.
29. Uddin S, Khan A, Hossain ME, Moni MA. Comparing different supervised machine learning algorithms for disease prediction. BMC Med Inform Decis Mak. 2019;281(19):281.
30. Juarez-Orozco LE, Martinez-Manzanera O, Nesterov SV, Kajander S, Knuut J. The machine learning horizon in cardiac hybrid imaging. European J Hybrid Imaging. 2018;15(2):1–15.
31. Dhawale CA, Dhawale K. Current trends in deep learning frameworks with opportunities and future prospectus. Adv Electr Comput Eng. 2020;63–77.
32. Mottet N, van den Bergh RCN, Briers E, Van den Broeck T, Cumberbatch MG, De Santis M, et al. EAU-EANM-ESTRO-ESUR-SIOG guidelines on prostate cancer-2020 update. Part 1: screening, diagnosis, and local treatment with curative intent. Eur Urol. 2021;79(2):243–62.
33. de Rooij M, Hamoen EH, Witjes JA, Barentsz JO, Rovers MM. Accuracy of magnetic resonance imaging for local staging of prostate cancer: a diagnostic meta-analysis. Eur Urol. 2016;70(2):233–45.
34. Rabaan AA, Bakhrebah M A, AlSaihati H, Alhumaid S, Alsubki RA, Turkistani SA, et al. Artificial intelligence for clinical diagnosis and treatment of prostate cancer. Cancers. 2022;14(22):5595.
35. Khanna NN, Maindarkar MA, Viswanathan V, Fernandes JFE, Paul S, Bhagawati M, et al. Economics of artificial intelligence in healthcare: diagnosis vs. treatment. Healthcare (Basel). 2022;10(12):2493.

Case Report/Series

Quadrigeminal plate arachnoid cyst presenting with eye movement related migraine: a rare case report

Yemima Graciela[1], Robert Shen[2,3], Mardjono Tjahjadi[4]

pISSN: 0853-1773 • eISSN: 2252-8083
https://doi.org/10.13181/mji.cr.236858
Med J Indones. 2023;32:129–36

Received: March 11, 2023
Accepted: September 06, 2023

Authors' affiliations:
[1]Faculty of Medicine, Universitas Tarumanagara, Jakarta, Indonesia, [2]Atma Jaya Neuroscience Research (ANR), Master Study Program in Biomedical Sciences, School of Medicine and Health Sciences, Universitas Katolik Indonesia Atma Jaya, Jakarta, Indonesia, [3]Bunda Pengharapan Hospital, Papua, Indonesia, [4]School of Medicine and Health Sciences, Universitas Katolik Indonesia Atma Jaya, Jakarta, Indonesia

Corresponding author:
Mardjono Tjahjadi
School of Medicine and Health Sciences, Universitas Katolik Indonesia Atma Jaya, Jalan Pluit Raya No. 2, North Jakarta 14440, DKI Jakarta, Indonesia
Tel/Fax: +62-21-6691944/ +62-21-6606122
E-mail: mardjono.tjahjadi@atmajaya.ac.id

This online publication has been corrected. The corrected version first appeared on December 22, 2023.

ABSTRACT

Type II arachnoid cyst of the quadrigeminal cistern is the rarest type of arachnoid cyst (10% prevalence) in adults and is generally asymptomatic. We reported an unusual case of chronic right-sided migraine provoked by right eye adduction, right eye adduction soreness, and dry eye symptoms in a 47-year-old woman with quadrigeminal arachnoid cyst confirmed by radiological findings with the compression of the tectal plate, vermis, and superomedial cerebellum's part. She was treated conservatively without improvement for 1 year before surgical intervention was conducted. Microsurgery for cyst excision and fenestration was done, followed by immediate relief from all her complaints after 3 months of follow-up. These findings should help clinicians consider surgical intervention for patients with chronic symptoms related to nerve function that have no improvement with the initial treatment.

KEYWORDS arachnoid cysts, eye movement, microsurgery, migraine disorder

Arachnoid cysts are non-neoplastic cerebrospinal fluid (CSF)-filled cysts lined with the arachnoid layer of the brain. The etiology of arachnoid cysts is yet to be determined. However, according to one theory, these cysts arise from abnormal formation of the arachnoid layer of the brain during embryogenesis and have been associated with a history of head trauma, surgery, intracranial hemorrhage, or infection.[1]

Arachnoid cysts are more common in men than women, with a lifetime prevalence of 1.4%. They are generally found in the middle cranial fossa, with a prevalence of 34%, or occur as retrocerebellar cysts, accounting for 33% of all arachnoid cysts.[2,3] Arachnoid cysts in the quadrigeminal cistern have a prevalence of 5% in children and 10% in adults and are usually asymptomatic, with only 10% of arachnoid cysts being symptomatic.[1,4,5]

Quadrigeminal arachnoid cysts are classified into the following three types: (1) type I with supratentorial and infratentorial extensions; (2) type II, when the location of the cyst is only infratentorial, mainly supracerebellar or supraretrocerebellar; and (3) type III, when the cyst has a lateral extension toward the temporal lobe.[6] Garg et al[7] reported that only four out of 18 cases of quadrigeminal arachnoid cysts were type II. Similarly, Cinalli et al[8] found only two cases of type II cysts among 14 patients with quadrigeminal cysts over a 13-year period. This suggests that type II

quadrigeminal arachnoid cysts are one of the rarest arachnoid cysts. To date, no multicenter studies have reported the prevalence of the three types of quadrigeminal arachnoid cysts.[1,7–9] We report a case of a 47-year-old woman with quadrigeminal cistern arachnoid cyst type II who presented with right-sided migraine accompanied by soreness and dryness of the right eye.

CASE REPORT

A 47-year-old Asian woman complained of a right-sided migraine for the past 1 year that was intermittent, chronically progressive, and almost disabling, affecting her daily routine and working ability. The migraine was often provoked by adduction of the right eye and was accompanied by soreness and dryness of the eye. She was referred to an ophthalmologist, who diagnosed multiple chalazia in the right eye. Surgical excision of all chalazia was performed to relieve her symptoms. However, 1 month after the chalazion excision, there was still no improvement in the migraine, eye soreness, and dryness. She was initially treated with minor tranquilizers and various painkillers, which slightly alleviated her symptoms.

Non-contrast head computed tomography (CT) showed a hypodense lesion of size 3.66 cm × 2.24 cm × 2.1 cm with attenuation of the CSF at the quadrigeminal cistern, which extends into the superior part of the cerebellum and compresses the tectal plate, superior vermis, and superomedial portion of the cerebellar hemisphere. Due to worsening symptoms, she was referred to a neurosurgeon (MT). Physical examination revealed impaired right eye adduction;

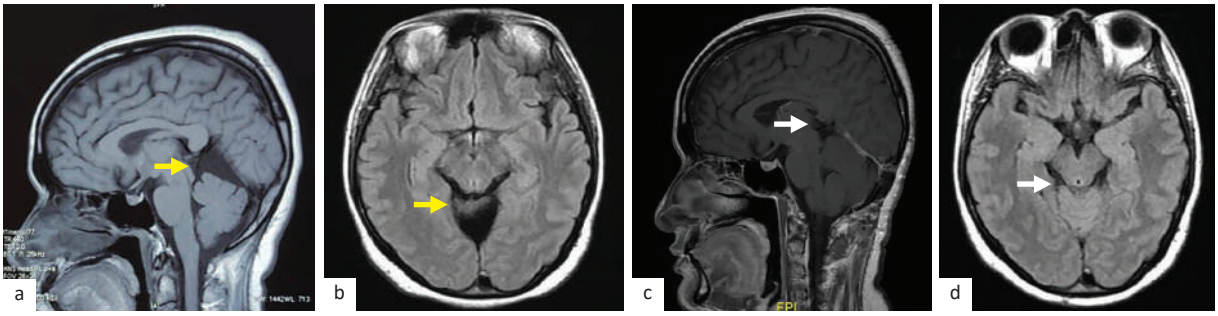

Figure 1. Preoperative non-contrast brain MRI of sagittal (a) and axial (b) views showing a hypointense lesion with a well-defined margin in T1WI that compressed cerebellar roof and tectal plate. An infratentorial extension confirmed the head CT findings of a type II quadrigeminal arachnoid cyst (yellow arrows) compared with the postoperative follow-up of the head MRI without contrast of sagittal (c) and axial (d) views that showed a complete resolution of the arachnoid cyst and a significant cerebellar roof decompression (white arrows). CT=computed tomography; MRI= magnetic resonance imaging; T1W1=T1-weighted images

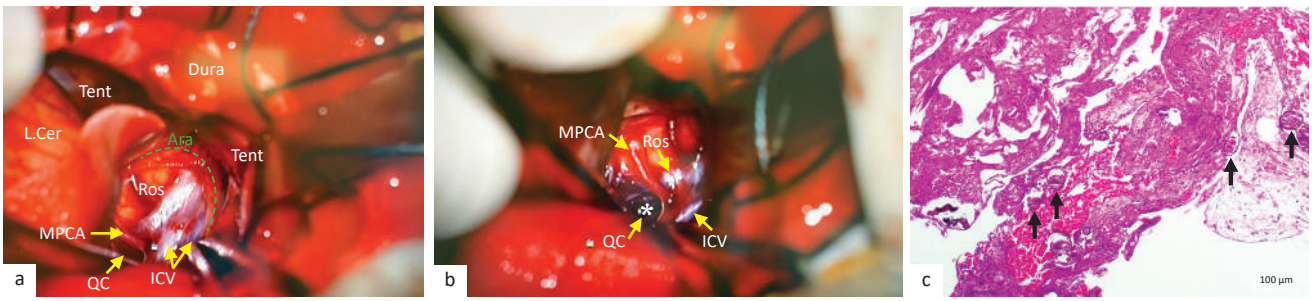

Figure 2. Arachnoid cyst. (a) Intraoperative findings at supracerebellar space showing the quadrigeminal supracerebellar area after some cyst walls removal with a microscope tilting inferolateral toward the brainstem and ambient cistern. The flap of the dura mater was mobilized superiorly to widen the surgical corridor. The remaining thick arachnoid cyst (green dashed line) was still visible at the level of incisura tentorium. In addition, the left side basal vein of Rosenthal and bilateral internal cerebral veins were visible and became the deepest border of the surgical dissection; (b) a more inferolateral tilting microscope aiming to fenestrate to the ambient cistern. The remaining arachnoid cyst wall shown in Figure 2a had already been removed; (c) histopathological examination results of the H&E stained cyst wall (200× magnification) showing a degenerative cyst wall without epithelial lining cells, several foci of calcification were present (black arrows). Ara=arachnoid cyst; Dura=dura mater of the posterior fossa; H&E=hematoxylin and eosin; ICV=internal cerebral veins; L.Cer=left cerebellum; MPCA=medial posterior choroidal artery; QC=quadrigeminal cistern toward quadrigeminal plate; Ros=basal vein of Rosenthal; Tent=tentorium. *Fenestration to the ambient cistern

eye movement was stalled and painful. The right-sided eye soreness was exacerbated when she performed eye adduction; otherwise, the other examinations were within normal limits. Brain magnetic resonance imaging (MRI) revealed a hypointense lesion in the supracerebellar area, confirming the findings of the head CT scan (Figure 1, a and b).

Cyst excision and fenestration to the surrounding basal cistern were performed by MT. The patient underwent microsurgery using the supracerebellar infratentorial (SCIT) technique while in the prone position. Meticulous arachnoid dissection was performed to access the superior cerebellar area and the cyst located in the quadrangular cistern under high magnification using a surgical microscope. All cerebellar bridging veins were preserved. Once the cyst wall was found, micro scissors were used to open and remove the cyst, followed by fenestration of the surrounding ambient cistern to ensure normal CSF flow. A hemostatic agent was used to manage minor post-dissection bleeding (Figure 2).

The surgery was successful and without any complications, and the patient experienced immediate relief from her chief complaints of migraine, right eye adduction soreness, and dry eye. She was hospitalized for 4 days and discharged with a modified Rankin Scale (mRS) score of 1 due to slight dizziness. Histological examination revealed a degenerative cyst wall with calcified foci (Figure 2).

Her condition had improved during the outpatient follow-up visit 2 weeks after surgery, with an mRS score of 0. Compared with the preoperative brain MRI, brain MRI performed after 3 months with gadolinium-diethylenetriamine pentaacetic acid contrast showed complete resolution of the quadrigeminal cistern arachnoid cyst and no further compression of the superior vermis and superomedial cerebellar hemisphere (Figure 1, c and d).

Written informed consent for the medical procedures and publication of this case report and accompanying images had been obtained from the patient. All ethical principles for medical research established by the hospital were followed.

DISCUSSION

During the last 30 years, only 38 cases of symptomatic quadrigeminal cistern arachnoid cysts have been reported (Table 1).[7,10–27] Of these, only 15 had visual disturbances as one of the main complaints. These complaints included decreased visual acuity, diplopia, nystagmus, worsening of eye vision, Parinaud's syndrome in the form of supraduction eye movement paralysis, and spasms of the orbicularis oculi muscle.[8,11–13] To the best of our knowledge, type II quadrigeminal cyst presenting with migraine related to eye adduction, eye adduction soreness, and dry eye has not been reported previously.

In early life, quadrigeminal cysts often cause hydrocephalus by compressing the aqueduct of Sylvius. Compared to cysts in other locations, cysts in the quadrigeminal cistern tend to cause symptoms because of obstructive hydrocephalus.[2] However, quadrigeminal cyst is commonly an incidental finding because it is usually asymptomatic. If symptomatic, the symptoms are usually nonspecific, such as headache, lethargy, nausea, vomiting, gait ataxia, papilledema, and visual disturbance.[1,5,25,28] Rarely, typical clinical signs may develop, such as impaired posture, nystagmus, diplopia, Parinaud's syndrome, hearing loss, hemiparesis, body spasticity, and weakness of the lateral rectus muscle of the eye.[5,25]

As many as 50% of patients with quadrigeminal arachnoid cysts are under 18 years of age and show signs of hydrocephalus in the form of developmental delays. In the present case, the clinical signs of eye adduction soreness were probably due to pressure on the superior vermis and tectal plate. The underlying mechanism may involve: (1) compression of the cerebellar vermis cortex, especially lobes VI and VII (declive, folium, and tuber), also referred to as the oculomotor vermis, which is responsible for initiating saccadic movement, projecting inhibitory signals to stop the gaze accurately at the target during saccadic movement, and calibrating saccadic amplitude, direction, and horizontal alignment of the eye;[29–31] (2) compression of the tectal plate, the deepest layer of the superior colliculus, which plays an essential role in the eye's motor function. The superior colliculus projects saccadic motion stimuli to the tegmentum and controls the oculocephalic reflex and gaze shift.[32] Hence, compression of these two anatomical structures may cause limited eye movement, eventually generating soreness and headaches.

Another interesting clinical presentation in our patient was chronic dry eye, which was relieved after cyst resection. The mechanism was unclear, but we believed that removing the cyst eventually released

Table 1. Adult symptomatic quadrigeminal cistern arachnoid cysts case report in the last 30 years

First author, year	Age/ sex	Clinical presentations	Radiologic findings	1st surgical procedure	2nd surgical procedure	Postoperative complications	Follow-up (months)	Outcomes
Garg,[7] 2015	34/F	Headache, gait ataxia, and vision diminution	Supratentorial extension of the cyst	ETV	Shunt followed by shunt revision	Pseudomeningocele	24	~
	22/F	Headache and vomiting	Supratentorial and infratentorial extension of the cyst	ETV	NA	NA	44	↑
	24/M	Parinaud's syndrome and ataxia	Supratentorial and infratentorial extension of the cyst and compression of the dorsal midbrain	Endoscopic ventriculostomy	Shunt	Intraoperative bleeding during endoscopic ventriculostomy	16	~
	22/F	Headache and vision diminution	Supratentorial and infratentorial extension of the cyst	Endoscopic ventriculostomy and ETV	NA	NA	27	↑
	50/F	Headache, gait ataxia, vision diminution, and Parinaud's syndrome	Supratentorial and infratentorial extension of the cyst and compression of the dorsal midbrain	Endoscopic ventriculostomy and ETV	NA	NA	12	↑
	28/M	Vision diminution, gait ataxia, and headache	Supratentorial and infratentorial extension of the cyst	Endoscopic ventriculostomy and ETV	NA	NA	6	↑
	19/M	Headache and vision diminution	Supratentorial and infratentorial extension of the cyst	Endoscopic ventriculostomy and cysto-cisternostomy	Shunt	NA	36	~
Silva,[10] 2022	33/F	Headache	Hydrocephalus	ETV	NA	Superficial skin infection	24	↑
	19/M	Headache and gait disturbance	Hydrocephalus	Endoscopic fenestration	NA	NA	60	↑
Takaki,[11] 2021	68/F	Intermittent spasms in the left orbicularis oculi and orbicularis oris muscles spasm as well as left upper and lower extremities cerebellar ataxia	Obstructed cerebral aqueduct and narrowing of the prepontine cistern with moderate ventriculomegaly and elongated left vertebral artery	Endoscopic ventriculostomy	NA	NA	NA	↑
Hayashi,[12] 1999	71/M	Gait instability, memory impairment, and disorientation	Supracollicular cyst, 3rd and lateral ventricle's anterior horn enlargement, and cerebellar vermis compression	ETV and ventricle-cystostomy	NA	NA	5	↑
Inamasu,[13] 2003	35/F	Headache	Hydrocephalus and infratentorial extension of the cyst	ETV and ventricle-cystostomy	NA	NA	6	↑
Gangemi,[14] 2005	45/F	Intracranial hypertension symptoms	NA	ETV and ventricle-cystostomy	NA	NA	NA	↑

Table continued on next page

Table 1. (continued)

First author, year	Age/ sex	Clinical presentations	Radiologic findings	1st surgical procedure	2nd surgical procedure	Postoperative complications	Follow-up (months)	Outcomes
Ohnishi,[15] 2007	62/F	Pain in 2nd division of right N V and papilledema	Infratentorial extension of the cyst and hydrocephalus	Ventriculo-cysto-cisternostomy	NA	NA	12	↑
Roka,[16] 2010	26/M	Migraine	Supratentorial and prepontine cistern extension of the cyst	Conservative treatment (carbamazepine)	NA	NA	12	Symptoms ↑, cyst size ~
Zanini,[17] 2013	66/F	Unsteady gait, headache, and cognitive impairment	Infratentorial extension of the cyst	Endoscopic fenestration	NA	Parinaud's syndrome	6	↑
Arakawa,[18] 2013	28/F	Headache and papilledema	Hydrocephalus and infratentorial extension of the cyst	ETV	NA	NA	12	↑
	26/F	Headache and nausea	NA	LVC and ETV	NA	NA	81	↑
	38/F	Headache and nausea	NA	LVC, third ventricle-cystostomy, and ETV	NA	NA	55	↑
Gui,[19] 2016	42/M	Headache, diplopia, and visual impairment	NA	LVC, third ventricle-cystostomy, and ETV	NA	NA	52	↑
	36/F	Headache and nausea	NA	LVC, third ventricle-cystostomy, and ETV	NA	NA	37	↑
	23/M	Nystagmus	NA	LVC and ETV	NA	NA	19	↑
	30/M	Headache, drowsiness, and ataxic gait	Infratentorial extension of the cyst	Third ventricle-cystostomy	NA	NA	70	↑
Yu,[20] 2016	19/M	Generalized convulsion and headache	Supratentorial and infratentorial extension of the cyst	Third ventricle-cystostomy	NA	NA	51	↑
	50/F	Headache and lassitude	Supratentorial and infratentorial extension of the cyst	ETV	NA	NA	64	↑
	35/M	Ataxic gait and visual complaints	Infratentorial extension of the cyst	Cysto-cisternostomy	NA	NA	50	↑
Yu,[20] 2016	26/F	Unsteady gait and visual complaints	Supratentorial and infratentorial extension of the cyst	ETV and third ventricle-cystostomy	NA	NA	65	↑
	20/F	Increased intracranial pressure	Supratentorial and infratentorial extension of the cyst	ETV and LVC	NA	NA	11	↑
Isaka,[21] 1995	37/M	Headache and visual impairment	Hydrocephalus	Ventriculoperitoneal shunt	NA	NA	NA	NA

Table continued on next page

Table 1. (continued)

First author, year	Age/ sex	Clinical presentations	Radiologic findings	1st surgical procedure	2nd surgical procedure	Postoperative complications	Follow-up (months)	Outcomes
Laviv,[22] 2017	31/F	Migraine, gait ataxia, cognitive impairment, and bilateral horizontal nystagmus	Supratentorial and infratentorial extension of the cyst and bilateral tonsil herniation	EVD and cystoperitoneal shunt	NA	NA	18	↑
Ohtsuka,[23] 1998	54/M	Trochlear nerve palsy (torsional diplopia) and mild truncal ataxia	3rd, 4th, and lateral ventricle enlargement, compression of the dorsal part of the brainstem, vermis cerebellar anterior, cisterna interpenduncularis, prepontine, and ambient	NA	NA	NA	NA	NA
Hayashi,[24] 2005	71/M	Ataxia	NA	NA	NA	NA	NA	NA
	54/F	Headache	NA	NA	NA	NA	NA	NA
Garg,[7] 2015	42/M	Headache and gait ataxia	Infratentorial extension of the cyst	Microsurgery cyst removal, ventricle-cystostomy, and cysto-cisternostomy	ETV	Air embolism hyponatremia	24	↑
	45/F	Headache and vision diminution	Infratentorial extension of the cyst	Midline suboccipital craniotomy with ventricle-cystostomy and cysto-cisternostomy	NA	NA	36	↑
Topsakal,[25] 2002	67/F	Lower cranial nerve paresis, pyramidal sign, respiratory disturbances, disorientation, and memory disturbances	Hydrocephalus, lateral extension, brainstem, tectal plate, cerebellum, and aqueduct compression, and lateral and 3rd ventricle dilation	Microsurgery cyst removal	NA	NA	18 days	↑
Wong,[26] 1996	42 /F	Right hemiparesis, dysarthria, dizziness, and hypesthesia	Supratentorial and infratentorial extension of the cyst	Microsurgery cyst removal and cysto-cisternostomy	NA	NA	18	↑
Sharifi,[27] 2013	52/F	Headache increased intracranial pressure signs.	Hydrocephalus and infratentorial extension of the cyst	Ventriculoperitoneal shunt, microsurgery cyst removal, and fenestration	Third ventriculostomy and third ventricle-cystostomy	Recurrence	28 days	↑

ETV=endoscopic third ventriculostomy; EVD=external ventricular drainage; F=female; LVC=lateral ventricle cystostomy; M=male; NA=not available; N V=trigeminal nerve. ~: unchanged; ↑: improved

the stretching and angulation of the ophthalmic branch (V1) of the trigeminal nerve (cranial nerve [CN] V). Previously, Hayashi et al[33] have also reported a relationship between quadrigeminal arachnoid cysts and CN V involvement. They suggested that trigeminal neuralgia was caused by stretching, angulation, and demyelination at the root entry zone by a quadrigeminal arachnoid cyst.

Microsurgical fenestration and excision of the quadrigeminal cyst using the SCIT technique were preferred, considering the clear evidence of cerebellar compression, cyst size, predominant infratentorial extension, and progressive worsening of the symptoms without hydrocephalus findings.[7,10,34] Microsurgery is preferred in type II quadrigeminal cysts without hydrocephalus, as sudden cyst decompression may invoke bleeding in the surrounding fragile neurovascular structures.[6,7,34] Bleeding can be more efficiently controlled with microsurgery than an endoscopic approach. The reported success rate of microsurgery (85%) is comparable to that of endoscopic fenestration (88.5%).[10,34]

In the present case, open surgery was preferred because of the degree of cyst wall removal required. A wide fenestration, with a minimum size of 10 to 15 mm, was made to reduce the possibility of cyst recurrence in the future.[1,34] Post-intervention cerebellar complications were minimized by preserving all the cerebellar bridging veins while avoiding coagulation to handle minor bleeding and using a hemostatic agent instead. The larger bridging veins, mainly located at the midline, must be preserved; however, some smaller bridging veins can be removed if they cover a limited surgical corridor.[34]

Intraoperative findings in the supracerebellar space showed the quadrigeminal supracerebellar area after removing some cyst walls with a microscope tilted inferolaterally toward the brainstem and ambient cistern. The remaining thick arachnoid cyst (green dashed line) was still visible at the level of the tentorium of the incisura. In addition, the left-side basal vein of Rosenthal and bilateral internal cerebral veins were visible and became the deepest border of the surgical dissection. Figure 2b shows an inferolateral tilting microscope aimed at fenestrating an ambient cistern. The remaining arachnoid cyst wall, shown in Figure 2a, had already been removed.

In conclusion, this was the first report of type II quadrigeminal arachnoid cyst presenting with migraine associated with eye adduction, eye adduction-induced eye soreness, and dry eye symptoms, which were immediately relieved after microsurgical cyst resection and fenestration. These findings may help clinicians consider surgical intervention in patients with chronic symptoms related to nerve function that do not improve with initial medical treatment.

Conflict of Interest

The authors affirm no conflict of interest in this study.

Acknowledgment

None.

Funding Sources

None.

REFERENCES

1. Mustansir F, Bashir S, Darbar A. Management of arachnoid cysts: a comprehensive review. Cureus. 2018;10(4):e2458.
2. Al-Holou WN, Terman S, Kilburg C, Garton HJ, Muraszko KM, Maher CO. Prevalence and natural history of arachnoid cysts in adults. J Neurosurg. 2013;118(2):222–31.
3. Samii M, Carvalho GA, Schuhmann MU, Matthies C. Arachnoid cysts of the posterior fossa. Surg Neurol. 1999;51(4):376–82.
4. Deopujari CE, Shaikh ST, Karmarkar VS, Sudke AY, Mohanty CB, Biyani NK. Experience with management of intracranial arachnoid cysts. J Neurol Surg A Cent Eur Neurosurg. 2021;82(1):43–52.
5. Choi SK, Starshak RJ, Meyer GA, Kovnar EH, Sty JR. Arachnoid cyst of the quadrigeminal plate cistern: report of two cases. AJNR Am J Neuroradiol. 1986;7(4):725–8.
6. Akutagawa K, Tamura G, Tsurubuchi T, Ishikawa E, Matsumura A, Inagaki T. Quadrigeminal arachnoid cyst with perinatal encephalocele. Childs Nerv Syst. 2020;36(7):1393–7.
7. Garg K, Tandon V, Sharma S, Suri A, Chandra PS, Kumar R, et al. Quadrigeminal cistern arachnoid cyst: a series of 18 patients and a review of literature. Br J Neurosurg. 2015;29(1):70–6.
8. Cinalli G, Spennato P, Columbano L, Ruggiero C, Aliberti F, Trischitta V, et al. Neuroendoscopic treatment of arachnoid cysts of the quadrigeminal cistern: a series of 14 cases. J Neurosurg Pediatr. 2010;6(5):489–97.
9. Spennato P, Ruggiero C, Aliberti F, Buonocore MC, Trischitta V, Cinalli G. Interhemispheric and quadrigeminal cysts. World Neurosurg. 2013;79(2 Suppl):S20.e1–7.
10. Silva MA, Chang H, Weng J, Hernandez NE, Shah AH, Wang S, et al. Surgical management of quadrigeminal cistern arachnoid cysts: case series and literature review. J Neurosurg Pediatr. 2022;29(4):427–34.
11. Takaki Y, Tsutsumi S, Teramoto S, Nonaka S, Okura H, Suzuki T, et al. Quadrigeminal cistern arachnoid cyst as a probable cause of hemifacial spasm. Radiol Case Rep. 2021;16(6):1300–4.
12. Hayashi N, Endo S, Tsukamoto E, Hohnoki S, Masuoka T, Takaku A. Endoscopic ventriculocystocisternostomy of a quadrigeminal cistern arachnoid cyst. Case report. J Neurosurg. 1999;90(6):1125–8.
13. Inamasu J, Ohira T, Nakamura Y, Saito R, Kuroshima Y, Mayanagi K, et al. Endoscopic ventriculo-cystomy for non-communicating hydrocephalus secondary to quadrigeminal cistern arachnoid cyst. Acta Neurol Scand. 2003;107(1):67–71.
14. Gangemi M, Maiuri F, Colella G, Magro F. Endoscopic treatment of quadrigeminal cistern arachnoid cysts. Minim Invasive Neurosurg. 2005;48(5):289–92.
15. Ohnishi YI, Fujimoto Y, Taniguchi M, Tsuzuki T, Taki T. Neuroendoscopically assisted cyst-cisternal shunting for

a quadrigeminal arachnoid cyst causing typical trigeminal neuralgia. Minim Invasive Neurosurg. 2007;50(2):124–7.
16. Roka YB, Nepal A. Unusual cause for unilateral headache: a quadrigeminal cistern arachnoid cyst. Ann Acad Med Singap. 2010;39(6):495–6.
17. Zanini MA, Rondinelli G, Fernandes AY. Endoscopic supracerebellar infratentorial parapineal approach for third ventricular colloid cyst in a patient with quadrigeminal cistern arachnoid cyst: case report. Clin Neurol Neurosurg. 2013;115(6):751–5.
18. Arakawa Y, Kita D, Ezuka I, Hayashi Y, Hamada J, Hayashi Y. Regression of cerebellar tonsillar descent and hydrocephalus after endoscopic third ventriculostomy in a patient with a quadrigeminal arachnoid cyst. Surg Neurol Int. 2013;4:142.
19. Gui S, Bai J, Wang X, Zong X, Li C, Cao L, et al. Assessment of endoscopic treatment for quadrigeminal cistern arachnoid cysts: a 7-year experience with 28 cases. Childs Nerv Syst. 2016;32(4):647–54.
20. Yu L, Qi S, Peng Y, Fan J. Endoscopic approach for quadrigeminal cistern arachnoid cyst. Br J Neurosurg. 2016;30(4):429–37.
21. Isaka T, Akai F, Kuroda R, Nakatani S, Taneda S. [The quadrigeminal giant cyst communicating with lateral ventricle as a cause of obstructive hydrocephalus: a case report]. CI Kenkyu. 1995;17:413–7. Japanese.
22. Laviv Y, Neto S, Kasper EM. Management of quadrigeminal arachnoid cyst associated with obstructive hydrocephalus: report on stereotactic ventricular - cystic stenting. Br J Neurosurg. 2019;33(4):418–21.
23. Ohtsuka K, Hashimoto M, Nakamura Y. Bilateral trochlear nerve palsy with arachnoid cyst of the quadrigeminal cistern. Am J Ophthalmol. 1998;125(2):268–70.
24. Hayashi N, Hamada H, Umemura K, Kurosaki K, Kurimoto M, Endo S. [Selection of surgical approach for quadrigeminal cistern arachnoid cyst]. No Shinkei Geka. 2005;33(5):457–65. Japanese.
25. Topsakal C, Kaplan M, Erol F, Cetin H, Ozercan I. Unusual arachnoid cyst of the quadrigeminal cistern in an adult presenting with apneic spells and normal pressure hydrocephalus--case report. Neurol Med Chir (Tokyo). 2002;42(1):44–50.
26. Wong CW, Lee ST, Lui TN, Wu T, WU LL. Fluctuating hemiparesis caused by a quadrigeminal arachnoid cyst: case report. Surg Neurol. 1996;45(2):193–5.
27. Sharifi G, Jahanbakhshi A. Quadrigeminal cistern arachnoid cyst treated by endoscopic ventriculocystostomy through the trigonal region. J Neurol Surg A Cent Eur Neurosurg. 2013;74 Suppl 1:e145–8.
28. White ML, M Das J. Arachnoid cysts. [updated 2022 Oct 3]. In: StatPearls [Internet]. Treasure Island (FL): StatPearls Publishing; 2022 Jan-. Available from: https://www.ncbi.nlm.nih.gov/books/NBK563272/.
29. Park IS, Lee NJ, Rhyu IJ. Roles of the declive, folium, and tuber cerebellar vermian lobules in sportspeople. J Clin Neurol. 2018;14(1):1–7.
30. Choi JH, Choi KD. Cerebellar control of saccades. Ann Clin Neurophysiol. 2013;15(2):37–41.
31. Kheradmand A, Zee DS. Cerebellum and ocular motor control. Front Neurol. 2011;2:53.
32. Ruchalski K, Hathout GM. A medley of midbrain maladies: a brief review of midbrain anatomy and syndromology for radiologists. Radiol Res Pract. 2012;2012:258524.
33. Hayashi Y, Takata S, Iizuka H. Endoscopic treatment for arachnoid cyst at the cerebellopontine angle presenting with bilateral trigeminal neuralgia: case report and literature review. Interdiscip Neurosurg. 2020;22:100815.
34. Campagnaro L, Bonaudo C, Capelli F, Della Puppa A. Microscope neuronavigation-guided microsurgical fenestration of quadrigeminal cistern arachnoid cysts: how I do it. Acta Neurochir (Wien). 2023;165(9):2561–5.

Basic Medical Research

Diversity of *Spa* gene between methicillin-resistant and methicillin-sensitive *Staphylococcus aureus* bacteria in a tertiary referral hospital, Indonesia

Sri Amelia[1], R. Lia Kusumawati[1], Ridwan Balatif[2], Tryna Tania[3], Lavarina Winda[4], Nadya Adlin Syamira[5]

pISSN: 0853-1773 • eISSN: 2252-8083
https://doi.org/10.13181/mji.oa.236862
Med J Indones. 2023;32:75–9

Received: March 13, 2023
Accepted: July 28, 2023
Published online: August 25, 2023

Authors' affiliations:
[1]Department of Microbiology, Faculty of Medicine, Universitas Sumatera Utara, Medan, Indonesia, [2]Faculty of Medicine, Universitas Sumatera Utara, Medan, Indonesia, [3]Whole Genome Sequence Laboratory, Department of Microbiology, Faculty of Medicine, Universitas Sumatera Utara, Medan, Indonesia, [4]Biomolecular Laboratory, Faculty of Medicine, Universitas Sumatera Utara, Medan, Indonesia, [5]Department of Biotechnology, Faculty of Science and Mathematics, Universitas Diponegoro, Semarang, Indonesia

Corresponding author:
Sri Amelia
Department of Microbiology, Faculty of Medicine, Universitas Sumatera Utara, Jalan Dr. Mansyur No. 5, Padang Bulan, Medan 20155, Indonesia
Tel/Fax: +62-61-8210555
E-mail: sriamelia@usu.ac.id

ABSTRACT

BACKGROUND Staphylococcal protein A *(spa)* typing is an effective and fast technique to identify the prevalence and spread of *Staphylococcus aureus* strains based on their *spa* gene profiles. The distribution of *spa* types will contribute to control the spread of *S. aureus*. Little is known regarding the *spa* types of *S. aureus* in Indonesia. This study aimed to investigate the diversity of *spa* gene among *S. aureus* carriage isolates in North Sumatra Province, Indonesia.

METHODS 79 *S. aureus* isolates consisting of 39 methicillin-resistant *S. aureus* (MRSA) and 40 methicillin-susceptible *S. aureus* (MSSA) carriage isolates were identified by VITEK2 Compact (BioMérieux, Indonesia) to detect *mecA* gene. All samples underwent *spa* typing and sequencing.

RESULTS *Spa* gene was detected among 31/39 (79%) of the MRSA isolates and 24/40 (60%) of the MSSA isolates. Most *spa* typing genes were identified between 350 and 400 base pair (bp). t258 and t852 were the most prevalence *spa* types among MRSA and MSSA isolates, respectively.

CONCLUSIONS Many MRSA and MSSA isolates encoded *spa* gene. The most genes detected were t258 and t852, identified in Germany and Portugal, respectively; while t18977 was initially identified in Malaysia. This result indicated a global spread of MRSA according to *spa* typing.

KEYWORDS bacterial typing techniques, *Staphylococcus aureus*, tertiary referral hospital

Staphylococcus aureus is a bacterium that often causes infections in the skin and soft tissue (furuncles, carbuncles, and cellulitis), as well as in the bones (osteomyelitis), lungs (pneumonia and empyema), blood (bloodstream infection), heart (endocarditis infective), gastrointestinal tract (gastroenteritis), and lining of the brain (meningitis). Morphologically, it is a cocci-shaped gram-positive bacterium arranged in clusters like grapes.[1] In 2019, *S. aureus* infection was the most common infection that caused death related to antimicrobial resistance in high-income countries and the Southeast Asian region.[2] According to Kuntaman et al,[3] there is an 8.1% incidence of methicillin-resistant *S. aureus* (MRSA) based on nose and throat swab results.

Virulence factors play a role in various infections caused by *S. aureus* bacteria, including cell wall-anchored (CWA) protein, a surface protein bounded to peptidoglycan. Protein A, the major group of CWA protein in the staphylococcal protein A (*spa*) gene, can bind to various ligands that result in different

effects, such as IgG fragment, IgM fragment antigen-binding, and tumor necrosis factor receptor 1. These bindings allow protein A to inhibit opsonization and phagocytosis, act as superantigen, and trigger inflammation. Additionally, protein A can bind to the von Willebrand factor and has a role in endovascular infection and endocarditis.[4]

To understand the epidemiology of *S. aureus*, both the methicillin-sensitive *S. aureus* (MSSA) and MRSA, molecular investigations of *S. aureus* strains are required. Molecular typing can assist in monitoring and limiting the spread of *S. aureus* in healthcare facilities. In clinical applications, it can be used to determine whether an episode or event of *S. aureus* infection is a relapse of the initial infection or a second infection from a different *S. aureus* strain.[5]

Among various molecular typing methods, single-locus sequence typing is the most effective and fastest way to differentiate *S. aureus* isolates. This technique is based on various sequences and the number of tandem repeats in the X region of the *spa* gene. These *spa* typing results are in good agreement with the results of pulsed-field gel electrophoresis.[6] Molecular *spa* typing studies in Indonesia are still limited and have never been performed in the North Sumatra Province. This study aimed to investigate the diversity of the *spa* gene in *S. aureus* isolates from patients with mucocutaneous infections in North Sumatra Province, provide information regarding epidemiological surveillance and public health tracing by *spa* typing, and identify MRSA and MSSA familial strains.

METHODS

Sample collection

Samples were collected from the isolates stored in our previous study.[6] A total of 79 isolate samples, consisting of 40 MSSA isolates and 39 MRSA isolates, were included. These samples were collected in 2021 from Adam Malik General Hospital. We began this study by isolating bacterial DNA, followed by examination using conventional polymerase chain reaction (PCR), electrophoresis, visualization, and DNA sequencing.

Bacterial DNA isolation

DNA was extracted from the bacterial cells using the Presto™ Mini gDNA Bacteria Kit (Geneaid, Taiwan). A total of 1×10^9 bacterial cell colonies were placed in a sterile 1.5 ml tube, centrifuged at 13,000 rpm for 1 min, and the supernatant was discarded. A volume of 200 µl of buffer was added to the tube (0.8 mg/200 µl of lysozyme had previously been added) and was vortexed. This mixture was then incubated at 37°C for 30 min, added 20 µl of proteinase K, and vortexed again. Subsequently, it was incubated again at 60°C for 10 min with an additional 200 µl genomic binding buffer in the tube and vortexed, followed by another incubation at 70°C for 10 min with an additional 200 µl absolute ethanol and vortexed again. The genomic depletion (GD) column was stringed into a collection tube, and the sample was inserted into a GD column series. Next, 400 µl of W1 buffer was added and centrifuged at 13,000 rpm for 30 sec; then, the liquid was discarded in a collection tube. The GD column was reassembled using the same collection tube, and 600 µl of wash buffer was added. The column was centrifuged again at 13,000 rpm for 30 sec, and the liquid was discarded from the collection tube. The GD column was reassembled and centrifuged for 3 min. The collection tube was discarded, and the GD column was transferred to a 1.5 ml tube. Then, 100 µl of elution buffer (previously heated to 70°C) was added and left for 3 min at room temperature. After centrifugation for 30 sec, the GD column was discarded. Tubes containing DNA were stored at –20°C. This assay was performed according to the Geneaid protocol.

Spa gene detection by conventional PCR

A PCR master mix was prepared by diluting GoTaq Green Master Mix 2X (Geneaid) with forward/reverse primers, nuclease-free water, and DNA templates. Initially, the samples were vortexed using a spindle for ± 10 sec. Then, the PCR mix was prepared with a mixture of GoTaq Green Master Mix 2X (Geneaid) (12.5 µl), 10 µM forward primer (1 µl), 10 µM reverse primer (1 µl), nuclease-free water (8.5 µl), and DNA template (2 µl), with a total mix volume of 25 µl for one sample. The PCR mix was transferred to a 1.5 ml tube, vortexed for homogeneity, and arranged on a 0.2 ml PCR cooling block tube. The 23 µl PCR mix was distributed into the PCR tubes, and 2 µl of DNA template was added to the PCR tube and spun down to reduce all reagents in the tube. PCR conditions in the thermal cycler were initially denatured at 94°C for 5 min, followed by denaturation at 94°C for 30 sec, annealing at 55°C for 30 sec, and extension at 72°C for 45 sec. This process was repeated 35 times. The final extension step was performed at 72°C for 5 min. PCR products were analyzed by

electrophoresis and visualization. This assay was performed according to the Geneaid protocol.

Electrophoresis and visualization

Initially, agarose gel electrophoresis was performed using 1 liter of Tris-acetate-EDTA (TAE) 1x buffer (100 ml TAE 10X + 900 ml distilled water). Next, 2 g of agarose was weighed to prepare a 2% agarose gel placed in an Erlenmeyer flask. Next, 100 ml of 1X TAE buffer solution was added. The solution was then heated until it boiled and became transparent. After cooling it down until warm, 1 µl of ethidium bromide was added and mixed thoroughly. The gel was poured into a caster and allowed to solidify for ± 30 min. TAE 1X buffer was then added, allowing the gel to submerge in the electrophoresis chamber. The PCR ladder for the marker was 100 base pairs (bp).

Next, 8 µl of PCR product was added to the agarose gel wells, and 5 µl of DNA ladder was added to the far left or right well. Results were visualized using the GelDoc tool (Bio-Rad, USA) and subsequently analyzed. Based on the PCR results, variations in the *spa* gene bands were categorized into five groups: <300, 300, 350, >400, and 500 bp. The target *spa* gene for both MRSA and MSSA was 350 bp long. Examples of the gel electrophoresis results are shown in Figures 1 and 2.

***Spa* typing sequencing**

The samples used for sequencing exhibited thick bands. Selection was carried out through discussions with three authors (SA, RLK, and RB). Fifteen samples of MRSA isolates and 15 samples of MSSA isolates were selected, whereas one ATCC sample of MSSA and MRSA (a total of 32 samples) was selected for sequencing. Region X of the *spa* gene was amplified by PCR using the primers 1095F (5-AGACGATCCTTCGGTGAGC-3) and 1517R (5-GCTTTTGCAATGTCATTTACTG-3).[7] Each 50 µl used 50 µl primer. Gene *spa* products were sent to the Apical Scientific Laboratory (Selangor, Malaysia). The *spa* gene results were entered into SeqSphere+ version 8.4 (http://spaserver.ridom.de/ [Ridom GmBH, Germany]) to analyze the *spa* type.[8]

RESULTS

The *spa* gene was detected in 31 MRSA (79%) and 24 MSSA isolates (60%). Based on the division of the bands, most MRSA bacteria (36%) had a *spa* gene length of 350 bp, whereas the majority of MSSA bacteria (38%) had a *spa* gene band length >400 bp (Table 1). One MSSA isolate (sample 17) showed two *spa* gene bands (Figure 3).

In the MRSA isolate group, several types of the *spa* genes were found, namely, two isolates for type t258 and one isolate each for types t1544, t148, t267, t050, t159, and t213. Three types of the *spa* genes

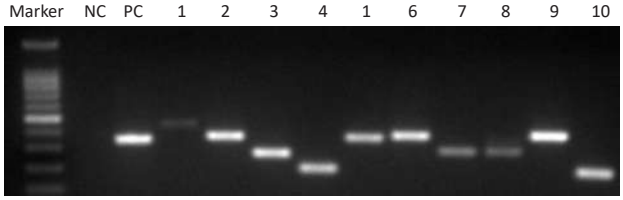

Figure 1. Gel electrophoresis results on MRSA isolates
MRSA=methicillin-resistant *Staphylococcus aureus*; NC=negative control; PC=positive control

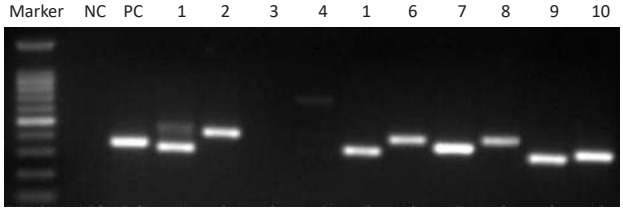

Figure 2. Gel electrophoresis results on MSSA isolates
MSSA=methicillin-susceptible *Staphylococcus aureus*; NC=negative control; PC=positive control

Table 1. *Spa* gene band length in isolates

Band (bp)	Frequency, n (%)	
	MRSA (N = 39)	MSSA (N = 40)
<300	3 (8)	0
300	8 (21)	3 (8)
350	14 (36)	7 (18)
>400	3 (8)	15 (38)
500	3 (8)	0

bp=base pairs; MRSA=methicillin-resistant *Staphylococcus aureus*; MSSA=methicillin-susceptible *Staphylococcus aureus*

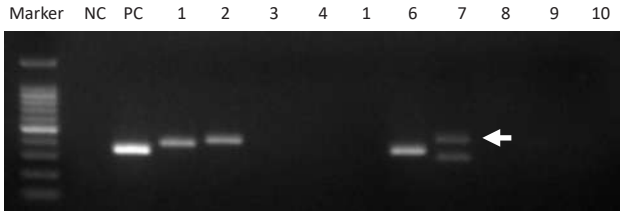

Figure 3. MSSA gel electrophoresis results, with the discovery of two bands on isolate number 17 (arrow)
MSSA=methicillin-resistant *Staphylococcus aureus*; NC=negative control; PC=positive control

were found in the MSSA isolates: t852 (five isolates), t701 (one isolate), and t18977 (one isolate). Owing to poor reliability, the remaining seven MRSA isolates and eight MSSA isolates did not show *spa* gene sequencing results.

DISCUSSION

In the present study, the *spa* gene was detected in 56 isolates (71%) of *S. aureus* (31 [79%] MRSA and 24 [60%] MSSA). In general, recent studies have revealed that approximately 63.5–97.5% of *S. aureus* bacteria have the *spa* gene. It was detected in 67.2–96.6% of MRSA isolates and 46.15–95% of MSSA isolates.[9–11] This study also revealed that one isolate had two bands of the *spa* gene in MSSA bacteria. This finding is in line with previous research reporting two *spa* gene bands in both MRSA and MSSA isolates.[11,12] *Spa* typing was used to study *S. aureus* familial strains. Although this method is not clinically significant, it is valuable for epidemiological tracing.

Based on data from https://*spa*.ridom.de/,[13] the seven types of the *spa* genes found in MRSA isolates were the gene types that have been detected in Indonesia for the first time. Previously, the gene types *spa* t1544 (two strains), t148 (one strain), t050 (one strain), and t159 (one strain) were detected in Indonesia (all in 2007), but in MSSA bacteria, not in MRSA bacteria as in this study. Only the t701 *spa* gene type was discovered in Indonesia out of the three types of the *spa* genes detected in MSSA isolates (2007). In 2019, Malaysian researchers identified a new type of the *spa* gene, t18977, in one strain.[13]

The lack of the *spa* gene in the *S. aureus* isolate might be explained by a mutation that prevented the *spa* primer from annealing to the target DNA, or by the fact that the isolate did not have the *spa* gene.[14] Baum et al,[14] conducted a study to analyze the non-*spa*-typeable in patients with invasive infections due to S. *aureus.* Sequencing of the *spa* locus revealed deletion mutations in the IgG-binding domain C, with only two strains showing unfavorable results. Despite lacking the *spa* gene, the bacteria remained virulent and caused invasive infections. In addition, the deficiency of forward *spa* primers in the IgG-binding region can lead to undetectable *spa* genes, making 1–2% of strains non-typeable.[16]

The majority of the *spa* gene band lengths in this study were 350 bp in MRSA isolates and >400 bp in MSSA isolates. In recent studies, MRSA bacteria have been shown to have a *spa* gene length of approximately 150–400 bp (the majority of the *spa* gene length is 300 bp),[13] but another study discovered that the length of the *spa* gene in *S. aureus* (MSSA and MRSA) ranged from 1,150 to 1,500 bp.[12] The sequencing results in this study showed that the dominant *spa* gene type was t258 and t852 in MRSA and MSSA bacteria, respectively. This study also identified the *spa* gene type t18977, which is the first to be identified in North Sumatra. Previously, Deurenberg et al[16] identified 62 MSSA isolates from 440 individuals in Yogyakarta and 37 different *spa* genes. Several types of *spa* genes were also found in this study, including the t701 type (in MSSA). Other *spa* gene types, such as t1544, t148, t050, and t159, were found in MSSA by Zukancic et al;[17] however, the present study found different *spa* gene types in MRSA. This difference might be due to the horizontal transfer of the genes between *S. aureus* bacteria (both MRSA and MSSA) or *S. aureus* bacteria and other *Staphylococcus* bacteria.[18]

Since December 22, 2022, *Spa*Server has discovered 20,838 *spa* gene types, with *spa* t032 being the most prevalent gene type globally (9.79%).[9] The dominant *spa* gene types in the Asian region are t030, t037, t002, t437, t1081, t004, t001, and t2460.[19] This type of *spa* gene represents a variety of tandem repeat sequences that often undergo polymerase staggering during DNA replication that are faster than most protein-encoding regions of the *S. aureus* genome. In addition, it is suspected that the variation in the *spa* type is a result of selection from the host immune system because the product of the *spa* gene is released as a virulence factor.[20] Although *spa* typing has no clinical impact, it can have an epidemiological impact. Two of the *spa* gene types identified were initially found in Germany and Portugal and then spread to China and Indonesia, while the newest one came from Malaysia before reaching Medan, a city destination for international travelers predominantly coming from Penang and Kuala Lumpur.

The *spa* gene encodes for protein A, a surface protein found in *S. aureus*. Protein A plays a role in the pathogenesis by binding to IgG. This will result in the bacteria being inaccessible to opsonins and could avoid phagocytosis.[14] Protein A can also act as a superantigen by binding to the V_H3 domain of the B cell receptor, triggering a disruption in the B cell response.[21] The expression of protein A can help colonize *S. aureus*

bacteria on the nose and skin surface.[22] The *spa* typing technique could allow sequencing of the X polymorphic region or short sequence repeats.

The limitations of this study were that not all *spa* genes were examined; the examined *spa* genes were selected based on the thickness of the *spa* band. Additionally, this study did not observe a clinical association in patients infected with *S. aureus* with the *spa* gene; therefore, we could not determine whether the *spa* gene's presence or absence affected the patient.

In conclusion, the number of detected *spa* genes in MRSA and MSSA isolates was 79% and 60%, respectively. Seven types of *spa* genes were identified in MRSA: t258, t1544, t148, t267, t050, t159, and t213, whereas three *spa* genes MSSA were identified: t852, t701, and t18977. The first *spa* gene detected in Indonesia was t18977.

Conflict of Interest

The authors affirm no conflict of interest in this study.

Acknowledgment

The authors are grateful to Nenni Dwi Aprianti Lubis who has helped to prepare administrative and funding matters from the college.

Funding Sources

This study was funded by Universitas Sumatera Utara through the TALENTA program with grant number 350/UN5.2.3.1/PPM/SPP-TALENTA USU/2021.

REFERENCES

1. Taylor TA, Unakal CG. *Staphylococcus aureus* infection. [Updated 2022 Jul 18]. In: StatPearls. Treasure Island (FL): StatPearls Publishing; 2023.
2. Antimicrobial Resistance Collaborators. Global burden of bacterial antimicrobial resistance in 2019: a systematic analysis. Lancet. 2022;399(10325):629–55.
3. Kuntaman K, Hadi U, Setiawan F, Koendori EB, Rusli M, Santosaningsih D, et al. Prevalence of methicillin resistant *Staphylococcus aureus* from nose and throat of patients on admission to medical wards of Dr Soetomo Hospital, Surabaya, Indonesia. Southeast Asian J Trop Med Public Health. 2016;47(1):66–70.
4. Arcenas RC. Molecular methods for healthcare-acquired infections. In: Coleman WB, Tsongalis GJ. Diagnostic molecular pathology: a guide to applied molecular testing. New York: Academic Press; 2017.
5. Hakimi Alni R, Mohammadzadeh A, Mahmoodi P. Molecular typing of *Staphylococcus aureus* of different origins based on the polymorphism of the *spa* gene: characterization of a novel *spa* type. 3 Biotech. 2018;8(1):58.
6. Amelia S, Wahyuni DD, Yunita R, Rozi MF. The active surveillance of *Staphylococcus aureus* using polymerase chain reaction-based identification method among hospitalized-patient of Haji Adam Malik General Hospital, Medan, Indonesia. Open Access Maced J Med Sci. 2021;9(A): 622–5.
7. Harmsen D, Claus H, Witte W, Rothgänger J, Claus H, Turnwald D, et al. Typing of methicillin-resistant *Staphylococcus aureus* in a university hospital setting by using novel software for *spa* repeat determination and database management. J Clin Microbiol. 2003;41(12):5442–8.
8. Ridom *Spa*Server. SpaServer database [Internet]. Ridom GmbH; [cited 2022 Dec 2022]. Available from: https://*spa*.ridom.de/index.shtml.
9. Kareem SM, Aljubori SS, Ali MR. Novel determination of *spa* gene diversity and its molecular typing among *Staphylococcus aureus* Iraqi isolates obtained from different clinical samples. New Microbes New Infect. 2020;34:100653.
10. Mohammed KAS, Abdulkareem ZH, Alzaalan AR, Yaqoob AK. *Spa* typing of *Staphylococcus aureus* isolated from clinical specimens from outpatients in Iraq. Pol J Microbiol. 2021;70(1):79–85.
11. Shakeri F, Shojai A, Golalipour M, Rahimi Alang S, Vaez H, Ghaemi EA. *Spa* diversity among MRSA and MSSA strains of *Staphylococcus aureus* in North of Iran. Int J Microbiol. 2010;2010:351397.
12. Omidi M, Firoozeh F, Saffari M, Sedaghat H, Zibaei M, Khaledi A. Ability of biofilm production and molecular analysis of *spa* and *ica* genes among clinical isolates of methicillin-resistant *Staphylococcus aureus*. BMC Res Notes. 2020;13(1):19.
13. Jones SU, Chua KH, Chew CH, Yeo CC, Abdullah FH, Othman N, et al. *spa* diversity of methicillin-resistant and -susceptible *Staphylococcus aureus* in clinical strains from Malaysia: a high prevalence of invasive European *spa*-type t032. PeerJ. 2021;9:e11195.
14. Baum C, Haslinger-Löffler B, Westh H, Boye K, Peters G, Neumann C, et al. Non-*spa*-typeable clinical *Staphylococcus aureus* strains are naturally occurring protein A mutants. J Clin Microbiol. 2009;47(11):3624–9.
15. Votintseva AA, Fung R, Miller RR, Knox K, Godwin H, Wyllie DH, et al. Prevalence of *Staphylococcus aureus* protein A (*spa*) mutants in the community and hospitals in Oxfordshire. BMC Microbiol. 2014;14:63.
16. Deurenberg RH, Beisser PS, Visschers MJ, Driessen C, Stobberingh EE. Molecular typing of methicillin-susceptible *Staphylococcus aureus* isolates collected in the Yogyakarta area in Indonesia, 2006. Clin Microbiol Infect. 2010;16(1):92–4.
17. Zukancic A, Khan MA, Gurmen SJ, Gliniecki QM, Moritz-Kinkade DL, Maddox CW, et al. Staphylococcal protein A (*spa*) locus is a hot spot for recombination and horizontal gene transfer in *Staphylococcus pseudintermedius*. mSphere. 2020;5(5):e00666–20.
18. Asadollahi P, Farahani NN, Mirzaii M, Khoramrooz SS, van Belkum A, Asadollahi K, et al. Distribution of the most prevalent *Spa* types among clinical isolates of methicillin-resistant and -susceptible *Staphylococcus aureus* around the world: a review. Front Microbiol. 2018;9:163.
19. Nübel U, Roumagnac P, Feldkamp M, Song JH, Ko KS, Huang YC, et al. Frequent emergence and limited geographic dispersal of methicillin-resistant *Staphylococcus aureus*. Proc Natl Acad Sci USA. 2008;105(37):14130–5.
20. Brignoli T, Manetti AGO, Rosini R, Haag AF, Scarlato V, Bagnoli F, et al. Absence of protein A expression is associated with higher capsule production in Staphylococcal isolates. Front Microbiol. 2019;10:863.
21. Hong X, Qin J, Li T, Dai Y, Wang Y, Liu Q, et al. Staphylococcal protein A promotes colonization and immune evasion of the epidemic healthcare-associated MRSA ST239. Front Microbiol. 2016;7:951.
22. Monaco M, Pimentel de Araujo F, Cruciani M, Coccia EM, Pantosti A. Worldwide epidemiology and antibiotic resistance of *Staphylococcus aureus*. Curr Top Microbiol Immunol. 2017;409:21–56.

Clinical Research

Prognostic value of neutrophil-to-lymphocyte ratio and fibrinogen levels in ovarian cancer

Roudhona Rosaudyn[1], Faradillah Mutiani[2], Indra Yuliati[1], Birama Robby Indraprasta[1]

pISSN: 0853-1773 • eISSN: 2252-8083
https://doi.org/10.13181/mji.oa.236880
Med J Indones. 2023;32:86–97

Received: March 23, 2023
Accepted: September 10, 2023
Published online: October 02, 2023

Authors' affiliations:
[1]Department Obstetrics and Gynecology, Faculty of Medicine, Universitas Airlangga, Dr. Soetomo General Hospital, Surabaya, Indonesia, [2]Faculty of Medicine, Universitas Airlangga, Dr. Soetomo General Hospital, Surabaya, Indonesia

Corresponding author:
Roudhona Rosaudyn
Department Obstetrics and Gynecology, Faculty of Medicine, Universitas Airlangga, Dr. Soetomo General Hospital, Jalan Mayjen Prof. Dr. Moestopo 47, Surabaya 60131, Indonesia
Tel/Fax: +62-31-5501640/ +62-31-5012632
E-mail: rosaudyn@gmail.com

ABSTRACT

BACKGROUND High neutrophil-to-lymphocyte ratio (NLR) and fibrinogen levels have been associated with mortality in several malignancies. However, the studies on the association between NLR or fibrinogen levels and ovarian cancer prognosis are inconsistent. This study aimed to investigate the prognostic roles of NLR and fibrinogen in ovarian cancer.

METHODS A systematic search of electronic databases was performed to analyze studies on the association of pre-treatment NLR and fibrinogen levels with overall survival (OS) and progression-free survival (PFS) among patients with ovarian cancer. The hazard ratio (HR) and corresponding 95% confidence intervals [CIs] were analyzed. All statistical analyses were done using RevMan version 5.4 (Cochrane, United Kingdom).

RESULTS A total of 7,312 patients from 27 studies were included. The median cut-off for high NLR was 3.6 for OS among 17 studies and 3.23 for PFS among 11 studies reporting an NLR HR. The median cut-off for fibrinogen levels was 4.0 in 9 studies reporting fibrinogen levels HR. High NLR was associated with lower OS (HR 1.35, 95% CI 1.18 to 1.55, $p<0.0001$, $I^2 = 76\%$) and PFS (HR 1.35, 95% CI 1.14 to 1.60, $p = 0.0005$, $I^2 = 71\%$). High fibrinogen levels were associated with lower OS (HR 1.44, 95% CI 1.14 to 1.82, $p = 0.002$, $I^2 = 81\%$) and PFS (HR 1.34, 95% CI 1.17 to 1.55, $p<0.0001$, $I^2 = 15\%$). This association occurred in all ovarian cancer types.

CONCLUSIONS High pre-treatment NLR and plasma fibrinogen levels were related to poor OS and PFS in ovarian cancer.

KEYWORDS meta-analysis, ovarian cancer, prognosis, progression-free survival, survival analysis

In 2020, ovarian cancer was the third most common gynecological cancer worldwide. Ovarian carcinoma accounts for over 90% of all ovarian cancers and is the deadliest gynecological cancer because it is often diagnosed at an advanced stage.[1] It is the foremost cause of death in patients with gynecological cancer and the fifth most common cause of death in women.[2]

The prognosis of ovarian cancer depends on the disease stage at diagnosis. The 5-year relative survival rate of patients with ovarian cancer is approximately 49%, mainly because at least half the patients are diagnosed with distant-stage disease.[3] In patients with advanced-stage ovarian cancer (stage IV), the 5-year survival rate falls to 17%, indicating a poor prognosis.[1,4] In women under 65 years of age, the rate is almost twice as high (61%) as in those aged 65 years and older (33%).[3] However, a better prognosis of ovarian cancer can be predicted by numerous favorable factors,

including younger age, good performance status, histological type other than clear cell or mucinous, well-differentiated tumor, early-stage tumor, smaller volume before debulking surgery, smaller residual tumor after primary cytoreductive surgery, BRCA1 or BRCA2 mutation carrier status, and lack of ascites.[5]

Cancer pathogenesis can be affected by inflammatory pathways. Hence, identifying the systemic inflammation status is a high priority.[6] Inflammation is a significant prognostic risk factor. Appropriate biological indicators, such as CA125, soluble cytokeratin, serum human kallikreins, serum cytokines, serum vascular endothelial growth factor, plasma D-dimer, and fibrinogen, may reflect the inflammatory state.[7] The neutrophil-to-lymphocyte ratio (NLR) is a marker of systemic inflammation assessed through a complete blood count examination, providing absolute neutrophil and lymphocyte counts.

A high pretreatment NLR is primarily associated with poor survival outcomes, based on several meta-analyses of patients with cancer.[6,8,9] In recent studies, plasma fibrinogen levels have been associated with tumor progression and poor prognosis in patients with several cancers. For example, increased plasma fibrinogen levels in hepatocellular carcinoma are independently associated with advanced disease stages and poor prognosis.[10] Other studies have also revealed that pretreatment with fibrinogen is a strong predictor of poor survival in gastric and digestive cancers with different traits.[11,12] Recent studies have revealed an association between the NLR or fibrinogen levels and ovarian cancer prognosis. However, these findings are varied. Therefore, this study aimed to investigate the prognostic roles of NLR and fibrinogen levels in ovarian cancer.

METHODS

Search strategy

This study followed the Preferred Reporting Items for Systematic Reviews and Meta-Analyses guidelines. A systematic literature search was performed using the PubMed and ScienceDirect databases for relevant studies published until July 7, 2023. The subsequent search phrases used were ("NLR ratio" OR "neutrophil-lymphocyte ratio" OR "Neutrophil to Lymphocyte ratio" OR "fibrinogen") AND ("ovarian cancer" OR "ovarian malignancy" OR "ovarian carcinoma" OR "cancer ovary" OR "carcinoma ovary").

Inclusion and exclusion criteria

Two investigators (RR and MF) independently identified all the articles. The included studies met all the following criteria: (1) studies in women with ovarian cancer that reported the prognostic effect of NLR and/or plasma fibrinogen; (2) NLR and/or plasma fibrinogen values collected before all treatments; (3) studies investigating the correlation of pretreatment NLR and/or fibrinogen levels with overall survival (OS) and/or progression-free survival (PFS); (4) studies with adequate data to evaluate the hazard ratio (HR) with a 95% confidence interval (CI); and (5) clinical trials, cohort, or case-control studies. The exclusion criteria were as follows: (1) overlapping or duplicate publications; (2) abstracts, reviews, letters, case reports, case series, editorials, and comments; (3) non-English studies; (4) non-human research; (5) unpublished trials; (6) studies presenting data in graphic form only (e.g., Kaplan–Meier curves) without reporting numerical HR values; and (7) full-text unavailability. Disagreements between the two researchers were resolved through discussion and consensus.

Data extraction

The following characteristics were extracted from each included study: name of the first author, year of publication, number of patients included in the analysis, mean or median age, disease stage, study design (prospective or retrospective), boundaries used to determine scores, high plasma NLR or fibrinogen levels, treatment gain, and HR with 95% CI for OS and/or PFS.

Quality assessment of primary study

The quality of the included studies was assessed using the Newcastle-Ottawa Quality Assessment Scale (NOS). An NOS score of more than five was considered high quality. Disagreements were resolved through discussion and consensus.

Statistical analysis

The extracted data were collected using the RevMan 5.4 software (Cochrane, United Kingdom). This analysis was conducted on all included studies for each relevant outcome. The main outcomes of interest were OS and PFS. HR estimates were pooled, weighted by generic inverse variance, and calculated using a random-effects model. Heterogeneity was evaluated

using Cochran's Q test and I^2 statistics. A random-effects model was used if significant heterogeneity was present (I^2>50% or Cochran's Q<0.1). Sensitivity analysis was performed to investigate the effect of omitting studies that could contribute to data heterogeneity, including studies that provided a multivariate HR or in which NLR or plasma fibrinogen levels were used as continuous variables. Predefined subgroup analyses were performed according to the disease stage and specific treatment. Disease stages were classified as per the International Federation of Gynecology and Obstetrics (FIGO) stages (I, II, III, and IV), and advanced stages referred to FIGO stages III and IV. Specific treatments were classified into surgery, chemotherapy, and mixed therapy (surgery and/or chemotherapy). Publication bias was assessed by visual inspection of funnel plots. All statistical tests were two-sided, and statistical significance was defined as p<0.05.

RESULTS

Extraction process and study characteristics

A total of 302 studies were identified using the search strategy. The initial search and study selection processes are presented in Figure 1. As a result, 27 studies published between 2009 and 2021, which included 7,312 patients, were included in this meta-analysis.

The majority of the patients included in the studies were above 50 years of age. Most ovarian cancers were of epithelial type. However, 15% of the 143 samples in the study by Wang et al[13] were non-epithelial ovarian cancers. Most ovarian cancers were classified as advanced stage III or IV based on the FIGO criteria. The studies used different cut-offs to classify high NLR (range 0.89 to 6.00) and high fibrinogen (range 3.63 to 4.85). The median cut-off for a high NLR was 3.6 for OS in 17 studies and 3.23 for PFS in 11 studies that reported an NLR HR. The median cut-off for high fibrinogen was 4.0 in nine studies reporting HR fibrinogen levels. The main characteristics of the included studies are summarized in Table 1.[13–39]

Characteristics of high NLR and high plasma fibrinogen

The pretreatment NLR and fibrinogen values were obtained from blood tests prior to the initial primary treatment in most studies, except for two studies[14,24] that included patients with recurrent disease and one study[21] that included patients with previous surgical treatment. Patients in eight studies[15,18,23,28,29,37–39] underwent surgical intervention or neoadjuvant chemotherapy (NACT), and patients in 13 studies[13,16,17,19,20,25–27,31–33,35,36] underwent primary surgery (primary staging or debulking surgery) with or without adjuvant chemotherapy as the initial intervention for treatment. Four studies[14,21,22,28] included patients who were treated with chemotherapy (Table 1).

Of the 5,018 patients in the studies evaluating NLR, 29.5% (1,482 patients) had high NLR levels, 74.0% (1,097 patients) were diagnosed with advanced-stage ovarian cancer, and the majority had serous carcinoma. Most patients with a high NLR were >50 years of age and had CA125 levels varying from <35 U/ml to 2,306 U/ml (Supplementary Table 1). High plasma fibrinogen levels were seen in 26.9% (618 of 2,294 patients in plasma

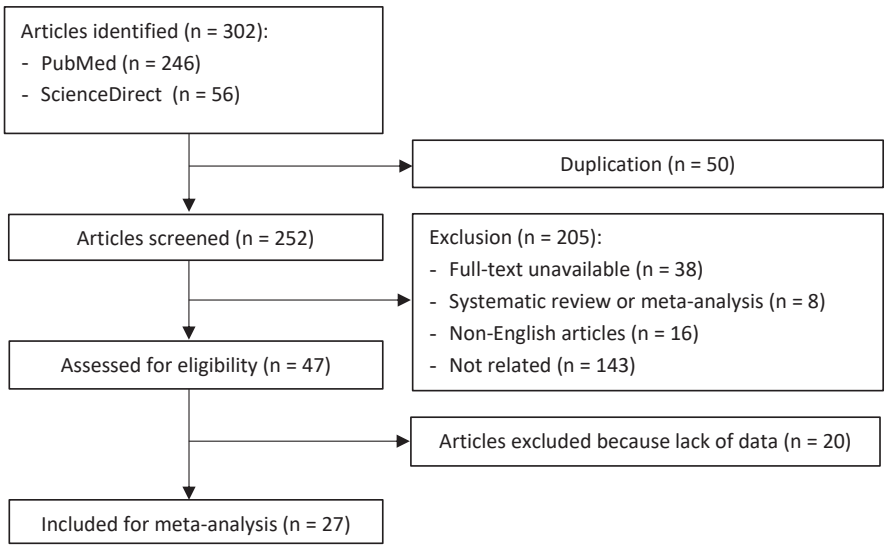

Figure 1. Flow chart of the study selection process

Table 1. Baseline characteristics of the included studies

First author, year	Study	Country	Outcomes	Cut-off	N	Duration of follow-up (months), median/ mean (range/SD)	Age (years), median/mean (range/SD)	FIGO stage, n (%)	Treatment strategy	NOS
NLR										
Henriksen,[14] 2020	Prospective cohort	Denmark	OS	≥4.1	69	19.3 (11.7–33.3)	69 (47–92)	NA	Chemotherapy	7
Marchetti,[15] 2021	Prospective cohort	Italy	PFS and OS	>4	397	24 (4–47)	60.2 (27–89)	1. III: 282 (71.8) 2. IV: 111 (28.2)	1. PDS: 76 (38.2%) 2. NACT: 123 (61.8%)	7
Asher,[16] 2011	Retrospective	United Kingdom	OS	>4	235	NA	62 (24–90)	1. I: 55 (23.4) 2. I: 28 (11.9) 3. III: 107 (45.5) 4. IV: 34 (14.5) 5. Missing: 11 (4.7)	Primary surgery	6
Komura,[17] 2018	Retrospective	Japan	PFS	≥4	344	NA	NA	1. I/II: 189 (54.9) 2. III/IV: 155 (45.1)	Primary surgery with/ without adjuvant chemotherapy	7
Wang,[13] 2016	Retrospective	China	PFS and OS	>3.43	143	NA	52.27 (14.09)	1. I/II: 54 (38) 2. III/IV: 89 (62)	Primary surgery	7
Baert,[18] 2018	Retrospective cohort	Belgium	PFS and OS	6	39	NA	NA	NA	PDS and NACT	6
Miao,[19] 2016	Retrospective	China	PFS and OS	>3.02	344	72 (61–97)	55 (45–84)	1. I/II: 168 (48.8) 2. III/IV: 176 (51.2)	Surgical staging or PDS and adjuvant chemotherapy	7
Zhou,[20] 2018	Retrospective	China	PFS and OS	>3.08	370	>10 years	54.3 (8.7)	IIIC	Surgery and adjuvant chemotherapy	7
Badora-Rybicka,[21] 2016	Retrospective	Poland	PFS and OS	0.89	315	NA	54 (22–77)	1. I: 61 (19.4) 2. II: 30 (9.5) 3. III: 186 (59) 4. IV: 38 (12.1)	Platinum-taxane regimen (after previous surgery)	6
Salman,[22] 2020	Retrospective cohort	Israel	OS	6	111	NA	NA	1. IIIC: 88 (79.3) 2. IV: 23 (20.7)	NACT 3–4 cycles then with/ without IDS	6
Jeerakornpassawat,[23] 2020	Retrospective	Thailand	OS	>3.38	306	NA	54.14 (9.72)	1. I: 92 (30.1) 2. II: 22 (7.19) 3. III: 129 (42.2) 4. IV: 18 (5.9)	1. NACT: 75 (24.5%) 2. Upfront surgery: 231 (75.5%) 3. Adjuvant chemotherapy	6
Cho,[24] 2009	Retrospective cohort	South Korea	OS	2.61	192	20.9	51.8 (12.9)	1. I/II: 59 2. III/IV: 125 3. Recurrence: 8	Elective surgery	8

Table continued on next page

Table 1. (continued)

First author, year	Study	Country	Outcomes	Cut-off	N	Duration of follow-up (months), median/ mean (range/SD)	Age (years), median/mean (range/SD)	FIGO stage, n (%)	Treatment strategy	NOS
Feng,[25] 2016	Retrospective	China	PFS and OS	>3.24	875	29 (1–115)	56 (30–90)	1. I/II: 75 (8.6) 2. III/IV: 800 (91.4)	PDS or primary staging with/without received platinum-based adjuvant chemotherapy	6
Wang,[26] 2015	Retrospective	China	PFS and OS	3.77	126	41.3 (3.3–70.4)	NA	1. I/II: 33 2. III/IV: 93	PDS or primary staging with/without received platinum-based adjuvant chemotherapy	7
Li,[27] 2017	Retrospective cohort	USA	OS	5.25	654	49.5 (0.1–175.3)	63 (28–93)	1. I: 87 (13.3) 2. II: 34 (5.2) 3. III: 416 (63.6) 4. IV: 117 (17.9)	PDS or primary staging with/without received platinum-based adjuvant chemotherapy	7
Kim,[28] 2018	Retrospective cohort	South Korea	PFS and OS	3.81 (OS) and 2.23 (PFS)	197	NA	57 (27–80)	1. IIIB: 7 (3.6) 2. IIIC: 45 (22.8) 3. IVA: 89 (45.2) 4. IVB: 56 (28.4)	NACT then underwent IDS	8
John-Olabode,[29] 2021	Retrospective cohort	Nigeria	PFS and OS	1.93	93	NA	47.1	1. I/II: 28 (30.2) 2. III/IV: 65 (69.8)	PDS and NACT	7
Williams,[30] 2014	Retrospective	USA	OS	NA	519	5.7 years (1 month–21 years)	NA	1. I: 150 (30) 2. II: 44 (9) 3. III: 266 (53) 4. IV: 42 (8)	NA	6
Fibrinogen										
Qiu,[31] 2012	Retrospective	China	OS	4.0	136	NA	44.42 (12.97)	1. I: 22 2. II: 26 3. III: 81 4. IV: 7	Primary surgical staging then platinum-based chemotherapy	7
Li,[32] 2019	Retrospective cohort	China	OS	3.63	186	NA	59.2 (51.1–65.9)	1. I/II: 52 (28.0) 2. III/IV: 134 (72.0)	Primary CRS	7
Polterauer,[33] 2009	Retrospective	Austria	OS	4.0	422	29.2 (25.1)	59.9 (13.9)	1. I: 88 2. II: 29 3. III: 252 4. IV: 53	Surgery and adjuvant chemotherapy	6
Hu,[34] 2020	Retrospective cohort	China	PFS and OS	4.0	104	NA	53 (37–81)	1. I/II: 23 2. III/IV: 81	NA	7

Table continued on next page

Table 1. (continued)

First author, year	Study	Country	Outcomes	Cut-off	N	Duration of follow-up (months), median/ mean (range/SD)	Age (years), median/mean (range/SD)	FIGO stage, n (%)	Treatment strategy	NOS
Feng,[35] 2016	Retrospective	China	PFS	4.0	724	29 (1–115)	56 (30–90)	1. I/II: 62 2. III/IV: 662	Primary staging or PDS with/without platinum-based adjuvant chemotherapy	6
Zhang,[36] 2015	Retrospective	China	OS and PFS	4.0	190	43 (2–164)	50.6 (11.1), (24–76)	1. I: 22 2. II: 31 3. III: 128 4. IV: 9	CRS and platinum-based adjuvant chemotherapy	7
Man,[37] 2015	Retrospective	China	PFS and OS	4.0	190	48 (2–150)	55 (25–8)	1. I/II: 89 2. III/IV: 101	1. PDS and adjuvant chemotherapy 2. NACT	7
Liu,[38] 2015	Retrospective	China	PFS	4.0	125	49 (5–85)	51 (25–73)	1. I/II: 39 2. III/IV: 86	1. CRS then adjuvant chemotherapy 2. NACT	7
Luo,[39] 2017	Retrospective cohort	NA	OS	4.852	217	44.5 (7–167.2)	54.4 (25–84)	1. IIIA: 3 (1.4) 2. IIIB: 15 (6.9) 3. IIIC: 149 (68.7) 4. IV: 50 (23)	NACT and non-NACT	7

CRS=cytoreductive surgery; FIGO=The International Federation of Gynecology and Obstetrics; IDS=interval debulking surgery; NA=not available; NACT=neoadjuvant chemotherapy; NLR=neutrophil-to-lymphocyte ratio; NOS=Newcastle-Ottawa Quality Assessment Scale; OS=overall survival; PFS=progression-free survival; PDS=primary debulking surgery; SD=standard deviation

fibrinogen studies), and 81.4% (503 patients) were diagnosed with advanced-stage ovarian cancer. Almost all the patients had serous epithelial ovarian cancer (Supplementary Table 1).

NLR and OS

Multivariate analysis demonstrated an association between an NLR greater than the cut-off value and a lower OS. In the subgroup analysis, a higher NLR was associated with lower OS in patients with ovarian cancer at all stages and at the advanced stage (Figure 2a). In addition, subgroup analyses based on the type of therapy administered revealed that patients with a higher NLR who underwent surgery and chemotherapy had a shorter OS (Supplementary Figure 1).

NLR and PFS

According to the multivariate analysis, an NLR higher than the cut-off was associated with a lower

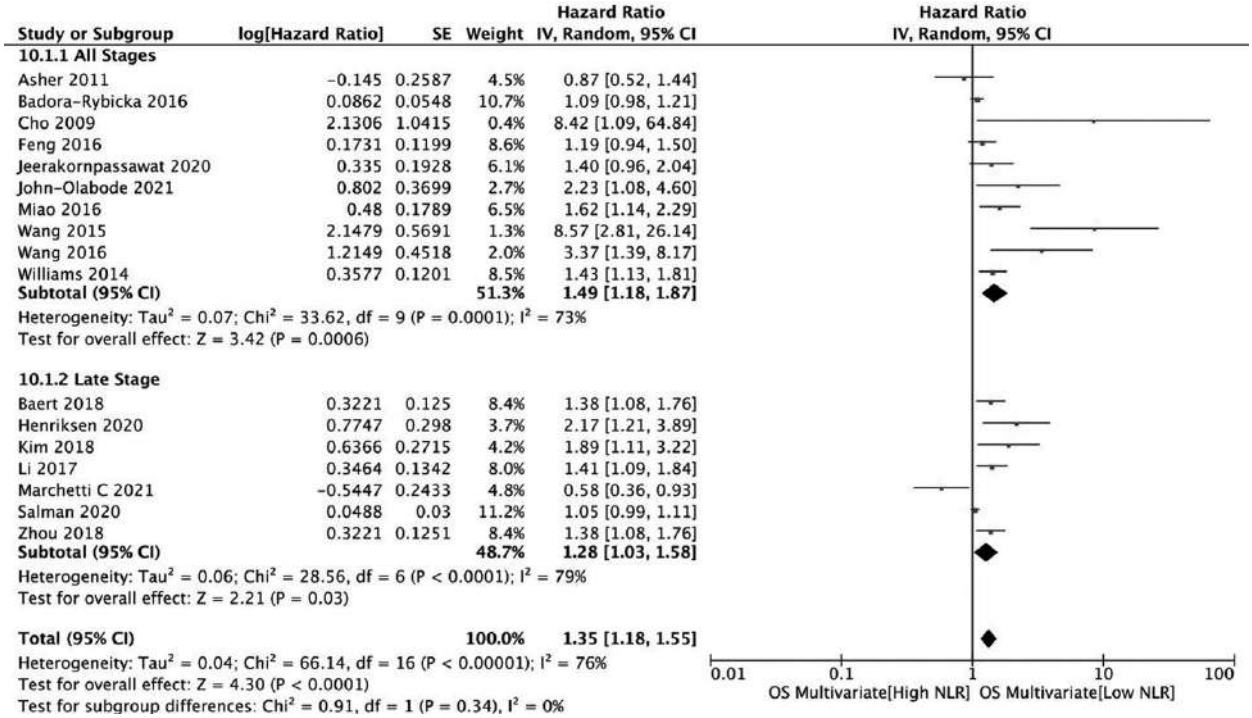

Figure 2. Forest plots showing HR of OS (a) and PFS (b) according to pretreatment NLR. CI=confidence interval; HR=hazard ratio; NLR=neutrophil-to-lymphocyte ratio; OS=overall survival; PFS=progression-free survival; SE=standard error

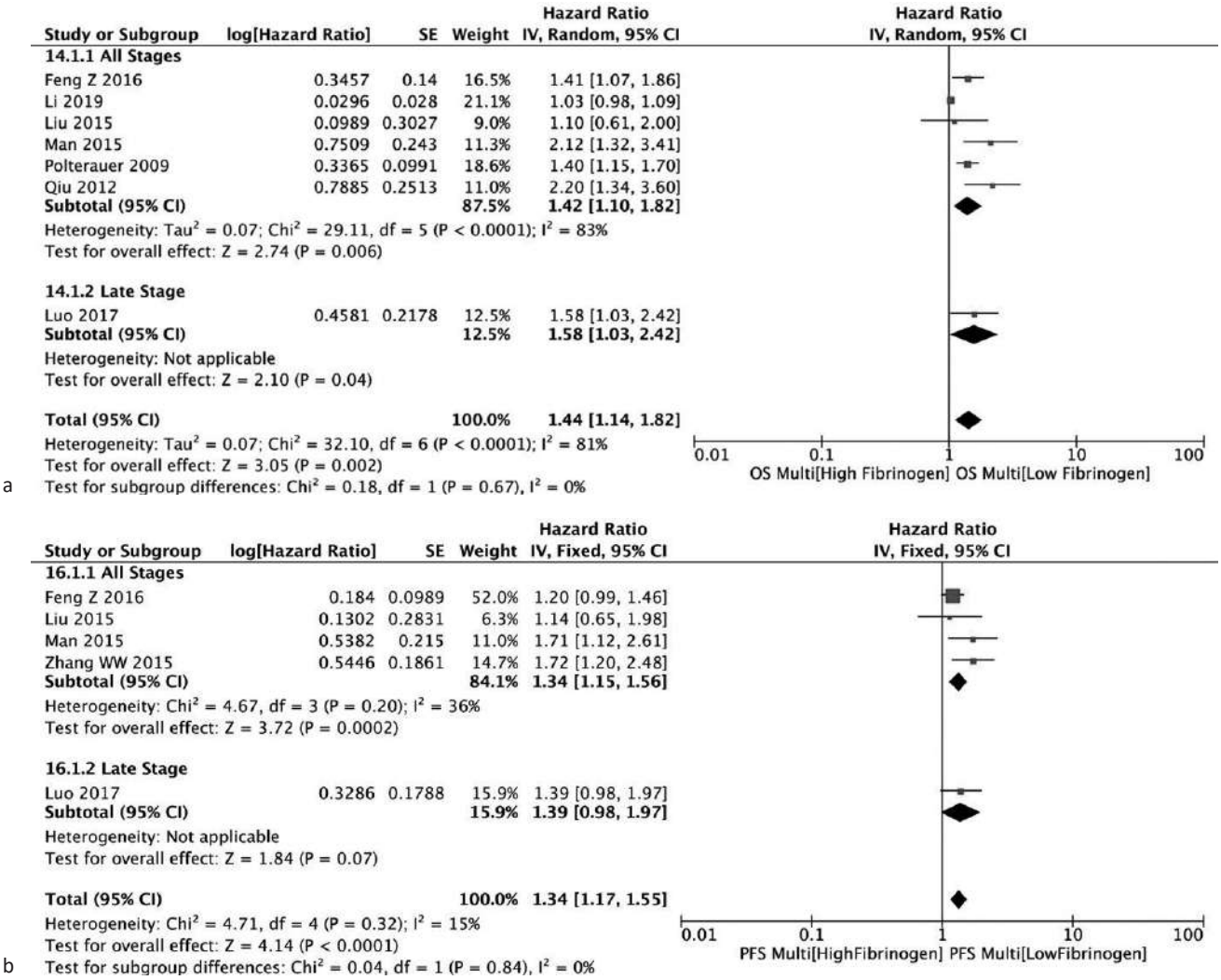

Figure 3. Forest plots showing HR of OS (a) and PFS (b) according to pretreatment fibrinogen level. CI=confidence interval; HR=hazard ratio; OS=overall survival; PFS=progression-free survival; SE=standard error

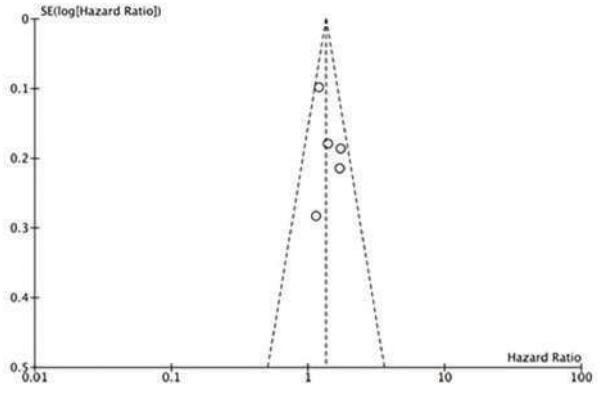

Figure 4. Funnel plots of HR of plasma fibrinogen according to the PFS in multivariate analyses (horizontal axis) and the SE for the HR (vertical axis). Each study is represented by one circle. The vertical line represents the pooled effect estimate. HR=hazard ratio; PFS=progression-free survival; SE=standard error

PFS. In subgroup analysis, a higher NLR was associated with shorter PFS in all stages of ovarian cancer (Figure 2b). Subgroup analysis based on the type of therapy administered revealed that patients with a higher NLR, both in those who underwent surgery and chemotherapy, had a lower PFS (Supplementary Figure 2).

Plasma fibrinogen level and OS

Multivariate analysis showed that plasma fibrinogen levels greater than the cut-off value were associated with a lower OS. According to the subgroup analysis, higher plasma fibrinogen levels were associated with lower OS in patients with ovarian cancer at all stages (Figure 3a) and in those who underwent surgical treatment (Supplementary Figure 3).

Plasma fibrinogen level and PFS

Fibrinogen levels greater than the cut-off were associated with lower PFS (Figure 3b) in patients who underwent surgical treatment (Supplementary Figure 4). In subgroup analysis, higher plasma fibrinogen levels were associated with lower PFS in patients with ovarian cancer at all stages.

Sensitivity analysis

A sensitivity analysis was performed to assess the effect of each study on the pooled HR. One study included in the pooled meta-analysis was omitted from each round of analysis. If the corresponding HR did not change significantly, this suggested that the meta-analysis results were credible (data not shown).

Publication bias

Funnel plots were used to evaluate publication bias. All NLR analyses exhibited asymmetric funnel plots, indicating a substantial publication bias. The funnel plots of the plasma fibrinogen analyses were asymmetric, except for the five-study analysis of plasma fibrinogen levels and PFS in ovarian cancer (Figure 4). Other funnel plots are shown in Supplementary Figures 5–7.

DISCUSSION

This meta-analysis pooled a large number of studies on the prognostic value of NLR and fibrinogen levels on OS and PFS in patients with ovarian cancer. Overall, higher NLR or plasma fibrinogen levels were associated with poor prognosis in patients with ovarian cancer. Patients with low NLR or plasma fibrinogen levels had higher OS and PFS despite heterogeneity. The prognostic effects of the NLR and plasma fibrinogen levels were reliable at all stages (FIGO stages I–IV) and advanced stages (FIGO stages III–IV). These results suggest that decreased NLR or plasma fibrinogen predicts a favorable prognosis in ovarian cancer, in agreement with a meta-analysis on pretreatment NLR or plasma fibrinogen and other cancer prognoses.[8,9,11,40,41] Analyses of sensitivity and publication bias indicated that our results were credible.

It is important to identify systemic inflammation status as the inflammatory pathway is known to play a role in many diseases, including cancer.[6] Inflammation is a hallmark of the development and progression of cancer.[42,43] Chronic inflammation has been suggested to cause the development of malignant tumors, which increases the probability of and accelerates mutations. Therefore, inflammation can affect the incidence, tumor stage, and development of cancer. Increasing evidence suggests an elevated systemic inflammatory response as an important indicator of cancer progression and prognosis.[44,45] Recent studies have shown that the interactions between tumor cells, immune cells, inflammatory cells, and interstitial components influence tumor metastasis.[43]

Various biochemical or hematological features routinely measured in general blood tests or as ratios derived from the measurements can be used to assess systemic inflammation. Previous studies have highlighted several ratios associated with morbidity and mortality, including NLR, platelet-to-lymphocyte ratio, lymphocyte-to-monocyte ratio, C-reactive protein/albumin ratio, and systemic immune-inflammation index.[44–46] However, most of these studies examined them as prognostic markers in patients newly diagnosed with cancer, even though this ratio has been associated with cancer risk and mortality.[44]

Lymphocytes, the primary antitumor response effectors, have prognostic and predictive values in cancer treatment.[22–24] The role of neutrophils in cancer is controversial, as they can either impede or promote tumor growth.[26,27] NLR, a marker of disease burden, was hypothesized to be an independent prognostic factor after adjusting for disease stage, metastatic site, and tumor markers.[10–12] However, data on blood parameters and the mechanical basis for the prognostic value of NLR remain unclear.[23,47] NLR is an affordable and promising index for cancer prognosis; however, some studies have shown conflicting results.[7,8,47–49]

Other markers of inflammation, such as plasma fibrinogen, are associated with tumor development and poor prognosis in several patients with cancer.[10,50] For example, studies on hepatocellular carcinoma,[10] gastrointestinal cancers of different types,[11] and gastric cancer[12] have revealed that elevated plasma fibrinogen levels before treatment are independently associated with poor prognosis or survival. Tumor growth, invasion, and distant metastasis are associated with coagulation disorders. Several studies have discussed the role of fibrinogen in cancer pathogenesis.[12–14] Fibrinogens can act as a platform to bind to tumor cells and platelets when they detach from the primary focus into the circulation,[14] contributing to tumor cell adherence to distant organs and facilitating tumor angiogenesis.

Evidence has shown that fibrinogen supplies nutrients and exchanges gases for the proliferation of tumor cells. Fibrinogen promotes tumor cell migration and protects cells from the innate immune system by acting as an extracellular matrix.[13] Zheng et al[51] reported that fibrinogen can accumulate and form dense fibrin layers around tumor cells, protecting them from natural killer cell-mediated cytotoxicity. Gropp et al[52] also found that fibrinogen breakup products repress immune reactions.

Based on the present meta-analysis, patients with low NLR and low plasma fibrinogen serum levels had greater OS and PFS. In a subgroup study of patients with ovarian cancer at any stage who were simultaneously receiving surgical treatment, those with lower OS and PFS had higher NLR and plasma fibrinogen levels. Moreover, multivariate analysis showed that a higher NLR was associated with lower OS and PFS in patients with ovarian cancer receiving chemotherapy. These results are similar to those of another study involving 2,919 patients, in which lower OS and PFS were found in the group with high NLR rates in multivariate and univariate analyses.[53] Luo et al[39] also showed that high plasma fibrinogen levels were associated with poor PFS and OS.

In contrast to the present study, a study on preoperative NLR in high-grade serous ovarian cancer found that high NLR was an independent predictor for PFS ($p = 0.011$) but not for OS ($p = 0.148$) in multivariate analysis.[25] A retrospective study in patients with ovarian cancer receiving NACT also stated that a high NLR was significantly associated with poor median OS ($p = 0.012$) but not significantly associated with median PFS ($p = 0.128$).[54] However, there is marked variability in the cut-off values of NLR among ovarian cancer studies.[49,54] Patients with a low NLR in the population have minimal systemic inflammation and better prognostic features, which may be the main reason why NLR lost prognostic significance in multivariate analysis.[54]

Some studies have added other prognostic scores such as combined NLR and fibrinogen levels (F-NLR) for different tumors, including non-small cell lung cancer,[40] esophageal squamous cell carcinoma,[41] and ovarian cancer,[55] with interesting results. Marchetti et al[55] revealed that patients with high F-NLR (NLR ≥3.24 and fibrinogen ≥450 mg/dl) had a significantly shorter PFS ($p = 0.023$) in ovarian cancer than patients with low F-NLR (NLR <3.24 and fibrinogen <450 mg/dl).

This study had several limitations. The varied cut-off values of NLR and plasma fibrinogen in several studies led to high heterogeneity. Additionally, there was publication bias in the NLR and plasma fibrinogen analyses. Some studies did not explicitly state the variables included in the multivariate model, thus generating uncertainty in interpreting the independent prognostic value of the NLR. Furthermore, only English articles were included, leading to language and publication biases. Most of the included studies were retrospective; therefore, additional clinical trials and research are essential to draw more accurate conclusions.

In conclusion, NLR and plasma fibrinogen levels were reliable indicators of ovarian cancer prognosis. These affordable tests are widely available at hospitals. The F-NLR score could also be a prognostic blood marker. However, these indicators could be affected by factors such as disease burden, age, and systemic inflammation. Further research is needed to understand the association between prognostic value and the combination of NLR and plasma fibrinogen levels.

Conflict of Interest
The authors affirm no conflict of interest in this study.

Acknowledgment
None.

Funding Sources
None.

REFERENCES

1. Huang J, Chan WC, Ngai CH, Lok V, Zhang L, Lucero-Prisno DE 3rd, et al. Worldwide burden, risk factors, and temporal trends of ovarian cancer: a global study. Cancers (Basel). 2022;14(9):2230.
2. Arora T, Mullangi S, Lekkala MR. Ovarian cancer. [updated 2023 Jun 18]. In: StatPearls [Internet]. Treasure Island (FL): StatPearls Publishing; 2023. Available from: https://www.ncbi.nlm.nih.gov/books/NBK567760/.
3. American Cancer Society. Cancer facts & figures 2022. Atlanta: American Cancer Society; 2022. p. 1–80.
4. Baldwin LA, Huang B, Miller RW, Tucker T, Goodrich ST, Podzielinski I, et al. Ten-year relative survival for epithelial ovarian cancer. Obstet Gynecol. 2012;120(3):612–8.
5. PDQ Adult Treatment Editorial Board. Ovarian epithelial, fallopian tube, and primary peritoneal cancer treatment (PDQ®): health professional version. 2023. In: PDQ Cancer Information Summaries. Bethesda (MD): National Cancer Institute (US); 2002.
6. Howard R, Kanetsky PA, Egan KM. Exploring the prognostic value of the neutrophil-to-lymphocyte ratio in cancer. Sci Rep. 2019;9(19673).
7. Chen G, Zhu L, Yang Y, Long Y, Li X, Wang Y. Prognostic role of neutrophil to lymphocyte ratio in ovarian cancer: a meta-analysis. Technol Cancer Res Treat. 2018;17:1533033818791500.
8. Gago-Dominguez M, Matabuena M, Redondo CM, Patel SP, Carracedo A, Ponte SM, et al. Neutrophil to lymphocyte ratio

and breast cancer risk: analysis by subtype and potential interactions. Sci Rep. 2020;10(1):13203. Erratum in: Sci Rep. 2020;10(1):20641.
9. Cupp MA, Cariolou M, Tzoulaki I, Aune D, Evangelou E, Berlanga-Taylor AJ. Neutrophil to lymphocyte ratio and cancer prognosis: an umbrella review of systematic reviews and meta-analyses of observational studies. BMC Med. 2020;18(1):360.
10. Zhang X, Long Q. Elevated serum plasma fibrinogen is associated with advanced tumor stage and poor survival in hepatocellular carcinoma patients. Medicine (Baltimore). 2017;96(17):e6694.
11. Lin Y, Liu Z, Qiu Y, Zhang J, Wu H, Liang R, et al. Clinical significance of plasma D-dimer and fibrinogen in digestive cancer: a systematic review and meta-analysis. Eur J Surg Oncol. 2018;44(10):1494–503.
12. Yu X, Hu F, Yao Q, Li C, Zhang H, Xue Y. Serum fibrinogen levels are positively correlated with advanced tumor stage and poor survival in patients with gastric cancer undergoing gastrectomy: a large cohort retrospective study. BMC Cancer. 2016;16:480.
13. Wang YQ, Jin C, Zheng HM, Zhou K, Shi BB, Zhang Q, et al. A novel prognostic inflammation score predicts outcomes in patients with ovarian cancer. Clin Chim Acta. 2016;456:163–9.
14. Henriksen JR, Nederby L, Donskov F, Waldstrøm M, Adimi P, Jakobsen A, et al. Prognostic significance of baseline T cells, B cells and neutrophil-lymphocyte ratio (NLR) in recurrent ovarian cancer treated with chemotherapy. J Ovarian Res. 2020;13(1):59.
15. Marchetti C, D'Indinosante M, Bottoni C, Di Ilio C, Di Berardino S, Costantini B, et al. NLR and BRCA mutational status in patients with high grade serous advanced ovarian cancer. Sci Rep. 2021;11(1):11125.
16. Asher V, Lee J, Innamaa A, Bali A. Preoperative platelet lymphocyte ratio as an independent prognostic marker in ovarian cancer. Clin Transl Oncol. 2011;13(7):499–503.
17. Komura N, Mabuchi S, Yokoi E, Kozasa K, Kuroda H, Sasano T, et al. Comparison of clinical utility between neutrophil count and neutrophil-lymphocyte ratio in patients with ovarian cancer: a single institutional experience and a literature review. Int J Clin Oncol. 2018;23(1):104–13.
18. Baert T, Van Camp J, Vanbrabant L, Busschaert P, Laenen A, Han S, et al. Influence of CA125, platelet count and neutrophil to lymphocyte ratio on the immune system of ovarian cancer patients. Gynecol Oncol. 2018;150(1):31–7.
19. Miao Y, Yan Q, Li S, Li B, Feng Y. Neutrophil to lymphocyte ratio and platelet to lymphocyte ratio are predictive of chemotherapeutic response and prognosis in epithelial ovarian cancer patients treated with platinum-based chemotherapy. Cancer Biomark. 2016;17(1):33–40.
20. Zhou M, Li L, Wang X, Wang C, Wang D. Neutrophil-to-lymphocyte ratio and platelet count predict long-term outcome of stage iiic epithelial ovarian cancer. Cell Physiol Biochem. 2018;46(1):178–86.
21. Badora-Rybicka A, Nowara E, Starzyczny-Słota D. Neutrophil-to-lymphocyte ratio and platelet-to-lymphocyte ratio before chemotherapy as potential prognostic factors in patients with newly diagnosed epithelial ovarian cancer. ESMO Open. 2016;1(2):e000039.
22. Salman L, Sabah G, Jakobson-Setton A, Raban O, Yeoshoua E, Eitan R. Neutrophil-to-lymphocyte ratio as a prognostic factor in advanced stage ovarian carcinoma treated with neoadjuvant chemotherapy. Int J Gynaecol Obstet. 2020;148(1):102–6.
23. Jeerakornpassawat D, Suprasert P. Potential predictors for chemotherapeutic response and prognosis in epithelial ovarian, fallopian tube and primary peritoneal cancer patients treated with platinum-based chemotherapy. Obstet Gynecol Sci. 2020;63(1):55–63.
24. Cho H, Hur HW, Kim SW, Kim SH, Kim JH, Kim YT, et al. Pre-treatment neutrophil to lymphocyte ratio is elevated in epithelial ovarian cancer and predicts survival after treatment. Cancer Immunol Immunother. 2009;58(1):15–23.
25. Feng Z, Wen H, Bi R, Ju X, Chen X, Yang W, et al. Preoperative neutrophil-to-lymphocyte ratio as a predictive and prognostic factor for high-grade serous ovarian cancer. PLoS One. 2016;11(5):e0156101.
26. Wang Y, Liu P, Xu Y, Zhang W, Tong L, Guo Z, et al. Preoperative neutrophil-to-lymphocyte ratio predicts response to first-line platinum-based chemotherapy and prognosis in serous ovarian cancer. Cancer Chemother Pharmacol. 2015;75(2):255–62.
27. Li Z, Hong N, Robertson M, Wang C, Jiang G. Preoperative red cell distribution width and neutrophil-to-lymphocyte ratio predict survival in patients with epithelial ovarian cancer. Sci Rep. 2017;7:43001.
28. Kim YJ, Lee I, Chung YS, Nam E, Kim S, Kim SW, et al. Pretreatment neutrophil-to-lymphocyte ratio and its dynamic change during neoadjuvant chemotherapy as poor prognostic factors in advanced ovarian cancer. Obstet Gynecol Sci. 2018;61(2):227–34.
29. John-Olabode SO, Okunade KS, Olorunfemi G, Soibi-Harry A, Rimi G, Osunwusi B, et al. Pretreatment neutrophil-to-lymphocyte ratio: a prognostic biomarker of survival in patients with epithelial ovarian cancer. Cureus. 2021;13(7):e16429.
30. Williams KA, Labidi-Galy SI, Terry KL, Vitonis AF, Welch WR, Goodman A, et al. Prognostic significance and predictors of the neutrophil-to-lymphocyte ratio in ovarian cancer. Gynecol Oncol. 2014;132(3):542–50.
31. Qiu J, Yu Y, Fu Y, Ye F, Xie X, Lu W. Preoperative plasma fibrinogen, platelet count and prognosis in epithelial ovarian cancer. J Obstet Gynaecol Res. 2012;38(4):651–7.
32. Li Y, Yang JN, Cheng SS, Wang Y. Prognostic significance of FA score based on plasma fibrinogen and serum albumin in patients with epithelial ovarian cancer. Cancer Manag Res. 2019;11:7697–705.
33. Polterauer S, Grimm C, Seebacher V, Concin N, Marth C, Tomovski C, et al. Plasma fibrinogen levels and prognosis in patients with ovarian cancer: a multicenter study. Oncologist. 2009;14(10):979–85.
34. Hu Q, Hada A, Han L. Platelet count as a biomarker for monitoring treatment response and disease recurrence in recurrent epithelial ovarian cancer. J Ovarian Res. 2020;13(78).
35. Feng Z, Wen H, Bi R, Duan Y, Yang W, Wu X. Thrombocytosis and hyperfibrinogenemia are predictive factors of clinical outcomes in high-grade serous ovarian cancer patients. BMC Cancer. 2016;16:43.
36. Zhang WW, Liu KJ, Hu GL, Liang WJ. Preoperative platelet/lymphocyte ratio is a superior prognostic factor compared to other systemic inflammatory response markers in ovarian cancer patients. Tumour Biol. 2015;36(11):8831–7.
37. Man YN, Wang YN, Hao J, Liu X, Liu C, Zhu C, et al. Pretreatment plasma D-dimer, fibrinogen, and platelet levels significantly impact prognosis in patients with epithelial ovarian cancer independently of venous thromboembolism. Int J Gynecol Cancer. 2015;25(1):24–32.
38. Liu P, Wang Y, Tong L, Xu Y, Zhang W, Guo Z, et al. Elevated preoperative plasma D-dimer level is a useful predictor of chemoresistance and poor disease outcome for serous ovarian cancer patients. Cancer Chemother Pharmacol. 2015;76(6):1163–71.
39. Luo Y, Kim HS, Kim M, Lee M, Song YS. Elevated plasma fibrinogen levels and prognosis of epithelial ovarian cancer: a cohort study and meta-analysis. J Gynecol Oncol. 2017;28(3):e36.
40. Wang H, Zhao J, Zhang M, Han L, Wang M, Xingde L. The combination of plasma fibrinogen and neutrophil lymphocyte ratio (F-NLR) is a predictive factor in patients with resectable non small cell lung cancer. J Cell Physiol. 2018;233(5):4216–24.
41. Kijima T, Arigami T, Uchikado Y, Uenosono Y, Kita Y, Owaki T, et al. Combined fibrinogen and neutrophil-lymphocyte ratio as a prognostic marker of advanced esophageal squamous cell carcinoma. Cancer Sci. 2017;108(2):193–9.
42. Diakos CI, Charles KA, McMillan DC, Clarke SJ. Cancer-related inflammation and treatment effectiveness. Lancet Oncol.

2014;15(11):e493–503.
43. Song XD, Wang YN, Zhang AL, Liu B. Advances in research on the interaction between inflammation and cancer. J Int Med Res. 2020;48(4):300060519895347.
44. Nøst TH, Alcala K, Urbarova I, Byrne KS, Guida F, Sandanger TM, et al. Systemic inflammation markers and cancer incidence in the UK Biobank. Eur J Epidemiol. 2021;36(8):841–8.
45. Dolan RD, McSorley ST, Horgan PG, Laird B, McMillan DC. The role of the systemic inflammatory response in predicting outcomes in patients with advanced inoperable cancer: Systematic review and meta-analysis. Crit Rev Oncol Hematol. 2017;116:134–46.
46. Sylman JL, Mitrugno A, Atallah M, Tormoen GW, Shatzel JJ, Tassi Yunga S, et al. The predictive value of inflammation-related peripheral blood measurements in cancer staging and prognosis. Front Oncol. 2018;8:78.
47. Uribe-Querol E, Rosales C. Neutrophils in cancer: two sides of the same coin. J Immunol Res. 2015;2015:983698.
48. Corbeau I, Jacot W, Guiu S. Neutrophil to lymphocyte ratio as prognostic and predictive factor in breast cancer patients: a systematic review. Cancers (Basel). 2020;12(4):958.
49. Ethier JL, Desautels DN, Templeton AJ, Oza A, Amir E, Lheureux S. Is the neutrophil-to-lymphocyte ratio prognostic of survival outcomes in gynecologic cancers? A systematic review and meta-analysis. Gynecol Oncol. 2017;145(3):584–94.
50. Sheng L, Luo M, Sun X, Lin N, Mao W, Su D. Serum fibrinogen is an independent prognostic factor in operable nonsmall cell lung cancer. Int J Cancer. 2013;133(11):2720–5.
51. Zheng S, Shen J, Jiao Y, Liu Y, Zhang C, Wei M, et al. Platelets and fibrinogen facilitate each other in protecting tumor cells from natural killer cytotoxicity. Cancer Sci. 2009;100(5):859–65.
52. Gropp C, Egbring R, Havemann K. Fibrinogen split products, antiproteases and granulocytic elastase in patients with lung cancer. Eur J Cancer (1965). 1980;16(5):679–85.
53. Yin X, Wu L, Yang H, Yang H. Prognostic significance of neutrophil-lymphocyte ratio (NLR) in patients with ovarian cancer: a systematic review and meta-analysis. Medicine (Baltimore). 2019;98(45):e17475.
54. Liontos M, Andrikopoulou A, Koutsoukos K, Markellos C, Skafida E, Fiste O, et al. Neutrophil-to-lymphocyte ratio and chemotherapy response score as prognostic markers in ovarian cancer patients treated with neoadjuvant chemotherapy. J Ovarian Res. 2021;14(1):148.
55. Marchetti C, Romito A, Musella A, Santo G, Palaia I, Perniola G, et al. Combined plasma fibrinogen and neutrophil lymphocyte ratio in ovarian cancer prognosis may play a role? Int J Gynecol Cancer. 2018;28:939–44.

Clinical Research

Risk of seizure recurrence in children with new-onset afebrile seizure

Mufeed Akram Taha[1], Noorjan Abdullah Muhammed[2]

pISSN: 0853-1773 • eISSN: 2252-8083
https://doi.org/10.13181/mji.oa.236927
Med J Indones. 2023;32:80–5

Received: April 18, 2023
Accepted: September 07, 2023
Published online: October 09, 2023

Authors' affiliations:
[1]Department of Medicine, College of Medicine, University of Kirkuk, Kirkuk, Iraq, [2]Department of Pediatric, College of Medicine, University of Kirkuk, Kirkuk, Iraq

Corresponding author:
Mufeed Akram Taha
Department of Medicine, College of Medicine, University of Kirkuk, Shorja Street, P.O. Box 2281, Kirkuk, Iraq
Tel/Fax: +964-7736935651
E-mail: mufeedakram@uokirkuk.edu.iq

ABSTRACT

BACKGROUND A seizure is a brief change in the normal neuronal electrical activity of the brain that causes changes in consciousness, perception, behavior, or movement. This study aimed to evaluate clinical findings, initial electroencephalography (EEG), and brain imaging findings as predictors of seizure recurrence after the first nonfebrile seizure.

METHODS This prospective follow-up study was conducted at Azadi Teaching Hospital, Kirkuk from July 2019 to January 2022 and enrolled 150 patients, ranging from 1 month to 15 years of age, who presented with their first afebrile seizure. The seizure types were classified based on the International League Against Epilepsy in 2017. A brain imaging with EEG was performed within 72 hours after admission.

RESULTS The median age of the patients was 5 years. A higher risk of seizure recurrence occurred in patients with focal seizure (relative risk [RR] = 6.604) (95% confidence interval [CI] 3.975–10.971), seizure occurrence at sleep (RR = 3.815) (95% CI 2.410–6.039), an abnormal neurological presentation such as Todd's paralysis (RR = 1.739) (95% CI 1.252–2.415), a positive family history of seizures (RR = 2.333) (95% CI 1.598–3.408), abnormal EEG (RR = 0.171) (95% CI 0.092–0.318), and abnormal brain image findings (RR = 0.681) (95% CI 0.492–0.941) within 72 hours. Seizure recurrence was not correlated with sex.

CONCLUSIONS Early and late childhood new-onset afebrile seizures with a positive family history, focal epilepsy, seizure during sleep, prolonged attack duration with frequent attacks within 24 hours, and abnormal initial EEG and brain image had a high risk of seizure recurrence.

KEYWORDS electroencephalography, neuroimaging, recurrence, seizure

A seizure refers to a short alteration in the typical electrical activity of brain cells, resulting in shifts in awareness, conduct, sense, or motion. Epilepsy represents a recognized neurological condition marked by recurrent seizure episodes, affecting approximately 65 million people worldwide.[1] Seizures are classified as febrile and afebrile. Various underlying pathological conditions, such as electrolyte imbalance, genetic triggers, brain injuries from either trauma or non-trauma, and neurodevelopmental and cardiovascular diseases, can cause abnormal neuronal activity without fever.[2] Therefore, seizure diagnosis is challenging and raises concerns about its underlying causes and the probability of recurrence.

Patients with the first unprovoked seizure should be closely reviewed to determine whether the index events constitute epilepsy or whether the patients are at a higher risk of experiencing seizure recurrence. This evaluation aims to guide diagnostic ceonsiderations, treatment initiation, and administration of anti-seizure

medications to reduce the life-threatening effects of prolonged seizures and status epilepticus,[3] as well as global cognitive impairment.[4]

The first seizure episode is a life-changing event with psychophysical consequences.[5] Patients must be appropriately assessed and managed immediately after an unprovoked seizure. Although the probability of seizure recurrence may be uncertain, clinicians should review the available evidence. When assessing patients after their first seizure, physicians must look for predisposing factors for seizure recurrence and accordingly stratify the risk of future events.

Despite extensive research on seizures and epilepsy, there remains a critical gap in the literature pertaining specifically to children with new-onset afebrile seizures. While previous studies have explored aspects of seizure diagnosis and management, there is a paucity of research dedicated to understanding the predictive factors associated with seizure recurrence following the initial nonfebrile seizure in pediatric patients. The significance of this study lies in its focus on filling this knowledge gap, as it seeks to provide valuable insights into the evaluation of children who experience their first unprovoked seizure. Therefore, this study aimed to evaluate clinical, initial electroencephalography (EEG), and brain imaging findings as predictors of seizure recurrence after the first nonfebrile seizure.

METHODS

This study was conducted from July 2019 to January 2022 and enrolled 150 patients who experienced their first afebrile seizure at the outpatient clinic and the Department of Emergency Pediatrics and Neurology of Azadi Teaching Hospital. The study population included 77 males and 73 females, ranging from 1 month to 15 years of age. Children who arrived at the hospital more than 72 hours after the seizure event, as well as patients whose caregivers and medical records did not provide sufficient information for the proper classification of seizures and mimics of seizures, were excluded from the study.

Seizures were classified according to the International League Against Epilepsy 2017 classification, distinguishing between generalized, partial, and unidentified seizure types. According to this classification, a second seizure attack more than 24 hours after the first afebrile seizure was considered a recurrence. All patients were questioned about their family history, number and duration of attacks, associations with vomiting, sphincter loss, Todd's paralysis, and seizure recurrence during follow-up. Follow-up assessments were conducted 1, 3, 6, and 12 months after the first seizure. Blood samples were drawn from all patients at admission for routine laboratory studies. Complete blood counts, blood sugar, serum potassium, sodium, magnesium, and calcium levels were assessed to exclude possible metabolic disturbances that might precipitate or contribute to future seizures, but was not presented in this paper. Brain imaging was performed on 95 patients (63.3%). EEG was performed on 117 (78.0%) patients within 72 hours of hospital admission using a 16-electrode machine (Nihon Kohden, Japan) for 30 min at a speed of 30 mm/s and an amplitude of 70 mV.

The study was conducted following the 2013 World Medical Association Declaration of Helsinki guidelines and was approved by the Research Ethics Committee of the University of Kirkuk College of Medicine, Iraq (decision no. 22, date: 18.1.2023). Informed oral consent was obtained from all participants prior to the study.

Statistical analyses were performed using the SPSS software version 26 (IBM Corp., USA). Continuous data are presented as mean (standard deviation), and categorical variables are summarized as numbers (n) and percentages (%). Groups were compared using chi-square tests (categorical variables) and independent sample *t*-tests (normally distributed continuous variables) for the number of seizures within 24 hours, duration of seizure episodes, and seizure recurrence. Relative risk (RR) was calculated to assess the risk of seizure recurrence for all independent variables. A *p*-value of <0.05 was considered statistically significant.

RESULTS

The median age of the patients was 5 years, with the majority (65.3%) being <6 years old. While 51.3% of patients were male, the remaining were female, and 68.0% experienced seizures lasting ≤5 min.

Generalized tonic-clonic seizures were the most common type, accounting for 61.0% of cases, and most seizures (54.0%) occurred while patients were awake. Approximately 44.0% of patients had a family history of seizures, while 50.0% experienced vomiting and loss of sphincter control during seizure attacks. Additionally,

Table 1. Demographic characteristics and the risk of seizure recurrence

Characteristics	Total cases (N = 150)	Recurrence		RR (95% CI)	*p*
		Yes, n (%) (N = 68)	No, n (%) (N = 82)		
Age (years)					**0.01**‡
1–5	98	43 (63)	55 (67)	1.00	
6–10	33	11 (16)	22 (27)	0.842 (0.625–1.134)	0.53§
11–15	19	14 (21)	5 (6)	2.133 (0.985–4.618)	**0.04**§
Sex					0.76¶
Female	73	34 (50)	39 (48)	1.00	
Male	77	34 (50)	43 (52)	0.948 (0.667–1.347)	
Duration of attack (min)					**0.0001****
≤5	102	23 (34)	79 (96)	1.00	
>5	48	45 (66)	3 (4)	12.392 (4.122–37.252)	
Vomiting					0.74¶
Yes	75	35 (51)	40 (49)	1.061 (0.746–1.508)	
No	75	33 (49)	42 (51)	1.00	
Sphincter loss					0.74¶
Yes	75	33 (49)	42 (51)	0.943 (0.663–1.340)	
No	75	35 (51)	40 (49)	1.00	
Todd's paralysis					**0.004**¶
Yes	29	20 (29)	9 (11)	1.739 (1.252–2.415)	
No	121	48 (71)	73 (89)	1.00	
Seizure type					**0.0001**¶
Generalized	91	13 (19)	78 (95)	1.00	
Focal	53	50 (74)	3 (4)	6.604 (3.975–10.971)	
Unidentified	6	5 (7)	1 (1)	1.143 (0.858–30.839)	
Family history of seizures					**0.0001**¶
Yes	66	44 (65)	22 (27)	2.333 (1.598–3.408)	
No	84	24 (35)	60 (73)	1.00	
Seizure occurrence					**0.001**¶
Awake	81	16 (24)	65 (79)	1.00	
Sleep	69	52 (76)	17 (21)	3.815 (2.410–6.039)	
EEG finding*					**0.0001**¶
Normal	57	12 (18)	45 (55)	1.00	
Abnormal	60	49 (72)	11 (13)	0.171 (0.092–0.318)	
Brain image type performed†					**0.0001**¶
CT	61	34 (50)	27 (33)	1.00	
CT/MRI	34	26 (38)	8 (10)	0.258 (0.154–0.432)	
Brain imaging results†					**0.0001**¶
Normal	47	24 (35)	23 (28)	1.00	
Abnormal	48	36 (53)	12 (15)	0.681 (0.492–0.941)	

CI=confidence interval; CT=computed tomography; EEG=electroencephalography; MRI=magnetic resonance imaging; RR=relative risk
*Missing data: 33 cases (26 no recurrence, 7 recurrence); †missing data: 55 cases (47 no recurrence, 8 recurrence); ‡one-way analysis of variance; §post-hoc Tukey with 1–5 years group as reference; ¶chi-square test, significant if $p<0.05$; **independent *t*-test

Table 2. Association between the risk of seizure recurrence and the results of EEG and brain imaging

Variables	Total cases (N = 150)	Recurrence		$p^{\ddagger}$
		Yes, n (%) (N = 68)	No, n (%) (N = 82)	
EEG findings*				**0.0001**
Normal	57	12 (18)	45 (55)	
Abnormal	60	49 (72)	11 (13)	
Focal spikes	16	13 (19)	3 (4)	
Focal spikes and slow wave	15	12 (18)	3 (4)	
Temporal sharp-wave discharges	6	5 (7)	1 (1)	
Generalized spikes and slow waves	6	4 (6)	2 (2)	
Frontal sharp wave discharges	6	6 (9)	0 (0)	
Centro-temporal spikes	5	5 (7)	0 (0)	
Focal slowing	5	3 (4)	2 (2)	
Occipital spikes	1	1 (1)	0 (0)	
Brain imaging results†				**0.0001**
Normal	47	24 (35)	23 (28)	
Abnormal	48	36 (53)	12 (15)	
White matter hyperintensities	15	8 (12)	7 (9)	
Volumetric reduction of the brain hemisphere	5	4 (6)	1 (1)	
Ventricular asymmetry	4	1 (1)	3 (4)	
Subdural/epidural collection	3	3 (4)	0 (0)	
Mesial temporal sclerosis	3	3 (4)	0 (0)	
Venous sinus thrombosis	3	3 (4)	0 (0)	
Focal cortical dysplasia	2	2 (3)	0 (0)	
Feature of tuberous sclerosis	2	2 (3)	0 (0)	
Vascular malformation	2	1 (1)	1 (1)	
Feature of Herpes simplex encephalitis	2	2 (3)	0 (0)	
Absent corpus callosum with severe cerebral atrophy	2	2 (3)	0 (0)	
Right temporal arachnoid cyst	1	1 (1)	0 (0)	
Acute disseminated encephalomyelitis	1	1 (1)	0 (0)	
Subcortical heterotopia	1	1 (1)	0 (0)	
Lissencephaly	1	1 (1)	0 (0)	
Rasmussen encephalitis	1	1 (1)	0 (0)	

EEG=electroencephalography
*Not performed: 33 cases (26 no recurrence, 7 recurrence) ; †not performed: 55 cases (47 no recurrence, 8 recurrence); ‡chi-square test, significant if $p<0.05$

19.3% of patients had Todd's paralysis after the attack. While 32.0% of the cases showed abnormal brain imaging, 31.3% had normal findings. Abnormal EEG findings were observed in 40% of patients.

The seizure recurrence rate was 45.3%. Factors significantly associated with seizure recurrence included seizure duration >5 min, Todd's paralysis, occurrence of focal seizures, family history of seizures, and seizures during sleep ($p<0.05$). However, based on the RR analysis, seizures occurring during sleep (RR = 3.815), Todd's paralysis (RR = 1.739), and a family history of seizures (RR = 2.333) were identified as factors associated with a significant rate ratio (Table 1).

Seizure recurrence was significant among individuals who initially showed abnormal EEG results, with focal spike waves being the most common finding (19%), followed by focal spikes and slow waves (18%). Furthermore, significant associations were

observed between seizure recurrence and specific abnormalities detected by brain imaging. White matter hyperintensities were the most frequently identified abnormality (12%), followed by volumetric reduction of the brain hemisphere (6%) (Table 2).

Furthermore, we examined the association between seizure recurrence and the (a) number of seizures within 24 hours and (b) duration of seizure episodes. While 2.19 (1.26) individuals experienced recurrent seizures within 24 hours, 1.33 (0.86) individuals had no recurrent seizures (p = 0.001). The duration of seizure episodes was 8.37 (4.63) min in individuals with recurrent seizures, in contrast to 3.62 (1.78) min in those without recurrence (p = 0.001). Overall, the number of seizures within 24 hours and the duration of seizure episodes were significantly associated with seizure recurrence.

DISCUSSION

The present study found that the highest percentage of first afebrile seizures (65.3%) occurred in patients under 5 years of age and gradually decreased with age. Consistent with the findings of Maia et al,[6] we found a 12.7% incidence of first afebrile seizures in patients aged 11–15 years. Furthermore, the recurrence of seizures was significantly higher in patients over 11 years than in those under 5 (RR = 1.316), which is in line with the findings of Woo et al.[7] Consistent with previous studies,[8,9] we also found that sex was not associated with recurrence following the first nonfebrile seizure. Studies investigating the risk factors associated with unprovoked seizure recurrence in children have reported recurrence rates of 27–50%,[10–12] consistent with our present findings (45.3%). We found that the recurrence of seizures after the first afebrile seizure was associated with a family history of epilepsy (RR = 2.333), seizures occurring during sleep (RR = 3.815), and seizure duration >5 min, consistent with previous studies.[13–15] Generalized seizures were more common (61.0%) than other types as the first afebrile seizure, congruent with the 63% (generalized seizures) reported by Poudyal et al.[16] In this study, Todd's paralysis was a significant predictor of seizure recurrence compared with sphincter loss and/or vomiting during the attack, although not significant. These findings are consistent with those of Woo et al,[17] who have reported abnormal neuroimaging findings for most cases of Todd's paralysis that predicted seizure recurrence.

EEG is crucial for examining patients with new-onset afebrile seizures. While previous studies have reported abnormal EEG findings in 18–63% of children with new-onset nonfebrile seizures,[18–20] the present study observed abnormal findings in 81.6% of patients with seizure recurrence. This inconsistency is attributed to the inclusion of patients who underwent EEG in the first 72 hours of admission in this study *versus* the first 24 hours of admission in the previous studies. In agreement with several previous studies highlighting the association between EEG with epileptiform activity and seizure recurrence,[21,22] this study found an increased risk of seizure recurrence when the first EEG showed abnormal epileptiform activity. Therefore, an early EEG after the first nonfebrile seizure is highly recommended to predict the recurrence of seizures.

Neuroimaging is essential in patients with new episodes of convulsions to identify tissue abnormalities or structural injuries that could be associated with seizures. Abnormal neuroimaging findings are seen in 7–67% of patients with seizures.[23–26] In the present study, 32.0% of patients had abnormal neurological imaging results. A significant correlation was seen between seizure recurrence and abnormal initial neuroimaging findings, consistent with the findings of Dedeoglu and Ardicli.[27]

This study had some limitations. First, it had a relatively small sample size, which might limit the generalizability of the findings to a larger population. Second, the study was conducted at a single center, increasing the possibility of bias and limitations. Third, the follow-up duration was limited to 1 year. While this allowed the assessment of seizure recurrence patterns within that timeframe, a large-scale, multicenter studies with longer follow-up durations would provide a more comprehensive understanding of long-term outcomes and factors that influence seizure recurrence. Additionally, exploring the potential impact of interventions and treatments on reducing seizure recurrence rates could further enhance our ability to improve the quality of life for these patients.

In conclusion, children with early- and late-onset afebrile seizures with a family history of seizures, focal epilepsy, seizures during sleep, recurrent seizures of prolonged duration within 24 hours of the first one, and abnormal initial EEG and brain imaging were at a higher risk of seizure recurrence. Seizure recurrence showed no correlation with sex. This study's implications extend to clinical practice by highlighting

the importance of early evaluation and risk assessment in children with afebrile seizures. Identifying key factors associated with seizure recurrence enables healthcare professionals to tailor their diagnostic and treatment approaches, ultimately enhancing patient care and safety. By recognizing the significance of family history, seizure characteristics, EEG findings, and neuroimaging results, clinicians can make informed decisions that may prevent life-threatening complications and minimize cognitive impairment in affected children.

Conflict of Interest
The authors affirm no conflict of interest in this study.

Acknowledgment
None.

Funding Sources
None.

REFERENCES

1. Hana NN, Taha MA, Abass KS. Vascular biomarkers study among epileptic patients with monotherapy. Biochem Cell Arch. 2020;20(1):859–68.
2. Ali N, Haider S, Mustahsan S, Shaikh M, Raheem A, Soomar SM, et al. Predictors of abnormal electroencephalogram and neuroimaging in children presenting to the emergency department with new-onset afebrile seizures. BMC Pediatr. 2022;22(1):619.
3. Ayanoğlu M, Ongun EA. The predictive factors for prolonged seizures and status epilepticus: a single center study. Med J Bakirkoy. 2021;17(1):53–63.
4. Harahap HS, Rizki M, Irawati D. Factors associated with global cognitive impairment in epilepsy patients: a cross-sectional study in Mataram, Indonesia. Med J Indones. 2022;31(3):155–9.
5. M P, Dudipala SC, Shankar R, Reddy RV, Ch AK. A prospective hospital-based study on the clinico-etiological profile of the first episode of a seizure in children. Cureus. 2022;14(11):e31242.
6. Maia C, Moreira AR, Lopes T, Martins C. Risk of recurrence after a first unprovoked seizure in children. J Pediatr (Rio J). 2017;93(3):281–6.
7. Woo S, Nah S, Kim M, Kim S, Lee D, Moon J, et al. Risk of epilepsy in children presenting to emergency departments with their first afebrile seizure: a retrospective multicenter study. Children (Basel). 2022;9(11):1741.
8. Khair AM, Ibrahim K, Alshami R, Veten A, Elmagrabi D, Mohamed K. EEG profile & yield in evaluation of first non-febrile seizures in children-first observational study in Qatar. J Neurol Neurophysiol. 2015;6(6).
9. Kumar R. Etiology, clinical profile and outcome of first episode of seizure in children. Eur J Mol Clin Med. 2023;10(01):6142–7.
10. Neligan A, Adan G, Nevitt SJ, Pullen A, Sander JW, Bonnett L, et al. Prognosis of adults and children following a first unprovoked seizure. Cochrane Database Syst Rev. 2023;1(1):CD013847.
11. Pellino G, Faggioli R, Madrassi L, Falsaperla R, Suppiej A. Operational diagnosis of epilepsy in children at undetermined risk: a meta-analysis of prognostic factors for seizure recurrence. Epilepsy Behav. 2022;127:108498.
12. Jomaa N, Nasreddine W, Hmeimess G, Beaini S, Beydoun A, Hotait M, et al. Risk of recurrence in patients with an unprovoked tonic-clonic seizure and generalized epileptiform discharges on EEG. Epilepsia. 2023;64(8):2153–61.
13. Momen AA, Davoodzadeh H, Morvaridnejad M. Evaluation of EEGs of children referred with first non-febrile seizure in Ahvaz, south west of Iran. Neuropsychiatr Neuropsychol. 2017;12(2):49–53.
14. Lawn ND, Pang EW, Lee J, Dunne JW. First seizure from sleep: clinical features and prognosis. Epilepsia. 2023. Epub ahead of print.
15. Rizvi S, Ladino LD, Hernandez-Ronquillo L, Téllez-Zenteno JF. Epidemiology of early stages of epilepsy: risk of seizure recurrence after a first seizure. Seizure. 2017;49:46–53.
16. Poudyal P, Shrestha RP, Shrestha PS, Dangol S, Shrestha NC, Joshi A, et al. Clinical profile and electroencephalogram findings in children with seizure presenting to Dhulikhel Hospital. Kathmandu Univ Med J (KUMJ). 2016;14(56):347–51.
17. Woo S, Nah S, Kim M, Kim S, Lee D, Lee J, et al. Factors associated with neuroimaging abnormalities in children with afebrile seizure: a retrospective multicenter study. West J Emerg Med. 2023;24(2):279–86.
18. Wirrell EC. Prognostic significance of interictal epileptiform discharges in newly diagnosed seizure disorders. J Clin Neurophysiol. 2010;27(4):239–48.
19. Wirrell E. Evaluation of first seizure and newly diagnosed epilepsy. Continuum (Minneap Minn). 2022;28(2):230–60.
20. Özdemir FMA, Öztoprak Ü, Atasoy E, Aksoy E, Çelik H, Ceylan N, et al. Characteristics and clinical value of early electroencephalography (EEG) after a first unprovoked seizure in children. Neurophysiol Clin. 2023;53(1):102848.
21. Ulusoy E, Uysal Ateş Ş, Çitlenbik H, Öztürk A, Şık N, Arslan G, et al. What is the safe observation period for seizure recurrence in pediatric emergency departments? Epilepsy Behav. 2023;139:109049.
22. Seneviratne U, Cook M, D'Souza W. Brainwaves beyond diagnosis: wider applications of electroencephalography in idiopathic generalized epilepsy. Epilepsia. 2022;63(1):22–41.
23. Amagasa S, Uematsu S, Tsuji S, Nagai A, Abe Y, Kubota M. Identification of children with first afebrile seizure for whom neuroimaging is unnecessary. Seizure. 2021;93:140–4.
24. Üner Ç, Tekeli A, Karacan CD. Evaluation of the results of patients with a first afebrile seizure admitted to a pediatric emergency department. J Pediatr Emerg Intensive Care Med. 2021;8:146–50.
25. Elfeshawy MS, Afia AA, Alsawah AY, Mohammed MI, Abdelkader AA. Role of neuroimaging and electroencephalogram in first unprovoked seizures in children from Cairo. The Scientific Journal of Al-Azhar Medical Faculty, Girls. 2019;3(2):503–16.
26. Ponnatapura J, Vemanna S, Ballal S, Singla A. Utility of magnetic resonance imaging brain epilepsy protocol in new-onset seizures: how is it different in developing countries? J Clin Imaging Sci. 2018;8:43.
27. Dedeoglu O, Ardicli D. Evaluation and management of the first unprovoked seizure in children: single-center experience first unprovoked seizure in children. Ann Med Res. 2022;29(11):1263–7.

Commentary

Metaverse in medical education

Agus Rizal Ardy Hariandy Hamid[1,4], Ferdiansyah Sultan Ayasasmita Rusdhy[2], Prasandhya Astagiri Yusuf[3,4]

Medicine is an ever-changing landscape, forced to continuously evolve in response to all challenges that come with constant advancements in the pursuit of better patient care. This has paved the way for implementing novel techniques, such as minimally invasive surgery and robotic surgery, minimizing complications, reducing hospital stays, and improving patient outcomes. This has increased the burden of the knowledge and skills that students and residents must acquire throughout their training. Despite this, increased considerations for patient safety result in limited clinical exposure, providing a glaring contrast between the knowledge and skills that trainees need to acquire and the opportunity and time available to acquire them. The coronavirus disease 2019 (COVID-19) pandemic has exacerbated this problem. Restrictions on controlling disease transmission have further constrained learning opportunities. This can prove detrimental because medical education is fundamentally rooted in face-to-face meetings as a means of learning.

However, the introduction of the metaverse may solve these challenges, perhaps initiating another evolution in medical education. The term metaverse, first coined in the 1992 science fiction book *Snow Crash* by Neal Stephenson, was described in the story as a virtual world in which people can communicate with each other through digital avatars. The characters in the story engage in activities in an interconnected virtual world designed as an alternate reality for its users.[1] This article discusses what metaverse is, its possible applications in medical education and medicine, and the concerns regarding its implementation to highlight the potential role of metaverse in medical education.

Definition of metaverse

Mark Zuckerberg explained the concept of metaverse as an integrated and immersive virtual ecosystem with seamless barriers between reality and virtuality where people can participate in a shared simulated experience through their personal avatars. This shared immersive virtual space is rooted in augmented reality (AR) and virtual reality (VR),[2] which can be accessed using AR and VR devices. VR is a technology capable of immersing a user in a virtual environment, whereas AR uses technology to project virtual presence into reality, superimposing it onto the real world. Metaverse is an integrated and connected virtual space accessed through VR/AR devices and can exist as a form of VR or AR. It can be considered a scaled-up and extended version of both VR and AR, where a user using VR/AR devices could experience a virtual world only they could interact with. In contrast, the metaverse allows users to experience a shared virtual world that multiple people can interact with and experience simultaneously. The Acceleration Studies Foundation,[3] a representative of metaverse research, categorizes metaverse into four types: lifelogging, the mirror world, and the aforementioned AR and VR. Lifelogging is the technology used to capture, store, and share personal experiences and information about a user's everyday life through social media platforms. The mirror world, as the name suggests, is a virtual mirrored version of our world equipped with additional information such as global positioning systems (GPS) or Google Earth. The four concepts are then connected and converge to form the metaverse.

Metaverse learning provides programmable, controlled, and safe learning environments in medical education. It can simulate classrooms and laboratories, enabling teachers and students to participate in learning similar to real-world settings through their avatars. Additionally, it can provide medical procedure training that allows trainees to practice continuously without safety concerns and prepare trainees before performing them on actual patients. Metaverse learning is also less resource-intensive

Table 1. Advantages and disadvantages of metaverse-based learning

Advantages	Disadvantages
- Time efficient - Facilitates distant learning in real time - Provides various interactive learning tools with 3D capabilities - Simulating multiple different medical procedures in a safe, controlled, and repeatable environment without compromising patient safety - Simulates a more immersive training experience	- Substantial initial cost of development - Lack of haptic and emotional feedback for students - Potential security, privacy, and ethical concerns - Possible motion sickness after prolonged use - Requires reliable high-speed internet network infrastructure

than its traditional real-world counterparts owing to the significant cost constraints in operating and maintaining laboratories and training devices. Further advantages and disadvantages are listed in Table 1.

Possibility of metaverse-based medical education

As the use of VR and AR has become more widespread in medical education, it is exciting to consider how the metaverse can potentially revolutionize the field. Classical classroom lectures featuring PowerPoint slides and textbooks can be simulated in a metaverse, with teachers and students equipped with their personal 3D models depicting the subject, essentially turning it into a laboratory environment. While teachers use large 3D models to demonstrate concepts, students can manipulate smaller, more detailed models to strengthen their understanding of a subject. Metaverse can be programmed to provide further information regarding the manipulated structure, highlighting how certain structures function and animate complex systems and pathways. This ability to visualize structures in 3D may impact knowledge acquisition and retention in students studying anatomy.[4] This was illustrated in a physiology course where a group of students using AR to learn cardiac physiology got higher scores and could illustrate cardiac physiology better than students learning using traditional methods comprising lectures, textbooks, and images.[5] The same concept can be applied in case presentations and multidisciplinary team meetings. A forum of physicians from various disciplines can benefit from these capabilities and bridge the knowledge gap between different fields.

As medical education increasingly relies on simulations, the objective structured clinical examination (OSCE) has been widely adopted for assessing students. While the assessment is conducted on real simulated patients, the process of studying and practicing for the exam is rooted in roleplaying the patient carer between students in a group. This dedicated group-centered learning approach may not always be feasible, especially with numerous other assignments and exams. An "OSCE Mock Exam" set in the metaverse can be the solution. Problem-based learning, another staple in medical education, relies on clinical cases as the point of discussion. Metaverse can help simulate virtual patients more realistically and engagingly to deliver clinical scenarios commonly presented in the text. The programmable nature of the metaverse also allows institutions to develop comprehensive programs suited to their curriculum requirements. An institution using an integrated block curriculum can develop fully integrated programs of the human body systems, providing all the necessary anatomy, physiology, and pathophysiology knowledge at the beginning of the block and later illustrating diagnoses and treatments of the diseases. Students may also use the program as a study guide, helping them focus on the topic and minimize the time spent learning irrelevant materials from other sources.

The ever-increasing burden of skills that students and residents must acquire during their training years, coupled with increasingly limited hospital exposure owing to patient safety concerns, may result in poor performance and lead to medical errors.[6,7] Thus, it is essential to provide an environment capable of replicating clinical scenarios in which trainees can safely and repeatedly practice different medical procedures before performing them on a patient. The immersive and programmable nature of the metaverse provides an optimally safe, controlled, yet customizable training environment. Although mannequins and task trainers, the mainstay of simulation-based training, can provide high-fidelity haptic feedback, they are single-purposed and unable to simulate patient interactions. Instead of only going through the motions of a procedure, trainees can indulge in a more comprehensive and realistic experience and follow a clinical scenario from the initial patient assessment to perform the procedure. This is especially helpful in essential

yet complex training such as advanced trauma and cardiac life support. In addition, mannequins and specific trainers are also resource-intensive and require significant costs and manpower to arrange and operate.[8] Metaverse-based training is particularly beneficial for surgery training, with the constant development of techniques with increasing difficulties paired with cost-ineffective training methods amidst the limited training hours. These considerations further push the claim to shift toward a more cost-effective alternative in metaverse-centered training. Various impelentations of VR/AR are already used to train different procedures, ranging from basic skill to advanced surgical techniques. Several studies have shown comparable or better learning outcomes in certain procedures.[9–11] Metaverse-based learning being more accessible than traditional training methods can increase the amount of training outside the operating room (OR), helping shorten learning curves, and improving OR performance, especially for novel surgical techniques.[12]

Current use of metaverse in medical education

While the possibilities seem enticing, various implementations ranging from knowledge transfer to skill training have mostly been experimental. These are confined to studies and trials that compare their efficacy with traditional teaching modalities. Anatomical education is one of the most popular medical education programs. Although the traditional practice of cadaver-centered anatomy learning aided by atlases has been used for centuries, it still has ethical issues.[13] Limitations due to decomposition and preservation techniques, such as changes in appearance and color, might hinder the ability to learn, not to mention the resources needed to preserve the cadaver itself.[14] Some studies have also documented the effects of cadaver dissection on students' emotional states, including anxiety and guilt.[15,16] While the sensation of real tissue manipulation and the multiple sensory feedback from cadaver dissection may not be replaceable, the metaverse can provide the necessary spatial visualization of structures from multiple viewpoints in 3D that atlases are incapable of. A German institution developed an immersive VR program to simulate an OR consisting of a dummy with precise human anatomy.[17] Students can then interact with the dummy as they interact with a real cadaver. Further information regarding the structure was provided when students held certain anatomical structures.

In medical training, VR/AR has already been widelys used to train for different procedures depending on the institution. These implementations are listed in Table 2.[18–28] In addition to training, VR/AR has been utilized in planning minimally invasive surgical procedures. The complex nature of some cases may require 3D models to better illustrate the anatomy of patients and help plan an optimal surgical approach. Data from routine preoperative imaging modalities can create a personalized 3D model, allowing surgeons to simulate surgical approaches and ultimately deliver better care. The models generated can also be viewed with AR technology in the OR, helping to visualize anatomical structures that would otherwise be difficult to localize owing to the restricted field of view and lack of spatial perception of laparoscopic systems. The possibility of using AR models as a real-time guiding tool for incision and instrumentation is currently being explored in neurosurgery[29] and orthopedics.[30]

The introduction of the metaverse during the COVID-19 pandemic geared its development toward providing a new social communication platform. The widely used teleconference apps such as Google Meet and Zoom have been shown to cause "zoom fatigue," which refer to feelings of emotional exhaustion due to a lack of social connection. Factors such as only seeing someone's face closely through the webcam without seeing their body movements or gestures contribute to this feeling.[31] The use of metaverse-based platforms with avatars can help alleviate these factors. A group of orthopedic surgeons held a virtual meeting in the metaverse to discuss clinical cases (Figure 1). Their discussion was aided by a 3D model of the patient's scapula, with which they could manipulate and interact with the model together.

The Seoul National University, Bundang Hospital, in South Korea showcased an even more exciting implementation.[32] Utilizing a smart OR, they held a virtual surgical training program as part of the Asian Society for Cardiovascular and Thoracic Surgery conference (illustrated in Figure 2), where participants joined a virtual conference room to observe lung cancer surgery.

The smart OR used multiple 360-8k-3D cameras to broadcast an unobstructed 3D view of the OR in its entirety. Instead of observing only a limited surgical field in traditional surgery footage, observers

Table 2. Implementations of metaverse-based learning in medical training

Field	Use of VR/AR	Institution
Neurosurgery[18]	Endoscopic neurosurgery Cranial tumor surgery Microvascular decompression Cerebral aneurysm clipping	Mount Sinai Hospital, Toronto, Canada Jichi Medical University, Tochigi, Japan Chinese PLA General Hospital, Beijing, China Kepler University Hospital, Linz, Austria
Maxillofacial surgery[18]	Orthognathic surgery Fixation of mandibular fracture	University of Basel, Basel, Switzerland Morristown Medical Center, Morristown, New Jersey, USA
General surgery[18]	Hepatobiliary surgery Open hepatic surgery Laparoscopic salpingectomy Laparoscopic pancreatectomy	University of Strasbourg, Straosbourg, France Paul Brousse Hospital, Villejuif, France Copenhagen Academy for Medical Education and Simulation, Copenhagen, Denmark Division of Gastroenterological and General Surgery, Showa University, Tokyo, Japan
Urology[19,20]	Transurethral resection of the prostate Ureteroscopy/cystoscopy	Linköping University Hospital, Linköping, Sweden Beijing Shijitan Hospital, Capital Medical University, Beijing, China
Cardiothoracic surgery[21]	Video-assisted thoracic surgery Robotic video-assisted thoracic surgery	Copenhagen Academy for Medical Education and Simulation, Copenhagen, Denmark Hospital Copa Star, Rio de Janeiro, RJ, Brazil
Ophthalmology[22]	Vitreoretinal surgery Cataract surgery	Nancy University Hospital, Nancy, France Imperial College London, London, UK
Otothinolaryngology[23]	Myringotomy Cochlear implantation	University of Western Ontario, Ontario, Canada University of Wolonggong, NSW, Australia
Orthopedics[24]	Arthroscopy Arthroplasty	Imperial College London, London, UK Nancy University Hospital, Nancy, France
Anesthesiology[25–27]	Bronchoscopy	Lausanne University Hospital, Lausanne, Switzerland Geneva University Hospital, Genève, Switzerland
	Regional anesthesia	University Hospital RWTH Aachen, Aachen, Germany
	Cricothyroidotomy	Baylor University Medical Center, Dallas, Texas, USA
Cardiology[28]	Cardiac catheterization	Terrence Donnelly Heart Centre, St Michael's Hospital, Toronto, Ontario, Canada
	Coronary angiography	Karolinska Institutet, Stockholm, Sweden

could see all the monitors and instruments used in the procedure. The nature of the 3D footage, in which scenes change as participants turn and move their heads, adds another layer of immersion to the experience.

Metaverse in medicine

Telemedicine has become a prominent example of the possibilities of the metaverse in healthcare. The remote healthcare provision enables patients to receive consultations, diagnoses, and treatment regardless of geographical barriers, eliminating the need for travel. This is particularly helpful in Indonesia, where specialists and consultants are limited to certain regions. Initial assessments and tests can be performed at a local center and subsequently reviewed by a specialist at a higher-level center. As discussed earlier, the metaverse-based case discussion can make the handover more effective, helping the specialist decide whether the patient requires referral to a tertiary center island, thus eliminating unnecessary travel costs for the patient. Although conventional telemedicine uses conference applications for communication, it has limitations in providing adequate care, restricting its usage to patient communication. In contrast, telemedicine in the metaverse provides a more immersive experience, enhanced patient care and consultations, and improved communication effectiveness. A virtual consultation room with a specialist walking a patient through the assessment, diagnosis, planning, and treatment procedures, which includes illustrations, models, and even demonstrations, would help patients better understand their condition and reduce their anxiety.

Several concepts have been proposed regarding how the metaverse can shape future health services. One of the key features is the live augmentation of

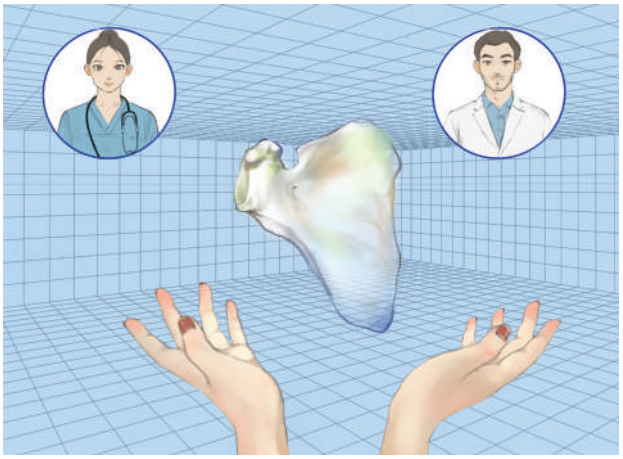

Figure 1. Metaverse usage in orthopedic case discussions

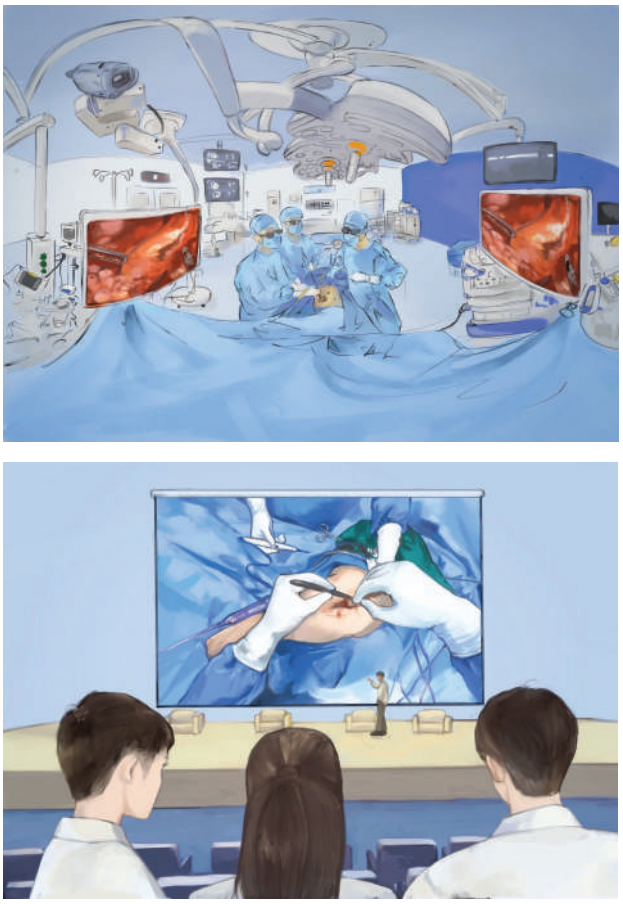

Figure 2. Broadcast of surgery in the metaverse

patients' medical data and imaging to help guide surgeons during procedures, particularly in minimally invasive and robotic surgeries. However, minimally invasive and robotic surgery have several issues regarding limited maneuverability and surgical view.[33] These systems can help identify landmarks and structures, especially in oncology, for selective resection and organ-sparing surgeries.[34] A study showcased these guiding capabilities in urology.[35] The advancement of robot-assisted kidney transplantation has shown several benefits over conventional open kidney transplant procedures; however, identifying atheromatous plaques can be challenging, with surgeons unable to manually palpate potential plaque in the iliac vessels.[36] A virtual 3D model is obtained from a computed tomography scan imaging and then superimposed in real-time on the actual iliac vessels of the patients. van Leeuwen and van der Hage[37] showed several concepts that the metaverse could help to advance minimally invasive and robotic surgery, including: (1) high-fidelity procedural planning based on preoperative 3D imaging roadmaps, (2) the superimposition of live data and 3D imagery on endoscopic views (e.g., mixed reality visualizations and GPS-like navigation strategies), (3) dynamic lesion/tissue characterization via intraoperative imaging (e.g., drop-in ultrasound for in-depth detection) or fluorescence imaging (superficial detection), and (4) the use of machine learning strategies to alleviate the mounting cognitive input, to advance the interpretation of the surgical data output, and to guide image-to-patient registration. While integrating these concepts presents considerable challenges, the development and standalone use of each key concept can still be helpful.

Metaverse can also improve neurorehabilitation. Currently, VR systems have been used in the rehabilitation of various conditions, including stroke, Parkinson's disease, Alzheimer's disease, and brain injury, and in delaying cognitive decline.[38] The resulting neurological deficits caused by these conditions often require a long period- and resource-consuming rehabilitation. Findings on improving cognitive function after interaction with virtual realities help cement its potential use in neurorehabilitation. A safe, repetitive, and controlled environment can be tailored to each individual's needs, especially those with differences in cognitive function. Although the digitization and virtualization of cognitive function assessment and rehabilitation tools are routinely practiced, the metaverse offers cognitive function assessment and training in real-life activities. Patients can engage in virtual simulations to assess their ability to perform daily tasks, such as driving, shopping, and cooking, without any real-life consequences of any mistakes. Studies have shown improvements in several cognitive attributes associated with the frontal lobe, such as

activities related to the immediate recall of memory and time- and event-based tasks. These improvements are associated with neuronal plasticity. Their fun and engaging nature also motivate patients to continue participating in each session. In motor function rehabilitation, highly interactive virtual realities strongly promote the activation and stimulation of the visual, proprioceptive, and vestibular regions of the brain, showing a significant increase in brain volume and activity levels in the VR-rehabilitated groups. It has been used to increase the active range of motion of the upper limbs and improve gait rehabilitation. While current advancements in gait rehabilitation rely on the use of treadmills with robot support to help gait and posture, the addition of VR devices can improve the patient's mood, perception of physical well-being, global cognitive functions, executive functions (such as perseveration, planning, and classification), cognitive flexibility, and selective attention. These findings regarding the effects of VR in neurobiology have been extensively discussed by Georgiev et al.[39]

Metaverse has also been used in the field of mental health. Virtual simulations may enhance aversion therapy, in which patients interact with objects or situations that cause anxiety and discomfort. Repeated exposure to the cause of anxiety helps increase the anxiety threshold and improve insensitivity to help alleviate anxiety and discomfort.[40] Metaverse can simulate various phobias, including fear of height, fear of insects, and even fear of flight. In addition, it provides patient monitoring, enabling the simulation to be stopped instantly when a patient is overwhelmed, thereby preventing full-blown anxiety and panic attacks. For soldiers with post-traumatic stress disorder, a simulated battle situation can mimic the triggers of their condition. This can also be applied to patients with agoraphobia or the fear of crowds. Patients who fear of social interaction can also benefit from the fact that people can freely interact in the metaverse. Metaverse can also be used in distraction therapy to alleviate pain and stress, allowing patients to shift their focus away from pain.[41] A study has shown the use of VR in assisting meditation and mindfulness sessions, significantly reducing sadness, anger, and anxiety and increasing relaxation.[40] Moreover, the metaverse allows patients with chronic conditions and long-term hospital stay to "get out" of the hospital and enjoy a change of scene, which could reduce their stress and shorten their hospital stays.[42]

Reality of metaverse

With sizeable investments made by numerous companies to enter the metaverse, the hype garnered from various fields, including medical education, should come as no surprise. Some ways in which the metaverse and its two key components in VR/AR have been adopted also help fuel the excitement behind the continuing development and implementation of this virtual world. As we look beneath its promises, several questions must be addressed before committing to its implementation. First, it is important to address its ability to achieve better outcomes than those of the traditional alternatives. A study in anatomy learning has shown conflicting reports on the use of the metaverse and traditional approach, with some showing better outcomes in VR- or AR-based learning, while others found no significant differences.[4] However, this study was conducted relatively short, which might show a slightly skewed result due to the initial excitement of trying a novel learning method and the perception of it being a more fun and enjoyable experience. More detailed studies over longer periods are necessary. After successfully establishing its effectiveness, further studies on its optimal role in medical education are required. Is it feasible to outright replace the need for a cadaver laboratory in favor of a "virtual" anatomy lab? If it can only be used as a complement to traditional methods, how should we best allocate time between these modalities? Which one provides better outcomes: a curriculum with more time allocation in metaverse-based learning or classical methods, or would it be better to make the time allocation equal? What about subjects other than anatomy?

In medical training, answers to these questions are straightforward. The inherent haptic nature of medical procedures will always require at least some training on real patients. Regardless of how immersive and high-fidelity the metaverse is programmed, trainees can never quite grasp the necessary force required for optimal chest compressions or the interaction between various surgical instruments and living tissues solely by training in the metaverse. Metaverse-based training is an introduction to basic and advanced procedures that helps trainees learn the core skills needed before performing them on patients. It provides a unique combination of immersive, repeatable, safe, programmable, and relatively cost-effective simulation. The goal is to determine the best way to incorporate these VR/AR simulations by analyzing the optimal

amount of virtual simulation training before moving to in-person training using mannequins or performing it in dry laboratory environments.

Then arise questions on the costs of metaverse implementation. However, the general use of VR/AR devices can cost thousands of dollars for a single device. Relatively affordable VR headsets such as Oculus Quest 2 costs approximately $300, excluding the necessary personal computer system required to run the software, pushing the cost to more than a thousand dollars per system. Microsoft HoloLens, regarded as one of the more advanced AR systems, costs $3,500. Regarding the software, the prices of ready-for-purchase third-party educational programs range from free of charge to hundreds of dollars, depending on the hardware utilized, with varying levels of detail and fidelity reflecting their prices. Developing custom-made software tailored to higher institution curriculum costs and setting up these devices for a large number of students should be performed simultaneously to reduce significant investments further. Virtual simulation systems used in medical training commonly include both software and hardware because of the need for special instruments depending on the simulated procedure. While customized VR systems used in surgical training do not need to be purchased for regular VR/AR devices, they can cost up to 6-figure expenses for a single system. Additionally, the potential lifespan of VR/AR systems should also be considered. With the rapid development of both hardware and software in the metaverse, it may only take a relatively short time before the software outdates the hardware, rendering it obsolete.

Cost-benefit analysis studies regarding its use in medical education and training are still scarce. A study examining the cost-utility ratio between virtual and mannequin-based simulations for nursing students showed that virtual-based simulations cost a third as much as mannequin-based simulations, although the study was conducted with a limited number of participants (n = 48) over one simulation course.[43] While this may be the case, early investments to set up the system can still prove costly. Will it be worthwhile for institutions with established traditional learning methods to implement metaverse-based learning modalities? Or will it be more beneficial for relatively new institutions without established traditional learning facilities? Ultimately, the analyses will differ for each institution depending on their needs and planned implementation. The faculty members must determine whether a significant investment is justified. Concerns regarding motion sickness and visual fatigue after long periods of VR/AR use are well-documented.[44] Although VR/AR systems have been used for some time, there has yet to be a definitive solution to this problem. VR/AR might also lead to oversimplification of training tasks, leading trainees to adopt habits detrimental to performance.[45] Thus, for now, metaverse-based learning seems best suited to facilitate and complement existing education and training modalities instead of replacing them.

In conclusion, introducing the metaverse could revolutionize medical education and training. The potential virtualization of knowledge transfer and skill acquisition in a programmable world is a possibility only the metaverse can offer. Early adoption of the metaverse, including its components VR and AR, has shown promise that warrants excitement. However, several concerns must be addressed before implementation in medical education. As the building blocks of its implementation continue to develop, it is perhaps best to slowly integrate metaverse-based learning to enhance learning and training modalities further because the technology, regardless of its continuous advancement, will never fully replace the traditional ones.

[1]From Medical Journal of Indonesia; Department of Urology, Faculty of Medicine, Universitas Indonesia, Cipto Mangunkusumo Hospital, Jakarta, Indonesia, [2]Faculty of Medicine, Universitas Airlangga, Surabaya, Indonesia, [3]Department of Medical Physiology and Biophysics, Faculty of Medicine Universitas Indonesia, Jakarta, Indonesia, [4]Medical Technology, Indonesia Medical Education and Research Institute (IMERI), Jakarta, Indonesia
pISSN: 0853-1773 • eISSN: 2252-8083
https://doi.org/10.13181/mji.com.236932
Med J Indones. 2023;32:67–74
Published online: September 19, 2023

Corresponding author:
Prasandhya Astagiri Yusuf
E-mail: prasandhya.a.yusuf@ui.ac.id

REFERENCES

1. Skalidis I, Muller O, Fournier S. CardioVerse: the cardiovascular medicine in the era of Metaverse. Trends Cardiovasc Med. 2022:S1050–1738(22)00071–8.
2. Zhang X, Chen Y, Hu L, Wang Y. The metaverse in education: definition, framework, features, potential applications, challenges, and future research topics. Front Psychol. 2022;13:1016300.
3. Smart J, Cascio J, Paffendorf J. Metaverse roadmap: pathway to the 3D web [Internet]. Ann Arbor (MI): Acceleration Studies Foundation; 2007 [cited 2021 Nov 29]. Available from: https://metaverseroadmap.org/MetaverseRoadmapOverview.pdf.
4. Alharbi Y, Al-Mansour M, Al-Saffar R, Garman A, Alraddadi A.

Three-dimensional virtual reality as an innovative teaching and learning tool for human anatomy courses in medical education: a mixed methods study. Cureus. 2020;12(2):e7085.
5. Gonzalez AA, Lizana PA, Pino S, Miller BG, Merino C. Augmented reality-based learning for the comprehension of cardiac physiology in undergraduate biomedical students. Adv Physiol Educ. 2020;44(3):314–22.
6. Al-Elq AH. Simulation-based medical teaching and learning. J Family Community Med. 2010;17(1):35–40.
7. Grant D, Marriage S. Training using medical simulation: Figure 1. Arch Dis Child. 2011;97(3):255–9.
8. Meerdink M, Khan J. Comparison of the use of manikins and simulated patients in a multidisciplinary in situ medical simulation program for healthcare professionals in the United Kingdom. J Educ Eval Health Prof. 2021;18:8.
9. Buttussi F, Chittaro L, Valent F. A virtual reality methodology for cardiopulmonary resuscitation training with and without a physical mannequin. J Biomed Inform. 2020;111:103590.
10. Abulfaraj MM, Jeffers JM, Tackett S, Chang T. Virtual reality vs. high-fidelity mannequin-based simulation: a pilot randomized trial evaluating learner performance. Cureus. 2021;13(8):e17091.
11. Sommer GM, Broschewitz J, Huppert S, Sommer CG, Jahn N, Jansen-Winkeln B, et al. The role of virtual reality simulation in surgical training in the light of COVID-19 pandemic: visual spatial ability as a predictor for improved surgical performance: a randomized trial. Medicine (Baltimore). 2021;100(50):e27844.
12. Kantamaneni K, Jalla K, Renzu M, Jena R, Kannan A, Jain R, et al. Virtual reality as an affirmative spin-off to laparoscopic training: an updated review. Cureus. 2021;13(8):e17239.
13. Ghazanfar H, Rashid S, Hussain A, Ghazanfar M, Ghazanfar A, Javaid A. Cadaveric dissection a thing of the past? the insight of consultants, fellows, and residents. Cureus. 2018;10(4):e2418.
14. Kovacs G, Levitan R, Sandeski R. Clinical cadavers as a simulation resource for procedural learning. AEM Educ Train. 2018;2(3):239–47.
15. Chia TI, Oyeniran OI, Ajagbe AO, Onigbinde OA, Oraebosi MI. The symptoms and stress experienced by medical students in anatomy dissection halls. J Taibah Univ Med Sci. 2020;15(1):8–13.
16. Chang HJ, Kim HJ, Rhyu IJ, Lee YM, Uhm CS. Emotional experiences of medical students during cadaver dissection and the role of memorial ceremonies: a qualitative study. BMC Med Educ. 2018;18(1):255.
17. Weyhe D, Uslar V, Weyhe F, Kaluschke M, Zachmann G. Immersive anatomy atlas-empirical study investigating the usability of a virtual reality environment as a learning tool for anatomy. Front Surg. 2018;5:73.
18. Lungu AJ, Swinkels W, Claesen L, Tu P, Egger J, Chen X. A review on the applications of virtual reality, augmented reality and mixed reality in surgical simulation: an extension to different kinds of surgery. Expert Rev Med Devices. 2021;18(1):47–62.
19. Hamacher A, Whangbo TK, Kim SJ, Chung KJ. Virtual reality and simulation for progressive treatments in urology. Int Neurourol J. 2018;22(3):151–60.
20. Cai JL, Zhang Y, Sun GF, Li NC, Yuan XL, Na YQ. Proficiency of virtual reality simulator training in flexible retrograde ureteroscopy renal stone management. Chin Med J (Engl). 2013;126(20):3940–3.
21. Rad AA, Vardanyan R, Thavarajasingam SG, Zubarevich A, Van den Eynde J, Sá MP, et al. Extended, virtual and augmented reality in thoracic surgery: a systematic review. Interact Cardiovasc Thorac Surg. 2022;34(2):201–11.
22. Iskander M, Ogunsola T, Ramachandran R, McGowan R, Al-Aswad LA. Virtual reality and augmented reality in ophthalmology: a contemporary prospective. Asia Pac J Ophthalmol (Phila). 2021;10(3):244–52.
23. Piromchai P. Virtual reality surgical training in ear, nose and throat surgery. Int J Clin Med. 2014;5(10):558–66.
24. Hasan LK, Haratian A, Kim M, Bolia IK, Weber AE, Petrigliano FA. Virtual reality in orthopedic surgery training. Adv Med Educ Pract. 2021;12:1295–301.
25. Casso G, Schoettker P, Savoldelli GL, Azzola A, Cassina T. Development and initial evaluation of a novel, ultraportable, virtual reality bronchoscopy simulator: the computer airway simulation system. Anesth Analg. 2019;129(5):1258–64.
26. Grottke O, Ntouba A, Ullrich S, Liao W, Fried E, Prescher A, et al. Virtual reality-based simulator for training in regional anaesthesia. Br J Anaesth. 2009;103(4):594–600.
27. Sankaranarayanan G, Odlozil CA, Hasan SS, Shabbir R, Qi D, Turkseven M, et al. Training on a virtual reality cricothyroidotomy simulator improves skills and transfers to a simulated procedure. Trauma Surg Acute Care Open. 2022;7(1):e000826.
28. Aslani N, Behmanesh A, Garavand A, Maleki M, Davoodi F, Shams R. The virtual reality technology effects and features in cardiology interventions training: a scoping review. Med J Islam Repub Iran. 2022;36:77.
29. Besharati Tabrizi L, Mahvash M. Augmented reality-guided neurosurgery: accuracy and intraoperative application of an image projection technique. J Neurosurg. 2015;123(1):206–11.
30. Dennler C, Jaberg L, Spirig J, Agten C, Götschi T, Fürnstahl P, et al. Augmented reality-based navigation increases precision of pedicle screw insertion. J Orthop Surg Res. 2020;15:174.
31. Lee H, Woo D, Yu S. Virtual reality metaverse system supplementing remote education methods: based on aircraft maintenance simulation. Appl Sci. 2022;12(5):2667.
32. Koo H. Training in lung cancer surgery through the metaverse, including extended reality, in the smart operating room of Seoul National University Bundang Hospital, Korea. J Educ Eval Health Prof. 2021;18:33.
33. Giannone F, Felli E, Cherkaoui Z, Mascagni P, Pessaux P. Augmented reality and image-guided robotic liver surgery. Cancers (Basel). 2021;13(24):6268.
34. Checcucci E, Verri P, Amparore D, Cacciamani GE, Rivas JG, Autorino R, et al. The future of robotic surgery in urology: from augmented reality to the advent of metaverse. Ther Adv Urol. 2023;15:17562872231151853.
35. Piana A, Gallioli A, Amparore D, Diana P, Territo A, Campi R, et al. Three-dimensional augmented reality-guided robotic-assisted kidney transplantation: breaking the limit of atheromatic plaques. Eur Urol. 2022;82(4):419–26.
36. Liu G, Deng Y, Zhang S, Lin T, Guo H. Robot-assisted versus conventional open kidney transplantation: a meta-analysis. Biomed Res Int. 2020;2020:2358028.
37. van Leeuwen FWB, van der Hage JA. Where robotic surgery meets the metaverse. Cancers (Basel). 2022;14(24):6161.
38. Calabrò RS, Cerasa A, Ciancarelli I, Pignolo L, Tonin P, Iosa M, et al. The arrival of the metaverse in neurorehabilitation: fact, fake or vision? Biomedicines. 2022;10(10):2602.
39. Georgiev DD, Georgieva I, Gong Z, Nanjappan V, Georgiev GV. Virtual reality for neurorehabilitation and cognitive enhancement. Brain Sci. 2021;11(2):221.
40. Park MJ, Kim DJ, Lee U, Na EJ, Jeon HJ. A literature overview of virtual reality (vr) in treatment of psychiatric disorders: recent advances and limitations. Front Psychiatry. 2019;10:505.
41. Cerasa A, Gaggioli A, Marino F, Riva G, Pioggia G. The promise of the metaverse in mental health: the new era of MEDverse. Heliyon. 2022;8(11):e11762.
42. Tashjian VC, Mosadeghi S, Howard AR, Lopez M, Dupuy T, Reid M, et al. Virtual reality for management of pain in hospitalized patients: results of a controlled trial. JMIR Ment Health. 2017;4(1):e9.
43. Haerling KA. Cost-utility analysis of virtual and mannequin-based simulation. Simul Healthc. 2018;13(1):33–40.
44. Chang E, Kim HT, Yoo B. Virtual reality sickness: a review of causes and measurements. Int J Hum-Comput Interact. 2020;36(17):1658–82.
45. Wang Z, Kasman M, Martinez M, Rege R, Zeh H, Scott D, et al. A comparative human-centric analysis of virtual reality and dry lab training tasks on the da Vinci surgical platform. J Med Robot Res. 2019;04(03n04):1942007.

Case Report/Series

Mutation of *PAX3* and *MITF* genes in a family with type 1 Waardenburg syndrome: a case series

Habibah Setyawati Muhiddin, Ulfah Rimayanti, Fadhlullah Latama, Andi Muhammad Ichsan, Marliyanti Nur Rahmah Akib, Adelina Titirina Poli, Budu, Andi Pratiwi

pISSN: 0853-1773 • eISSN: 2252-8083
https://doi.org/10.13181/mji.cr.236954
Med J Indones. 2023;32:137–42

Received: May 09, 2023
Accepted: September 04, 2023
Published online: October 04, 2023

Authors' affiliations:
Department of Ophthalmology, Faculty of Medicine, Universitas Hasanuddin, Makassar, Indonesia

Corresponding author:
Ulfah Rimayanti
Department of Ophthalmology, Faculty of Medicine, Universitas Hasanuddin, Jalan Perintis Kemerdekaan KM. 11, Tamalanrea, Makassar 90245, Indonesia
Tel/Fax: +62-411-580678
E-mail: rimayantiu@gmail.com

ABSTRACT

Waardenburg syndrome (WS) is a rare genetical disorder, characterized with pigmentary abnormalities of the eyes, skin, hair, dystopia canthorum, and sensorineural deafness. In Majene, West Sulawesi, 12 members of a 4-generation family presented manifestations of WS. We examined the presence of mutations in 5 family members with type 1 WS and the other 5 normal phenotype family members to identify mutations of *PAX3* and *MITF* genes. Ophthalmic examination and peripheral blood test were done. Conventional polymerase chain reaction and direct Sanger sequencing were then performed to detect the mutation. 26 mutations of *PAX3* gene were only identified in patients with major and minor criteria, including 7 missense mutations (substitutions) and 2 insertions in exons 1, 2, and 6, as well as 17 intronic changes in intron 8. No mutations were detected in *MITF* gene.

KEYWORDS genes, Waardenburg syndrome

Waardenburg syndrome (WS) is a rare genetic disorder of the neural crest, characterized by pigment abnormalities in the eyes, skin, and hair, dystopia canthorum, and sensorineural deafness.[1,2] WS is divided into four subtypes based on specific clinical signs. Type 1 WS (WS1) is characterized by the presence of dystopia canthorum, whereas type 2 WS usually presents with hearing loss without dystopia canthorum. In type 3 WS, dystopia canthorum is observed, along with musculoskeletal abnormalities in the arms and hands. In type 4 WS, the patient also has Hirschsprung disease, in which intestinal blockage and severe constipation may happen.[3,4]

The major, minor, and rare diagnostic features of WS1 were defined based on the WS1 consortium. The major diagnostic features include pigmentary disorders of the iris, hair hypopigmentation, congenital sensorineural deafness, dystopia canthorum, and having a first-degree relative with WS1. Minor diagnostic features include synophrys or medical eyebrow flare, congenital leukoderma, hypoplasia of the alae nasi, broad and high nasal roots, and premature graying of the hair (<30 years of age). An individual must meet either (a) at least two of the major criteria or (b) one of the major criteria and two of the minor criteria (not including the rare criteria, such as Hirschsprung disease, Sprengel anomaly, spina bifida, cleft lip and/or palate, limb defects, congenital heart abnormalities, abnormalities of vestibular function, broad square jaw, and low anterior hairline) to be diagnosed with WS1.[5,6]

At the molecular level, WS1 can be influenced by six genes, namely paired box 3 transcription factor (PAX3), endothelin-3, SRY-box transcription factor

10, microphthalmia-associated transcription factor (MITF), endothelin receptor type B, and snail homolog 2.[5] Each of which has interfamilial and intrafamilial variabilities.[3] These genes are responsible for the establishment and development of specific cell types, such as melanocytes. Abnormalities caused by defects in these cells contribute to the clinical signs of WS1. This disorder is caused by the absence of melanocytes from hair, skin, eyes, and/or cochlear stria vascularis.[4] Furthermore, any pigmentary changes in the eye do not only affect the iris but also the choroid.[7,8] The affected choroid areas are slightly thinner compared to normal tissues but without lipofuscin abnormalities.[8]

In Majene, West Sulawesi, Indonesia, 12 members of the same family were diagnosed with WS1. To our knowledge, there have been no studies presenting data about genetic mutations of this rare genetic disease in Indonesia. Therefore, this case study aimed to investigate the presence and type of mutations in *PAX3* and *MITF* genes and compare them with normal family members. We hope this will provide insight into the genetic factors influencing WS1.

CASE REPORT

Twelve members of a family across four generations presented with manifestations of WS (Figure 1). Among them, three had bright blue irides in both eyes, and four had heterochromia. Of the members with bright blue irides, two had sensorineural hearing loss and poliosis accompanied by a broad nasal bridge. Three other patients exhibited only hypertelorism and poliosis. One family member passed away prior to this case study, and one other was not present during the assessment. All the participants had normal visual acuity. No history of consanguineous marriage was reported.

The presence of genetic mutations was examined in five of the family members with WS1, including the proband and the proband's sister, brother, niece, and grandson. Five unaffected family members with normal phenotypes were also examined.

The diagnosis of WS1 was confirmed by ophthalmological and otorhinolaryngological examinations. Normal participants were family members without the WS1 phenotype. The blood samples were examined at the Hasanuddin University Medical Research Center (HUMRC) laboratory, Makassar, Indonesia.

Cases

The procedures were performed following Declaration of Helsinki and approved by the Ethics Committee of Universitas Hasanuddin (No: 644/UN4.6.4.5.31/PP36/2021). Written and signed informed consent from the patients or the parents was obtained before the examinations done.

Of the five patients with WS1, three exhibited major criteria for WS1, and two exhibited minor criteria (Figure 2). The proband (case 1) had blue irides, congenital leukoderma, and poliosis. Other family members with WS1 had varied signs of WS1, such as blue irides, congenital leukoderma, poliosis, premature hair graying, and congenital sensorineural deafness.

In this study, we identified 74 variations in *PAX3* expression in patients with WS1. Of these, 53 were found in normal family members. Twenty-one mutations of the *PAX3* gene were only identified in patients with major and minor criteria, including 11 missense mutations (substitutions), 1 nonsense mutation, 2 insertion mutations in exons 6 and 10, and 7 intronic changes in introns 2 and 9. An example of a *PAX3* heterozygous mutation in exon 10 is shown in Figure 3. Five variations of the *PAX3* gene are known,

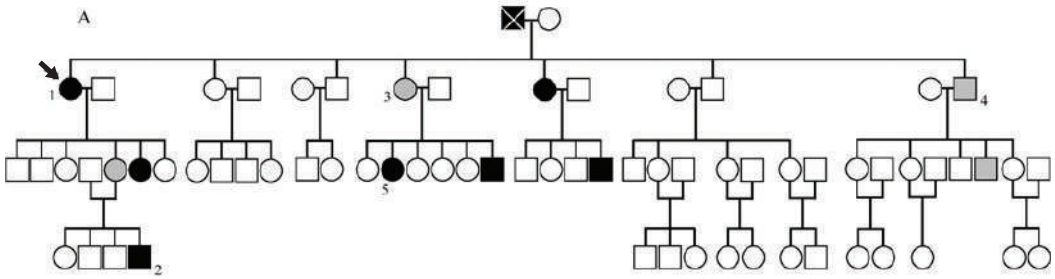

Figure 1. Pedigree of the family with type 1 Waardenburg syndrome (WS1) cases. Square represented male, and round represented female. Number showed orders of cases. Cross symbol represented deceased person. Arrow showed the proband (case no. 1). Solid black represented person with major criteria, while solid gray represented those with minor criteria

Figure 2. Five patients with Waardenburg syndrome (WS)

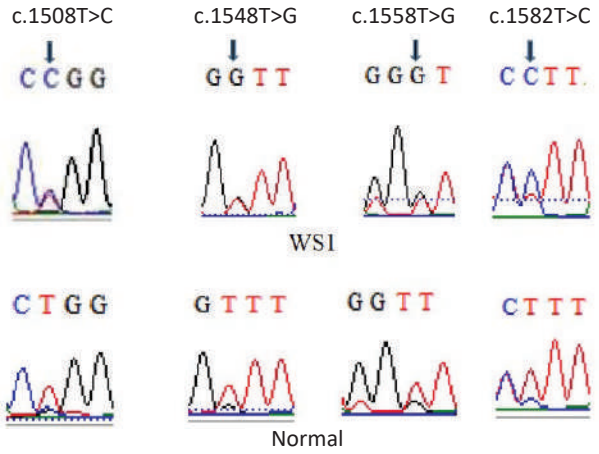

Figure 3. Sequencing result of PAX3 heterozygous mutations in exon 10. PAX3=paired box 3 transcription factor; WS1=type 1 Waardenburg syndrome

all of which were also found in family members. Mutations of the *PAX3* gene that were found only in patients with WS1 are shown in Table 1. Variations in the *MITF* gene, which were also observed in healthy individuals, are presented in Table 2.

Sample collection and DNA extraction

A total of 5 ml of peripheral blood was collected into standard EDTA tubes and stored at –20°C until DNA extraction. Blood samples were analyzed at the HUMRC laboratory. DNA was isolated from peripheral blood leukocytes using a gSYNC DNA Extraction Kit (Geneaid Biotech Ltd, Taiwan) according to the manufacturer's protocol.[9] DNA quality was evaluated by 2% agarose gel electrophoresis at 100 V (Bio-Rad, USA); the DNA quantity was not calculated.

Polymerase chain reaction (PCR) and sequencing

Mutational screening of whole exons from the *PAX3* and *MITF* genes was performed using direct Sanger sequencing. The primer sequences used are listed in Table 3. A total volume of 50 µl of DNA was amplified in a PCR DNA thermal cycler (Bio-Rad). The reaction components were 1 µl forward and 1 µl reverse *PAX3* and *MITF* gene primers (Table 3), 25 µl KAPA2G fast enzyme, 18 µl nuclease-free water, and 5 µl DNA template. The PCR conditions were as follows: denaturation at 95°C for 15 min, then cycles of 94°C for 1 min, annealing at 55°C for 30 sec, and extension at 72°C for 1.5 min, followed by 72°C for 10 min for final extension, and then 12°C for 30 min. Sequencing was performed and examined using the BioEdit Sequence Alignment Editor version 7.0.5.1 (Hall, Tom; North Carolina State University, USA). The results and data from GenBank of the National Center for Biotechnology Information GRCh37 database were compared using a basic local alignment search tool. Additional information regarding mutations in the *PAX3* and *MITF* genes was obtained from The Human Gene Mutation Database and the Leiden Open Variation Database.

DISCUSSION

In this study, all five patients with WS1 had dystopia canthorum. The other most common signs were congenital leukoderma (80%), pigmentary iris disorder (60%), and poliosis (60%). Two patients had premature hair graying, and one had congenital sensorineural deafness. Unfortunately, we could not examine the remaining six family members with WS1.

Most genetic mutations were found in exon 10. The most common PAX3 protein is formed by a stop codon in exon 8.[4,10] Differential splicing before the exon 8 stop codon and within exons 9 and 10 will produce a different C-terminal end of the protein.[11] Although the significance of these changes is unknown, they may have functional abilities analogous to the most common isoform.[3,4]

We found one mutation in exon 1 and six mutations in exon 2 of the *PAX3* gene. Mutations in exon 2 have also been commonly reported in previous studies.[3,12,13] Approximately 95% of *PAX3* mutations were found in the DNA-binding domains. The highest number of pathogenic variants were found in exon 2 of the paired domain, followed by exons 5 and 6, which encode the homeodomain.[3] Missense mutations in

Table 1. *PAX3* gene mutations in patients with WS1

Patient ID	Exon/intron no	g. position	c. position	Protein change	Type of mutation
WS 1	Intron 2	g.7077T>C	c.321+73T>C	-	Intronic
WS 5	Intron 2	g.7078T>C	c.321+74T>C	-	Intronic
WS 5	Exon 6	g.82613InsC	c.811InsC*	-	Insertion
WS 5	Exon 6	g.82664InsC	c.862InsC*	-	Insertion
WS 1	Intron 9	g.102699A>C	c.1452-43A>C	-	Intronic
WS 1	Intron 9	g.102701T>A	c.1452-41T>A	-	Intronic
WS 1	Intron 9	g.102709A>C	c.1452-33A>C	-	Intronic
WS 1	Intron 9	g.102720A>G	c.1452-22A>G	-	Intronic
WS 1	Intron 9	g.102724A>G	c.1452-18A>G	-	Intronic
WS 1	Exon 10	g.102764A>C	c.1474A>C*	His>Pro	Missense
WS 1	Exon 10	g.102779A>C	c.1489A>C*	Gln>Pro	Missense
WS 1	Exon 10	g.102781T>G	c.1491T>G*	Trp>Gly	Missense
WS 1	Exon 10	g.102798T>C	c.1508T>C*	Pro>Thr	Missense
WS 1	Exon 10	g.102820A>C	c.1530A>C*	Asn>His	Missense
WS 1	Exon 10	g.102823A>C	c.1533A>C*	Ile>Leu	Missense
WS 1	Exon 10	g.102838T>G	c.1548T>G*	Phe>Val	Missense
WS 1	Exon 10	g.102844A>C	c.1554A>C*	Met>Leu	Missense
WS 1	Exon 10	g.102848T>G	c.1558T>G*	Val>Gly	Missense
WS 1	Exon 10	g.102855T>A	c.1565T>A*	Tyr>Stop	Nonsense
WS 1	Exon 10	g.102862A>C	c.1572A>C*	Ile>Leu	Missense
WS 1	Exon 10	g.102872T>C	c.1582T>C*	Leu>Pro	Missense

*Novel mutation
Based on *PAX3* gene transcript 205 ensembl Asia
ID=identity; *PAX3*=paired box 3 transcription factor; WS1=type 1 Waardenburg syndrome

Table 2. *MITF* gene variations in patients with WS1

Patient ID	Exon/intron no	g. position
WS 1	Promoter	g. 1554&1555 AT>TA
WS 3	Promoter	g. 1554&1555 AT>TA
WS 5	Promoter	g. 1554&1555 AT>TA
WS 6	Promoter	g. 1554&1555 AT>TA
WS 10	Promoter	g. 1554&1555 AT>TA

ID=identity; *MITF*=microphthalmia-associated transcription factor; WS1=type 1 Waardenburg syndrome

the *PAX3* gene cause amino acid changes from glycine to glutamic acid in exon 1, and valine to alanine and threonine to serine in exon 2. Most human genetic mutations are caused by single-nucleotide changes.[14,15] Amino acid changes caused by mutations in the DNA-binding domain may alter the structure of the paired DNA-binding sites, causing functional impairment. Those possessing a mutation in *PAX3* develop several phenotypes, including abnormalities of the central nervous system, eye, and nose, and pigmentation abnormalities affecting the skin, hair, and otic pigment cells that are important for normal hearing, as found in WS1.[16,17]

In the present study, most of the mutations in exons were missense mutations (71.43%). Pingault et al[3] identified trimmed variations in approximately half of the mutations, while the remaining half were missense mutations in the *PAX3* gene. Other studies have reported a low amount of recurrency among approximately 100 sequence changes in the *PAX3* gene.[3,18] Previously reported mutations include missense mutations (38%), small deletions (20%), nonsense mutations (15%), gross deletions (11%), small insertions (8%), and splicing mutations (8%).[19] Among these variants, seven intronic mutations were identified in the present study. Only a small number of bases in introns are functional targets for pathogenic mutations;[20] however, point mutations deep within introns may alter normal splicing,

Table 3. Primer sequences used in PCR

Exons no	Length (bp)	Forward primers (5'-3')	Reverse primers (5'-3')	Annealing temp (°C)
PAX3				
1	788	GATGGGAAGAGAAAGTGGTC	TGCAGAAAGGAAATCGAGTA	62
2	503	CCGATGTCGAGCAGTTTCAG	CGCACCTTCACAAACCTCAG	64
3	420	TGGGATGTGTTCTGGTCTG	TCCCAATAGCTGAGATCGA	60
4	383	CTGGAGAAGGATGAGGATGT	CGTCAGATCACCAATGTCAG	62
5	508	TACGGATTGGTTAGACTTGT	AACAATATGCATCCCTAGTAA	57
6	445	CAACACAGAAGGCAGAGA	ATAGGTACGTTCAGGACAA	57
7	586	TGTGCAGAGATAGGTGTGAC	TTTGATGAAGCCAGTAGGA	57
8	480	TCTCCTGGACAGCTCTTTAA	GGCATGTGTGGCTTAATCT	57
9 & 10	580	GGTCAGCTCCAGGATCATAT	GCAAATGGAATGTTCTAGCT	60
MITF				
1		GGATACCTTGTTTATAGTACCTTC	AAAAGAGCAGATTTATACTTATTG	
2		TCTGAAACTCACAAATAACAGCGC	TATTCAACAGACAAGTTATTTAGC	
3		CCATCAGCTTTGTGTGAACAGGTC	TTTCAGGAAGGTGTGATCCACCAC	
4		AACTAAAGACCATTATTGCTTTGG	AGAAAAGAACCCTGGAAACACCTC	
5		ATAAATCCTAGAGTAGGATATAGG	ACTTTGTCTTATCAGGAAATGGAC	
6		TCAAGTCAAATAAGCTTCTGTATG	GTAGGAATCAACTCTCCTCTACAG	
7		GTGCTAAATGCATACATGGCACGT	TTAGGAATAGAACCAAAGGGAGAG	
8		TTCATTGAGCCTCAAATCCTAAAG	CTGTTTCTACTGTCTTGAAGTCGG	
9		AGTCCTCTGTGCTCGTCCTATTTC	AAGCTAAAGTCTGTGGTGAATTC	

bp=base pair; *MITF*= microphthalmia-associated transcription factor; *PAX3*= paired box 3 transcription factor; PCR=polymerase chain reaction

transcription regulators, and non-coding RNA genes.[21,22] Additional analysis, such as minigene assays, are needed to confirm the pathogenicity of intronic mutations.[23,24]

In the present study, no mutations of the *MITF* gene were detected in patients with WS1. *MITF* gene mutations occur in approximately 15% of WS2 cases.[3,4] Studies have indicated that WS2 tends to be associated with clinical signs influenced by MITF gene mutations.[25] The absence of *MITF* gene mutations in this study might be because all patients were classified as having WS1. The limitations of this study included having a relatively small sample size and incomplete family mapping. Moreover, additional analyses, such as minigene assays, were not performed. In conclusion, when observing genetic mutations in related WS1 patients, 26 mutations in the *PAX3* gene were found, including 7 missense mutations and 2 insertions in exons 1, 2, and 6, as well as 17 intronic changes in intron 8; no mutations were found in the *MITF* gene. The finding has implications for genetic counseling and risk prediction for the families with this genetic disorder.

Conflict of Interest

The authors affirm no conflict of interest in this study.

Acknowledgment

We thank John Ellis, Handayani Halik, and Asep M. Ridwanulloh who provided insight and expertise that greatly assisted the research.

Funding Sources

None.

REFERENCES

1. Pandya A, Xia XJ, Landa BL, Arnos KS, Israel J, Lloyd J, et al. Phenotypic variation in Waardenburg syndrome: mutational heterogeneity, modifier genes or polygenic background? Hum Mol Genet. 1996;5(4):497–502.
2. Bondurand N, Pingault V, Goerich DE, Lemort N, Sock E, Le Caignec C, et al. Interaction among *SOX10*, *PAX3* and *MITF*, three genes altered in Waardenburg syndrome. Hum Mol Genet. 2000;9(13):1907–17.
3. Pingault V, Ente D, Dastot-Le Moal F, Goossens M, Marlin S, Bondurand N. Review and update of mutations causing Waardenburg syndrome. Hum Mutat. 2010;31(4):391–406.
4. Read AP, Newton VE. Waardenburg syndrome. J Med Genet. 1997;34(8):656–65.
5. Farrer LA, Grundfast KM, Amos J, Arnos KS, Asher JH Jr, Beighton P, et al. Waardenburg syndrome (WS) type I is caused by defects at multiple loci, one of which is near ALPP on chromosome 2: first report of the WS consortium. Am J Hum Genet. 1992;50(5):902–13.

6. Rawlani SM, Ramtake R, Dhabarde A, Rawlani SS. Waardenburg syndrome: a rare case. Oman J Ophthalmol. 2018;11(2):158–60.
7. Sharma K, Arora A. Waardenburg syndrome: a case study of two patients. Indian J Otolaryngol Head Neck Surg. 2015;67(3):324–8.
8. Shields CL, Nickerson SJ, Al-Dahmash S, Shields JA. Waardenburg syndrome: iris and choroidal hypopigmentation: findings on anterior and posterior segment imaging. JAMA Ophthalmol. 2013;131(9):1167–73.
9. Umar BT, Rimayanti U, Pagarra H, Massi N, Muhiddin HS. Novel point mutation and intronic mutations of RB1 gene in retinoblastoma patients in Indonesia. Med J Indones. 2023;31(4):218–24.
10. Lalwani AK, Brister JR, Fex J, Grundfast KM, Ploplis B, San Agustin TB, et al. Further elucidation of the genomic structure of PAX3, and identification of two different point mutations within the PAX3 homeobox that cause Waardenburg syndrome type 1 in two families. Am J Hum Genet. 1995;56(1):75–83.
11. Barber TD, Barber MC, Cloutier TE, Friedman TB. *PAX3* gene structure, alternative splicing and evolution. Gene. 1999;237(2):311–9.
12. Farrer LA, Arnos KS, Asher JH Jr, Baldwin CT, Diehl SR, Friedman TB, et al. Locus heterogeneity for Waardenburg syndrome is predictive of clinical subtypes. Am J Hum Genet. 1994;55(4):728–37.
13. Baldwin CT, Hoth CF, Macina RA, Milunsky A. Mutations in PAX3 that cause Waardenburg syndrome type I: ten new mutations and review of the literature. Am J Med Genet. 1995;58(2):115–22.
14. Halushka MK, Fan JB, Bentley K, Hsie L, Shen N, Weder A, et al. Patterns of single-nucleotide polymorphisms in candidate genes for blood-pressure homeostasis. Nat Genet. 1999;22(3):239–47.
15. Cargill M, Altshuler D, Ireland J, Sklar P, Ardlie K, Patil N, et al. Characterization of single-nucleotide polymorphisms in coding regions of human genes. Nat Genet. 1999;22(3):231–8. Erratum in: Nat Genet. 1999;23(3):373.
16. Tassabehji M, Read AP, Newton VE, Harris R, Balling R, Gruss P, et al. Waardenburg's syndrome patients have mutations in the human homologue of the *Pax-3* paired box gene. Nature. 1992;355(6361):635–6.
17. Kubic JD, Young KP, Plummer RS, Ludvik AE, Lang D. Pigmentation PAX-ways: the role of Pax3 in melanogenesis, melanocyte stem cell maintenance, and disease. Pigment Cell Melanoma Res. 2008;21(6):627–45.
18. Boudjadi S, Chatterjee B, Sun W, Vemu P, Barr FG. The expression and function of PAX3 in development and disease. Gene. 2018;666:145–157.
19. Jalilian N, Tabatabaiefar MA, Farhadi M, Bahrami T, Noori-Daloii MR. A novel mutation in the *PAX3* gene causes Waardenburg syndrome type I in an Iranian family. Int J Pediatr Otorhinolaryngol. 2015;79(10):1736–40.
20. Zhang K, Nowak I, Rushlow D, Gallie BL, Lohmann DR. Patterns of missplicing caused by *RB1* gene mutations in patients with retinoblastoma and association with phenotypic expression. Hum Mutat. 2008;29(4):475–84.
21. Vaz-Drago R, Custódio N, Carmo-Fonseca M. Deep intronic mutations and human disease. Hum Genet. 2017;136(9):1093–111.
22. Highsmith WE, Burch LH, Zhou Z, Olsen JC, Boat TE, Spock A, et al. A novel mutation in the cystic fibrosis gene in patients with pulmonary disease but normal sweat chloride concentrations. N Engl J Med. 1994;331(15):974–80.
23. Gámez-Pozo A, Palacios I, Kontic M, Menéndez I, Camino I, García-Miguel P, et al. Pathogenic validation of unique germline intronic variants of *RB1* in retinoblastoma patients using minigenes. Hum Mutat. 2007;28(12):1245.
24. Imperatore V, Pinto AM, Gelli E, Trevisson E, Morbidoni V, Frullanti E, et al. Parent-of-origin effect of hypomorphic pathogenic variants and somatic mosaicism impact on phenotypic expression of retinoblastoma. Eur J Hum Genet. 2018;26(7):1026–37.
25. Wildhardt G, Zirn B, Graul-Neumann LM, Wechtenbruch J, Suckfüll M, Buske A, et al. Spectrum of novel mutations found in Waardenburg syndrome types 1 and 2: implications for molecular genetic diagnostics. BMJ Open. 2013;3(3):e001917.

Clinical Research

Food-induced brain activity in adult obesity: a quantitative electroencephalographic study

Kemas Abdurrohim[1,2], Pradana Soewondo[3], Fiastuti Witjaksono[4], Hasan Mihardja[2], Wresti Indriatmi[5], Heri Wibowo[6], Selfi Handayani[7], Nurhadi Ibrahim[8,9,10]

pISSN: 0853-1773 • eISSN: 2252-8083
https://doi.org/10.13181/mji.oa.236974
Med J Indones. 2023;32:98–104

Received: May 19, 2023
Accepted: July 21, 2023
Published online: October 03, 2023

Authors' affiliations:
[1]Doctoral Program in Medical Sciences, Faculty of Medicine, Universitas Indonesia, Jakarta, Indonesia, [2]Department of Medical Acupuncture, Faculty of Medicine, Universitas Indonesia, Cipto Mangunkusumo Hospital, Jakarta, Indonesia, [3]Department of Internal Medicine, Faculty of Medicine, Universitas Indonesia, Cipto Mangunkusumo Hospital, Jakarta, Indonesia, [4]Department of Nutrition, Faculty of Medicine, Universitas Indonesia, Cipto Mangunkusumo Hospital, Jakarta, Indonesia, [5]Department of Dermatology & Venereology, Faculty of Medicine, Universitas Indonesia, Cipto Mangunkusumo Hospital, Jakarta, Indonesia, [6]Department of Parasitology, Faculty of Medicine, Universitas Indonesia, Cipto Mangunkusumo Hospital, Jakarta, Indonesia, [7]Department of Anatomy, Faculty of Medicine, Universitas Sebelas Maret, Surakarta, Indonesia, [8]Department of Medical Physiology and Biophysics, Faculty of Medicine, Universitas Indonesia, Jakarta, Indonesia, [9]Neuroscience & Brain Development Cluster, Indonesian Medical Education and Research Institute (IMERI), Faculty of Medicine, Universitas Indonesia, Jakarta, Indonesia, [10]Medical Technology Cluster, Indonesian Medical Education and Research Institute (IMERI), Faculty of Medicine, Universitas Indonesia, Jakarta, Indonesia

Corresponding author:
Nurhadi Ibrahim
Department of Medical Physiology and Biophysics, Faculty of Medicine, Universitas Indonesia, Jalan Salemba Raya No. 6, Kenari, Senen, Central Jakarta 10430, DKI Jakarta, Indonesia
Tel/Fax: +62-21-31930373/ +62-21-3912477
E-mail: ibmnurhadi@gmail.com

ABSTRACT

BACKGROUND Obesity may be associated with declined food consumption control through neurological and behavioral processes, as well as heightened responsiveness of the brain's reward systems. Performing neuroimaging and neurophysiological methods such as electroencephalography (EEG) can examine the connection between brain function and behavior. This study aimed to identify brain regulation of feeding behavior to food cues, which could be a potential neuromodulatory intervention target in adult obesity.

METHODS This cross-sectional study was conducted at Cipto Mangunkusumo Hospital, Jakarta, involving 40 adults with obesity. EEG analysis was performed to measure electrophysiological brain activity during eyes-open condition and during exposure to high-calorie food cues. Student's *t*-tests were performed to identify any significant differences between the groups ($p<0.05$).

RESULTS Beta waves in the frontal (channel F7) and gamma waves in the central (channels C3 and C4) and parietal (channels P3 and P4) regions were significantly increased during food cues compared to resting state/eyes-open condition without stimulation. Theta waves in the frontal (channels F7 and F8), central (channel C3), and parietal (channels P3 and P4) regions and alpha waves in the central (channels C3 and C4) and parietal (channels P3 and P4) regions were significantly decreased during food cues compared with resting state.

CONCLUSIONS In adults with obesity, increased beta activity in the frontal and gamma in the central and parietal regions suggested increased food-cue awareness and heightened attentional focus toward food stimuli. Additionally, decreased alpha and theta activities in frontal regions could underline deficits in executive functions and higher motivation.

KEYWORDS brain wave, food, electroencephalography, obesity

Obesity is a major public health challenge worldwide.[1] An increasing trend in obesity prevalence has been observed in Indonesia since 2007 and 2018, growing from 10.3–21.8%.[2] A recent study suggested that obesity might be associated with alterations in how the body and mind respond to food cues, particularly with increased reactivity to high-calorie foods. This reactivity can manifest as elevated neural activity, salivation, or physiological arousal and is known as high food-cue reactivity. According to the meta-analysis findings, significant medium-to-large effects were observed for food-related stimuli responsiveness, which was linked to overeating, weight gain, and becoming

overweight or obese in both children and adults, in cross-sectional and longitudinal studies.[3]

Studies have revealed a significant increase in attentional processing triggered by environmental food cues, which have been linked to weight gain and obesity. This neurophysiological response can be measured using electroencephalography (EEG) event-related potentials.[4,5] Neuroimaging research has identified various important brain regions and networks that respond differently to visual food cues depending on the context, including fasting, weight loss, overfeeding, exercise, hormones, and cognitive control. These areas include those involved in visual processing and networks related to motivation and food cravings, particularly high-energy and palatable foods, located in the frontal cortex, striatum, and amygdala. This network, referred to as the "salience network," shows greater activation in obese individuals than in lean individuals.[1] Neuroimaging studies have shown that specific brain parts are associated with food-cue reactivity. Greater orbitofrontal cortex activity was observed in children with obesity than in those of normal weight when passively viewing high-calorie food images, which is related to the reward and motivation systems.[6,7] However, evidence regarding the relationship between the dorsolateral prefrontal cortex (PFC) and cognitive control is mixed.[4,7] This study aimed to identify the brain's regulation of feeding behavior in response to food cues, which could be a potential neuromodulatory intervention target in adults with obesity.

METHODS

This was a cross-sectional study with no control group that examined the effects of brain activity on adult obesity using EEG. The study was conducted at Cipto Mangunkusumo Hospital from October 2022 to May 2023 on participants who fulfilled the study criteria. The study protocol was approved by the Ethics Committee of the Faculty of Medicine, Universitas Indonesia, Cipto Mangunkusumo Hospital, Jakarta (No: KET-1236/UN2.F1/ETIK/PPM.00.02/2022).

Sample size

This was a large pre-intervention study employing a sample size formula designed for unpaired analytical research. Based on the research by Yeo et al,[8] the analysis of weight loss in patients with obesity had a mean difference of –2.05 (experimental mean –4.25 and control mean –2.2), standard deviation (SD) 2.03 in the experimental group, the SD was 1.9 in the control group ($p<0.05$), and the ratio of sample sizes between groups was 0.20. Calculations were performed using the MedCalc® statistical software version 20.111 (MedCalc Software Ltd., Belgium), and a minimum sample size obtained was 40, with an anticipation of 20% dropout.

Participants selection

Participants were recruited through advertisements on social media and banners placed at Cipto Mangunkusumo Hospital. Telephone screening was performed to evaluate the inclusion and exclusion criteria before scheduling the direct interviews and examinations. The inclusion criteria were females or males aged 19–35 years, body mass index (BMI) of ≥25.0 kg/m^2, waist circumference of ≥80 cm (woman) or ≥90 cm (man), agreed on signing informed consent. Participants were measured using calibrated scales and defined as obese according to the Asia-Pacific guidelines. Exclusion criteria for both groups were a history of epilepsy, diabetes mellitus, thyroid disease, medication intake affecting body weight, history of hormonal contraception, and pregnancy. Clinical data were obtained from direct observation and medical records. Figure 1 shows a flow diagram of the participant recruitment process and the number of eligible participants.

Procedure

Eligible participants (n = 40) were selected based on their medical history and physical examination screening. The screening and anthropometric examinations were conducted by a trained medical doctor using standardized procedures. Body weight was measured to the nearest 0.1 kg (in light clothes and without shoes) using a body composition analyzer (TANITA, BC-541, Tanita Corporation, Japan). The participants were instructed to stand at the center of the scale and look straight ahead with both arms in the resting position.[9] Height was measured to the nearest 0.1 cm without shoes on a stadiometer (Charder version ADE M320600-01, ADE Germany GmbH, Germany). Participants were instructed to stand barefoot on the stadiometer, and body height was measured as the distance between the soles of the feet and crown of the head. The back of the head, shoulder blades, buttocks,

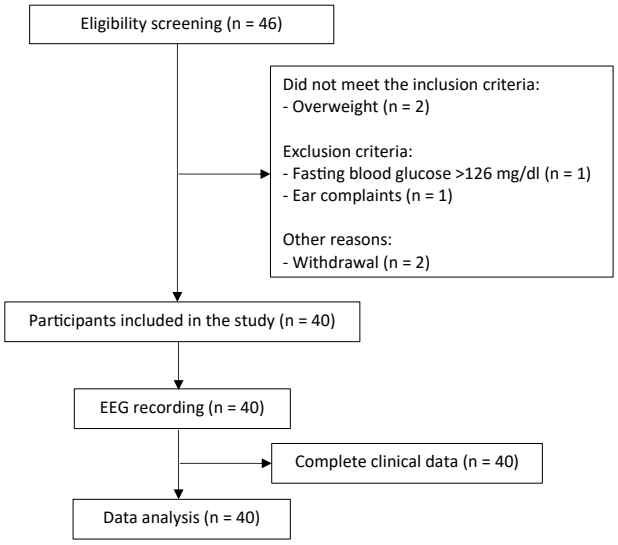

Figure 1. Flow diagram of the eligible participants. EEG= electroencephalography

Table 1. PSD during eyes-open condition *versus* food provocation

Scalp sites	Delta	Theta	Alpha	Beta	Gamma
FP1	0.4296	0.4326	0.7275	0.2261	0.8963
FP2	0.9744	0.8149	0.6874	0.6828	0.5987
F7	0.1303	**0.0327***	0.7535	**0.0407***	0.0799
F8	0.2377	**0.0229***	0.8483	0.1846	0.1685
F3	0.7709	0.2577	0.8409	0.4916	0.6872
F4	0.4068	0.6224	0.9839	0.8630	0.5503
C3	0.3897	**0.0464***	**0.0201***	0.6166	**0.0019***
C4	0.1023	0.0529	**0.0392***	0.4589	**0.0237***
P3	0.4034	**0.0252***	**0.0170***	0.9612	**0.0002***
P4	0.2332	**0.0081***	**0.0012***	0.8561	**0.0001***

C3=left central; C4=right central; FP1=left prefrontal; FP2=right prefrontal; F3=left frontal; F4=right frontal; F7=left frontal; F8=right frontal; PSD=power spectrum density; P3=left parietal; P4=right parietal
*Student's *t*-test, significant if $p<0.05$

and heels should be aligned with the stadiometer.[9] BMI was calculated by dividing the weight (kg) by the square of the height (m^2). Based on the Asia-Pacific guidelines, participants were classified as obese I (BMI of ≥25 kg/m^2) and II (BMI of ≥30 kg/m^2).[10] Waist circumference (cm) was measured at the midpoint between the lower margin of the least palpable rib and the top of the iliac crest at the umbilicus. The measurement was recorded at the end of a normal expiration.[11] All participants gave written informed consent before participating in the study, followed by EEG recordings.

EEG recordings

Participants fasted for 4–6 hours prior to EEG recordings. A 32-channel Easy III amplifier (Cadwell, USA) was used, and EEG signals were recorded over 19 scalp sites: prefrontal (channels FP1 and FP2); frontal (channels F3, F4, F7, F8, and Fz); central (channels C3, C4, and Cz); medial temporal (channels T3 and T4); posterior temporal (channels T5 and T6); parietal (channels P3, P4, and Pz); and occipital (channels O1 and O2) regions.[12] The gold cup electrodes were positioned according to the standard 10–20 international placement. The patient laid back in a semi-Fowler position in a silent room and was positioned in a quiet room for approximately 20 min. The recordings comprised specific segments, including 3 min of eyes-closed and 3 min of eyes-open condition without food cues. Following this, there was a 3-min period with high-calorie food cues, followed by another 3 min of eyes-closed and 3 min of eyes-open condition without food cues. Participants were presented with prepared instant noodles, a high-calorie food popular among Indonesians. The provocation of high-calorie food was provided 30 cm away from the participants for 3 min of eye-open condition. Artifact rejection (eye movements, blinks, muscular activations, or movement artifacts) was visually performed on the raw EEG, and the recordings were attended by trained technicians.

Pre-processing and analysis of EEG recordings

EEG was compared between participants during eyes-open condition *versus* provocation with food for each frequency band. A high-pass filter of 1 Hz, band-stop filter of 49–51 Hz, and low-pass filter of 100 Hz were used to filter the EEG signals. Following this, the EEG was filtered using a fourth-order Butterworth filter. Independent component analysis and visual rejection were applied to filter out artifacts and remaining impurities.

The extracted filtered EEG data included delta (1–4 Hz), theta (4–8 Hz), alpha (8–13 Hz), beta (13–30 Hz), and gamma (30.5–60 Hz). The EEG signals analyzed were 10 channels, and the extracted absolute power for each frequency band was grouped for frontal (FP1, FP2, F3, F4, F7, and F8); central (C3 and C4); and parietal (P3 and P4) and converted to a signal spectrum (microVolt^2/Hz).

Data analysis

Power spectral density (PSD) was processed using the P-Welch method, and PSD normalization

was performed for comparison. The plot spectrum and topographic plot are visually presented. Shapiro–Wilk tests were conducted to examine data normality, and Levene's test was performed to examine the homogeneity of variance. Student's *t*-tests were performed to assess significant differences between groups and are presented as bar plots. The level of significance was set at a *p*-value of <0.05. All EEG analysis and statistics were performed by the Matlab® R2021a software (Mathworks Inc., Germany).

RESULTS

EEG recordings suitable for analysis were obtained from all patients. The total mean PSD and topographic PSD plots are shown in Figure 2, consisting of 10 subfigures representing the 10 selected channels. The x-axis of the figure shows the frequency (Hz), and the y-axis of the figure shows the normalized PSD (microVolt^2/Hz). The topographic plot was divided into five frequency ranges (delta, theta, alpha, beta, and gamma). The color bar shows the normalized PSD values based on the mean frequency ranges and the mean of all participants.

Bar plots PSD comparison between eyes-open and provocation of all participants are shown in Figure 3. Beta activity was significantly increased in the left frontal (F7) during the food-cue condition compared with the eyes-open condition. Additionally, gamma activity showed an overall increase, with significant increases in the left and right central (C3 and C4 [p<0.05]) and the left and right parietal (P3 and P4 [p<0.001]).

In contrast, theta activity decreased across all channels. However, the decrease was significant in specific areas, namely, the left and right frontal (F7 and F8), left central (C3), and left and right parietal (P3 [p<0.05] and P4 [p<0.01]). Finally, alpha activity exhibited a significant decrease in the left and right central (C3 and C4) and left and right parietal (P3 [p<0.05] and P4 [p<0.01]) (Tables 1 and 2).

DISCUSSION

Food consumption is influenced by both physiological hunger and the rewarding properties of food, indicating that human eating behavior results from a combination of needs (homeostasis) and desires (reward). The brain plays a crucial role in mediating the incentive value of food, attention allocation to food cues, and the motivation to obtain food rewards. It involves complex interactions within key brain regions, including the amygdala/hippocampus, insular cortex, orbitofrontal cortex, and striatum.[4,5,12] Pleasurable sensations and rewards are achieved by activating various neural circuits such as the dopaminergic, gamma-aminobutyric acid, opioid, and serotonergic pathways. These neural pathways, originating from the ventral tegmental area and substantia nigra pars compacta, regulate food consumption, and are implicated in addiction-related behaviors. The mesocortical and mesolimbic tracts of these circuits are particularly active during reward-seeking behaviors, including those related to pleasurable food intake. Interestingly, individuals with obesity and drug addicts show similar abnormalities in these neural pathways, such as increased anticipation of pleasure in response to rewards; however, a blunted pleasure response upon reward attainment.[5] Brain wave alterations in specific areas related to food regulation were identified in adult obesity when stimulated with food, suggesting an enhanced recognition of food cues, intensified concentration of food-related stimuli, and underlying impairments in executive functions.

This study showed greater beta activity in the left frontal lobe (F7) (p = 0.0407) during food cues than during the eyes-open condition. Consistent with the present study, Kösling et al[7] showed that overweight or obese children had increased beta activity when provoked by images of high-calorie food. The food stimulus was more effective than the landscape picture as it triggered higher levels of beta activity in the brain during the experiment. The human brain appears to be particularly responsive to food-related stimuli; studies have shown that displaying such stimuli can significantly increase brain metabolism in fasting, normal-weight individuals.[13] This result aligns with some studies showing a significant elevation in frontal beta activity, suggesting increased awareness of food cues and heightened attentional focus toward food stimuli.[13,14] Unlike the present study, Tammela et al[13] did not find differences in beta activity between the left and right frontal regions in their study. Greater increases in gamma activity were identified in the left and right central (C3 [p = 0.0019] and C4 [p = 0.0237]) and the left and right parietal (P3 [p = 0.0002] and P4 [p = 0.0001]) regions. Elevated gamma activity

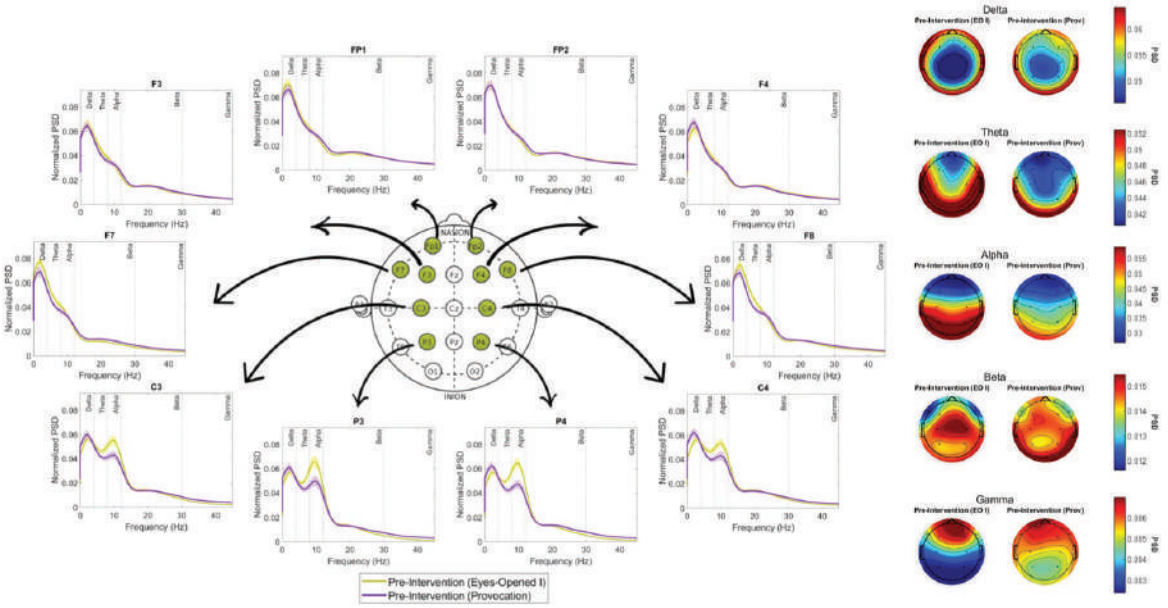

Figure 2. Total mean (grand mean) PSD along with the SEM of all participants (n = 40) during eyes-open condition and provocation (left). Yellow PSD and SEM represented eyes-open condition, while purple represented provocation. Topographic PSD plot of pre-intervention participants (n = 40) during eyes-open condition and provocation (right). Dark blue indicated low, and dark red indicated high. C3=left central; C4=right central; EO=eyes-open; FP1=left prefrontal; FP2=right prefrontal; F3=left frontal; F4=right frontal; F7=left frontal; F8=right frontal; O1, O2=occipital region; PSD=power spectrum density; P3=left parietal; P4=right parietal; SEM=standard error of the mean; T3, T4=medial temporal; T5, T6=posterior temporal

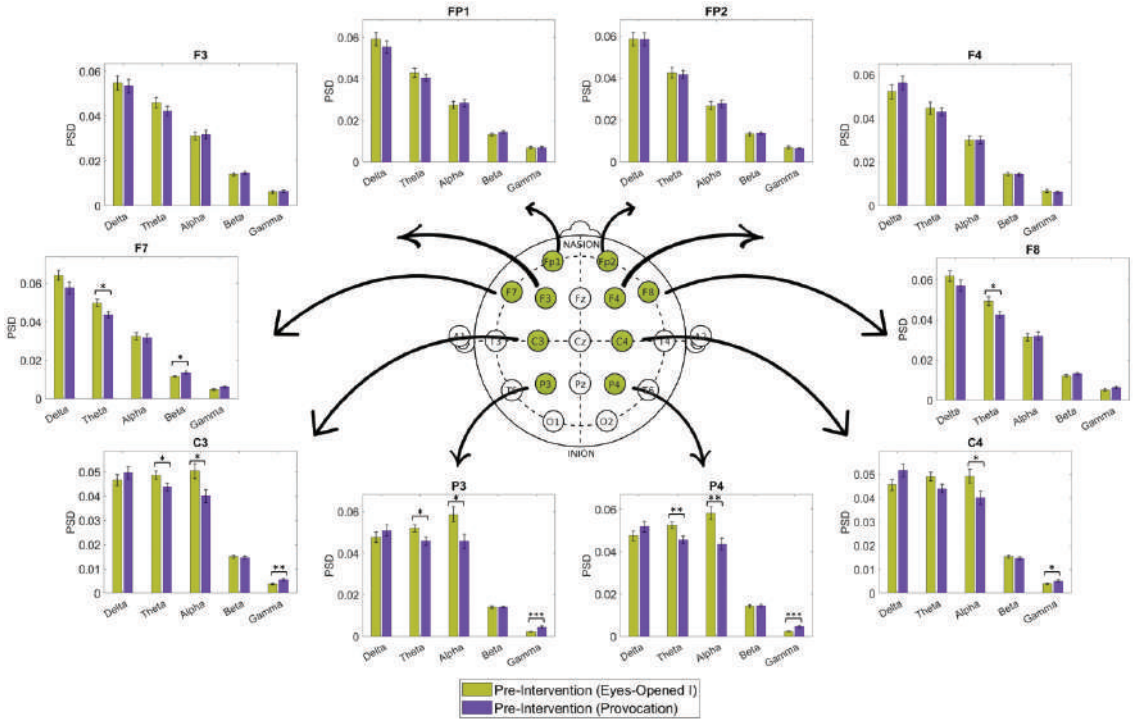

Figure 3. Bar plot PSD comparison between eyes-open and provocation of all participants. It consisted of 10 subfigures, representing the 10 selected channels/electrodes. The x-axis showed frequency ranges respectively (delta, theta, alpha, beta, and gamma), while the y-axis showed the normalized PSD (unit: microVolt^2/Hz) for each frequency range. The yellow bar showed the normalized grand mean PSD during eyes-open, the purple bar showed the normalized grand mean PSD during provocation. The line at the top of each bar represented the normalized mean (SEM) of PSD for each frequency range. *Significant if $p \leq 0.05$. C3=left central; C4=right central; EO=eyes-open; FP1=left prefrontal; FP2=right prefrontal; F3=left frontal; F4=right frontal; F7=left frontal; F8=right frontal; O1, O2=occipital region; PSD=power spectrum density; P3=left parietal; P4=right parietal; SEM=standard error of the mean; T3, T4=medial temporal; T5, T6=posterior temporal

Table 2. PSD during eyes-open condition *versus* food provocation

Scalp sites	Mean (SEM)									
	Delta		Theta		Alpha		Beta		Gamma	
	EO	Provocation	EO	Provocation	EO	Provocation	EO	Provocation	EO	Provocation
FP1	0.0592 (0.0033)	0.0554 (0.0031)	0.0429 (0.0022)	0.0405 (0.0018)	0.0274 (0.0017)	0.0284 (0.0018)	0.0131 (0.0007)	0.0145 (0.0007)	0.0069 (0.0007)	0.0070 (0.0005)
FP2	0.0585 (0.0032)	0.0584 (0.0031)	0.0425 (0.0024)	0.0417 (0.0018)	0.0267 (0.0019)	0.0278 (0.0017)	0.0133 (0.0007)	0.0137 (0.0007)	0.0070 (0.0007)	0.0065 (0.0005)
F7	0.0642 (0.0026)	0.0576 (0.0031)	0.0498 (0.0020)	0.0436 (0.0018)	0.0324 (0.0019)	0.0315 (0.0020)	0.0116 (0.0006)	0.0135 (0.0007)	0.0048 (0.0005)	0.0060 (0.0005)
F8	0.0617 (0.0026)	0.0569 (0.0028)	0.0493 (0.0022)	0.0425 (0.0018)	0.0314 (0.0018)	0.0319 (0.0020)	0.0121 (0.0006)	0.0133 (0.0006)	0.0051 (0.0005)	0.0062 (0.0005)
F3	0.0548 (0.0032)	0.0534 (0.0031)	0.0460 (0.0023)	0.0423 (0.0021)	0.0312 (0.0018)	0.0317 (0.0020)	0.0139 (0.0007)	0.0146 (0.0008)	0.0061 (0.0006)	0.0064 (0.0005)
F4	0.0522 (0.0032)	0.0562 (0.0032)	0.0448 (0.0027)	0.0431 (0.0020)	0.0300 (0.0020)	0.0301 (0.0017)	0.0144 (0.0008)	0.0142 (0.0008)	0.0067 (0.0007)	0.0062 (0.0005)
C3	0.0467 (0.0023)	0.0498 (0.0026)	0.0488 (0.0016)	0.0438 (0.0017)	0.0504 (0.0031)	0.0401 (0.0027)	0.0152 (0.0007)	0.0147 (0.0006)	0.0037 (0.0003)	0.0056 (0.0005)
C4	0.0456 (0.0022)	0.0517 (0.0027)	0.0491 (0.0018)	0.0439 (0.0018)	0.0492 (0.0029)	0.0402 (0.0029)	0.0155 (0.0007)	0.0147 (0.0007)	0.0039 (0.0003)	0.0052 (0.0005)
P3	0.0477 (0.0026)	0.0510 (0.0027)	0.0521 (0.0016)	0.0459 (0.0020)	0.0588 (0.0037)	0.0458 (0.0035)	0.0142 (0.0007)	0.0141 (0.0006)	0.0024 (0.0002)	0.0045 (0.0005)
P4	0.0474 (0.0023)	0.0518 (0.0025)	0.0524 (0.0016)	0.0455 (0.0018)	0.0581 (0.0030)	0.0435 (0.0029)	0.0144 (0.0007)	0.0145 (0.0006)	0.0025 (0.0002)	0.0047 (0.0005)

C3=left central; C4=right central; EO=eyes-open; FP1=left prefrontal; FP2=right prefrontal; F3=left frontal; F4=right frontal; F7=left frontal; F8 = right frontal; PSD=power spectrum density; P3=left parietal; P4=right parietal; SEM=standard error of the mean
Normalized PSD (per participant, per channel) was PSD per frequency point (per participant, per channel) divided by sum of the data (per participant, per channel)

suggests that a higher conflict situation needs to be resolved during food stimuli. However, studies on gamma radiation activity are limited.

Theta activity was significantly decreased in the left and right frontal (F7 [p = 0.0327] and F8 [p = 0.0229]), left central (C3) (p = 0.0464), left parietal (P3) (p = 0.0252), and right parietal (P4) (p = 0.0081) regions during food cues compared to when eyes were open. Hume et al[5] found that adults with obesity displayed lower theta activity than that in those without obesity. However, no significant effects were observed on theta activity during food cues. In contrast, Imperatori et al[15] observed increased frontal theta activity in adults who were overweight or obese and had symptoms of food addiction compared to weight-matched controls without food addiction after consuming a single milkshake. Theta activity may indicate cognitive control and is potentially relevant for food cue reactivity in obesity.[16]

The alpha activity was significantly decreased in the left and right central (C3 [p = 0.0201] and C4 [p = 0.0392]) and the left and right parietal (P3 [p<0.05] and P4 [p<0.01]) regions. This result contrasts with that of Kösling et al[7] who found no significant differences in alpha and theta activities between overweight/obese and normal-weight children. The specific areas mentioned above are similar to those in a functional magnetic resonance imaging study by Davids et al,[4] which showed increased activity in the dorsal PFC of individuals during food-related stimuli. This increased PFC activity is associated with various cognitive processes related to top-down control, particularly executive function, goal selection, planning, information manipulation, and response inhibition. As the level of emotional or cognitive conflict increases, the PFC activation also increases. In particular, food cues may induce a higher level of conflict as they exclusively result in heightened PFC activation. Intensified dorsal PFC activity may suppress appetitive reactions or approach behaviors triggered by food cues, leading to avoidance. Greater activation of the PFC indicates a greater need for inhibitory

control, suggesting that when faced with food-related cues, stronger regulation by the PFC is necessary to generate appropriate behavior. These specific areas of the PFC are often referred to as the "satiation domain" since they contribute to the termination of the feeding period by suppressing subcortical areas associated with hunger, such as the limbic/paralimbic areas, basal ganglia, thalamus, and hypothalamus. In individuals with obesity, the network responsible for promoting hunger (known as the orexigenic network) is consistently hyperactive, requiring increased effort from the PFC areas to suppress these hunger centers. Reduced neural activation in the putamen and amygdala results in difficulties activating the reward system in response to food cues. Furthermore, reduced hippocampal activation contributes to a decreased ability to regulate feeding behavior.

The results of this study can potentially serve as neuromodulatory intervention targets for adult obesity. However, this study was limited by the small number of EEG channel analyses (10); a greater number of electrodes would have allowed more detailed topographical analyses to assess other brain activity changes. Additional longitudinal studies are required to determine the association between feeding behavior and EEG changes.

In conclusion, increased beta activity in the frontal and gamma in the central and parietal regions suggested increased awareness of food cues and heightened attentional focus toward food stimuli. Additionally, decreased alpha and theta activity in the frontal regions may underlie deficits in executive function and higher motivation.

Conflict of Interest

Pradana Soewondo is the editorial board member but was not involved in the review or decision making process of the article.

Acknowledgment

This work was supported by Universitas Indonesia and Cipto Mangunkusumo Hospital, Jakarta.

Funding sources

None.

REFERENCES

1. Gadde KM, Martin CK, Berthoud HR, Heymsfield SB. Obesity: pathophysiology and management. J Am Coll Cardiol. 2018;71(1):69–84.
2. Health Research and Development Agency (*Balitbangkes*) Ministry of Health Republic of Indonesia. Basic health research (*RISKESDAS* 2018) [Internet]. Health Research and Development Agency (*Balitbangkes*) Ministry of Health Republic of Indonesia; 2018 [cited 2021 Aug 3]. Available from: http://www.depkes.go.id/resources/down load/info- terkini/materi_rakorpop_2018/Hasil%20 Riskesdas%202018.pdf.
3. Boswell RG, Kober H. Food cue reactivity and craving predict eating and weight gain: a meta-analytic review. Obes Rev. 2016;17(2):159–77.
4. Davids S, Lauffer H, Thoms K, Jagdhuhn M, Hirschfeld H, Domin M, et al. Increased dorsolateral prefrontal cortex activation in obese children during observation of food stimuli. Int J Obes (Lond). 201;34(1):94–104.
5. Hume DJ, Howells FM, Rauch HG, Kroff J, Lambert EV. Electrophysiological indices of visual food cue-reactivity. Differences in obese, overweight and normal weight women. Appetite. 2015;85:126–37.
6. World Health Organization (WHO). Waist circumference and waist-hip ratio: report of a WHO expert consultation, Geneva, 8–11 December 2008. World Health Organization (WHO); 2011. p. 3.
7. Kösling C, Schäfer L, Hübner C, Sebert C, Hilbert A, Schmidt R. Food-induced brain activity in children with overweight or obesity versus normal weight: an electroencephalographic pilot study. Brain Sci. 2022;12(12):1653.
8. Samara A, Li X, Pivik RT, Badger TM, Ou X. Brain activation to high-calorie food images in healthy normal weight and obese children: a fMRI study. BMC Obes. 2018;5:31.
9. van Meer F, van der Laan LN, Charbonnier L, Viergever MA, Adan RA, Smeets PAet al,. Developmental differences in the brain response to unhealthy food cues: an fMRI study of children and adults. Am J Clin Nutr. 2016;104(6):1515–22.
10. Yeo S, Kim KS, Lim S. Randomised clinical trial of five ear acupuncture points for the treatment of overweight people. Acupunct Med. 2014;32(2):132–8.
11. Centers for Disease Control and Prevention (CDC). National Health and Nutrition Examination Survey (NHANES): anthropometry procedures manual. Centers for Disease Control and Prevention (CDC); 2007.
12. World Health Organization (WHO) Regional Office for the Western Pacific. The Asia-Pacific perspective: redefining obesity and its treatment. Sydney: Health Communications Australia; 2000.
13. Tammela LI, Pääkkönen A, Karhunen LJ, Karhu J, Uusitupa MI, Kuikka JT. Brain electrical activity during food presentation in obese binge-eating women. Clin Physiol Funct Imaging. 2010;30(2):135–40.
14. Hume DJ, Howells FM, Karpul D, Rauch HG, Kroff J, Lambert EV. Cognitive control over visual food cue saliency is greater in reduced-overweight/obese but not in weight relapsed women: An EEG study. Eat Behav. 2015;19:76–80.
15. Imperatori C, Fabbricatore M, Innamorati M, Farina B, Quintiliani MI, Lamis DA, et al. Modification of EEG functional connectivity and EEG power spectra in overweight and obese patients with food addiction: an eLORETA study. Brain Imaging Behav. 2015;9(4):703–16.
16. Blume M, Schmidt R, Hilbert A. Abnormalities in the EEG power spectrum in bulimia nervosa, binge-eating disorder, and obesity: a systematic review. Eur Eat Disord Rev. 2019;27(2):124–36.

Clinical Research

Coagulation factors as potential predictors of COVID-19 patient outcomes

Dwi Anggita, Irawaty Djaharuddin, Harun Iskandar, Nur Ahmad Tabri, Jamaluddin Madolangan, Harry Akza Putrawan, Edward Pandu Wiriansya

pISSN: 0853-1773 • eISSN: 2252-8083
https://doi.org/10.13181/mji.oa.236992
Med J Indones. 2023;32:105–11

Received: June 01, 2023
Accepted: September 18, 2023

Authors' affiliations:
Department of Pulmonology and Respiratory Medicine, Faculty of Medicine, Universitas Hasanuddin, Makassar, Indonesia

Corresponding author:
Irawaty Djaharuddin
Department of Pulmonology and Respiratory Medicine, Universitas Hasanuddin Hospital Building A 2nd Floor, Jalan Perintis Kemerdekaan, Tamalanrea, Makassar, South Sulawesi 90245, Indonesia
Tel/Fax: +62-411-591210/ +62-411-591332
E-mail: irawatydjaharuddin@unhas.ac.id

ABSTRACT

BACKGROUND Causes of death and length of hospitalization in patients with COVID-19 have been associated with coagulopathy. The coagulopathy mechanism involves the process of coagulation and endothelial damage triggered by an inflammatory response of the SARS-CoV-2 infection due to excessive release of proinflammatory cytokines. This study aimed to determine the association of coagulation factors as potential predictors of COVID-19 patient outcomes.

METHODS This retrospective study was performed on 595 patients at Wahidin Sudirohusodo Hospital, Makassar, from June 2020 to June 2021. Participants were recruited using total sampling and assessed for COVID-19 severity using the World Health Organization classification and coagulation factors (D-dimer, fibrinogen, thrombocyte, and prothrombin time [PT]). Patient outcome assessments were survival and length of hospitalization.

RESULTS We found a significant sex-based disparity, with a higher COVID-19 incidence in males. Severe cases were more common among those aged >50 years, with prolonged hospitalization (>10 days) linked to higher severity (odds ratio [OR] = 2.22, 95% confidence interval [CI] = 1.31–3.77, $p<0.001$). Elevated fibrinogen and D-dimer levels, as well as prolonged PT, predicted severe cases. However, D-dimer had the highest influence compared to other coagulation factors (OR = 14.50, 95% CI = 5.85–35.95, $p<0.001$), while prolonged PT influenced mortality rates (OR = 4.02, 95% CI = 1.35–12.00, $p = 0.01$).

CONCLUSIONS Coagulation factors, such as elevated D-dimer and fibrinogen levels and prolonged PT, predicted the severity of COVID-19 patients leading to death.

KEYWORDS blood coagulation factors, COVID-19, patient outcome assessment

The World Health Organization (WHO) has reported more than 583 million confirmed coronavirus disease 2019 (COVID-19) cases and more than six million deaths by August 2022. The prevalence of COVID-19 demonstrates how effectively it spreads through droplet respiration in local populations. Although symptom variability exists among individuals, the average incubation period of COVID-19 is predicted to be 6.57 days.[1–3] COVID-19 symptoms include fever, chills, cough, runny nose, sore throat, breathing difficulties, myalgia, nausea, vomiting, and diarrhea. Although some patients remain asymptomatic, others may experience severe respiratory conditions such as acute respiratory distress syndrome or systemic infections, leading to multiorgan failure and death.[4–6] The inflammatory reaction in patients with COVID-19 releases proinflammatory cytokines that activate the coagulation system and host defense mechanisms, leading to disseminated intravascular coagulation. The cytokine storm enabled by the excessive inflammatory

response also causes increased coagulation factors and D-dimer levels, called COVID-19-associated coagulopathy.[7,8]

Coagulation abnormalities are also associated with severe cases of COVID-19. Several studies have agreed that coagulation factors strongly influence the outcomes of patients with COVID-19, such as prolonged prothrombin time (PT), elevated D-dimer and fibrinogen levels, and thrombocytopenia.[9–15] However, other studies have found standard coagulation factors, such as platelets and fibrinogen. These factors are influenced by various individual and population factors related to race and ethnicity.[16,17] Few studies exist, especially in Indonesia, that examine the relationship between coagulation factors and outcomes in patients with COVID-19, with a variable focus on confounding factors. Therefore, this study aimed to determine the influence of coagulation factors as potential predictors of the outcomes in patients with COVID-19 based on disease severity, survival, and length of hospitalization.

METHODS

Research design and patient selection

This retrospective study used the medical records of all patients with COVID-19 at Wahidin Sudirohusodo Hospital, Makassar, from June 2020 to June 2021. Participants who met the inclusion and exclusion criteria were selected using total sampling. The inclusion criteria were patients who tested positive for the virus that causes COVID-19, at least 18 years of age, and had complete laboratory data on D-dimer, fibrinogen, platelets, and PT levels, as well as data on the length of hospitalization and discharge status. Patients who requested hospital discharge were excluded. Additionally, we included data on comorbidities that contributed to the development of COVID-19, including active smoking, pulmonary tuberculosis, chronic liver disease, malignancy, diabetes mellitus, hypertension, cardiovascular diseases (coronary artery disease, hypertensive heart disease, and congestive heart failure), chronic kidney disease, autoimmune disease, and HIV infection.

Severity classification and measurement of patient outcomes

The severity of COVID-19 was evaluated using the WHO severity classification. Severe illness was defined as oxygen saturation below 90% with room air, signs of pneumonia, respiratory distress characterized using accessory respiratory muscles, inability to complete a sentence, and respiratory rate >30 breaths per min. Non-severe illness classification was based on the absence of signs of a severe illness. Coagulation factors that were measured during hospitalization, but not limited to hospital admission, such as platelet/thrombocyte (normal range 150×10^3–400×10^3/µl), PT (normal value 10–14 sec), D-dimer (normal value <0.5 µg/ml), and fibrinogen (normal value 150–375 mg/dl) were obtained through medical records. Additionally, patient outcomes such as survival status and length of hospitalization were obtained from medical records. Based on Lucijanic et al,[18] a median of 10 days was the cut-off for determining the length of hospitalization.

Statistical analysis

The collected data samples were grouped according to their purpose and were not normally distributed. Statistical analyses were performed using Microsoft Excel 2020 (Microsoft Corp., USA) and SPSS software version 26 (IBM Corp., USA). Univariate analysis was used to describe the general characteristics, and bivariate analysis using the chi-square test was used to determine the correlation between categorical data. Multivariate binary logistic regression analysis was performed to determine the influence of variables on COVID-19 severity and patient survival. Ethical approval was obtained from the Ethics Committee of the Faculty of Medicine, Universitas Hasanuddin (No: 38/UN4.6.4.5.31/PP36/2023).

RESULTS

The review of medical records was conducted from January to April 2023, with a total sample of 595 patients screened based on the inclusion and exclusion criteria. We efficiently assessed the severity of COVID-19, coagulation factors, and patient outcomes, all at a relatively low cost. The participant selection flowchart is shown in Figure 1.

Furthermore, we reported the distribution of baseline demographic characteristics (age and sex), comorbidities, independent variables of coagulation factors (thrombocytes, fibrinogen, D-dimer, and PT), patient outcomes (survival, non-survival, and length of hospitalization), and COVID-19 severity (severe and non-severe) as dependent variables (Table 1).

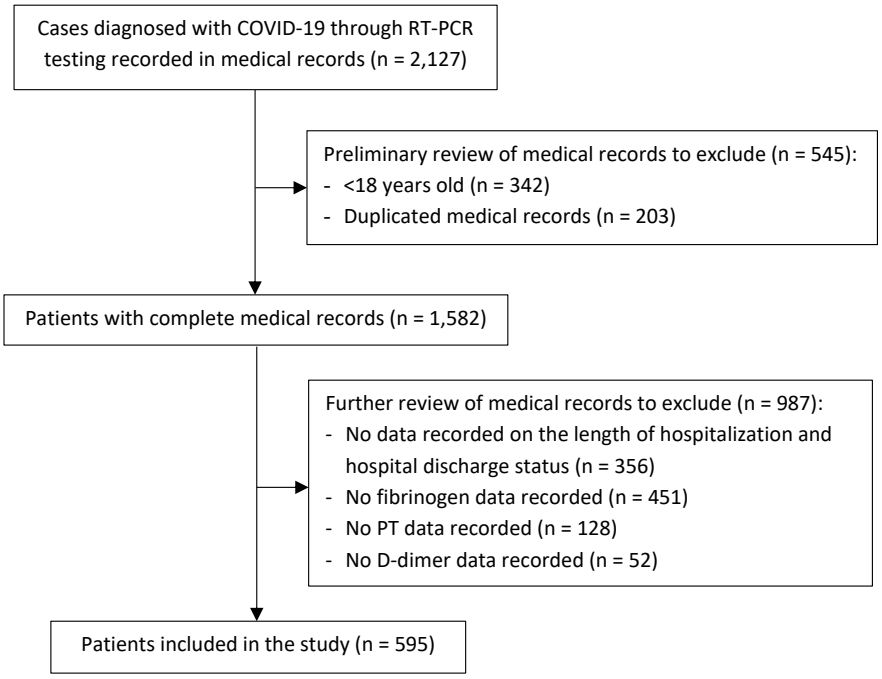

Figure 1. Patient selection diagram. COVID-19=coronavirus disease 2019; PT=prothrombin time; RT-PCR=real time-polymerase chain reaction

Table 1. Patient characteristics

Characteristics	N = 595
Male sex, n (%)	291 (48.9)
Age (years), n (%)	
≤50	362 (60.8)
>50	233 (39.2)
Comorbidities, n (%)	
Smoker	78 (13.1)
Lung tuberculosis	14 (2.4)
Liver disease	40 (6.7)
Malignancies	65 (10.9)
Diabetes mellitus	106 (17.8)
Hypertension	138 (23.2)
Cardiovascular disease	104 (17.5)
Chronic kidney disease	53 (8.9)
Autoimmune	5 (0.8)
HIV	3 (0.5)
Length of stay (days), mean (SD)	10 (6)
Survive, n (%)	520 (87.4)
Severe COVID-19, n (%)	75 (12.6)
Coagulation factors, mean (SD)	
Thrombocyte (/µl)	286.078 (121.347)
Fibrinogen (mg/dl)	360.61 (158.44)
D-dimer (mg/l)	3.90 (11.14)
PT (sec)	11.23 (1.64)

COVID-19=coronavirus disease 2019; PT=prothrombin time; SD=standard deviation

Subsequently, bivariate and multivariate analyses were performed to ascertain the interplay between the variables and their impact on the severity of COVID-19 (Table 2) and survival groups (survivor and non-survivor) (Table 3). Analyses of these two dependent variables revealed a notable sex-based disparity with a higher incidence in males. A distinct distribution pattern in age stratification was observed; most patients with COVID-19 aged >50 years had severe disease and high mortality rates. Exploring the impact of the length of hospitalization on severity, the severe group generally required a significantly extended hospitalization of more than 10 days (odds ratio [OR] = 2.22, 95% confidence interval [CI] = 1.31–3.77, $p<0.001$). The survivor group had an average stay within 10 days, but there was no statistically significant effect (OR = 0.77, 95% CI = 0.46–1.29, $p = 0.32$). In terms of coagulation factors, elevated D-dimer levels (OR = 14.50, 95% CI = 5.85–35.95, $p<0.001$) had the highest statistically significant OR to predict severe COVID-19 cases. Among all variables examined, only prolonged PT significantly influenced the mortality rate of patients with COVID-19.

DISCUSSION

This study found a statistically significant relationship between the severity of COVID-19, coagulation factors, and patient outcomes. Several previous studies

Table 2. Variables associated with COVID-19 severity

Variables	Severe (N = 138)	Non-severe (N = 457)	Bivariate analysis*		Multivariate analysis†	
			OR (95% CI)	*p*	OR (95% CI)	*p*
Sex, n (%)				**<0.001**		**0.004**
Male	90 (65.2)	201 (44.0)	1.00		1.00	
Female	48 (34.8)	256 (56.0)	0.42 (0.28–0.62)		0.44 (0.25–0.77)	
Age (years), n (%)				**<0.001**		**<0.001**
≤50	47 (34.1)	315 (68.9)	4.23 (2.87–6.43)		2.97 (1.66–5.32)	
>50	91 (65.9)	142 (31.1)	1.00		1.00	
Length of stay (days), mean (SD)	11.78 (7.59)	9.83 (5.99)				
>10, n (%)	68 (49.3)	167 (36.5)	1.68 (1.15–2.47)	**<0.001**	2.22 (1.31–3.77)	**<0.001**
Platelets (/µl), mean (SD)	265,442.03 (118,680.95)	292,309.19 (121,580.27)				
<150,000, n (%)	21 (15.2)	36 (7.9)	2.09 (1.18–3.73)	0.10	0.80 (0.34–1.85)	0.60
Fibrinogen (mg/dl), mean (SD)	405.54 (195.14)	347.05 (143.05)				
>375, n (%)	73 (52.9)	153 (33.5)	2.23 (1.51–3.28)	**<0.001**	1.52 (0.88–2.61)	**0.02**
D-dimer (µg/ml), mean (SD)	9.85 (18.61)	2.10 (6.61)				
≥0.5, n (%)	131 (94.9)	217 (47.5)	20.69 (9.46–45.25)	**<0.001**	14.50 (5.85–35.95)	**<0.001**
PT (sec), mean (SD)	12.25 (2.28)	10.93 (1.25)				
≥14	19 (13.8)	12 (2.6)	5.92 (2.79–12.54)	**<0.001**	2.16 (0.77–6.03)	**0.01**

CI=confidence interval; COVID-19=coronavirus disease 2019; OR=odds ratio; PT=prothrombin time; SD=standard deviation
*Chi-square test, significant if $p<0.05$; †binary logistic regression test, significant if $p<0.05$

have been conducted on the relationship between fibrinogen levels and COVID-19 severity,[19–23] showing significant fibrinogen values in severe COVID-19 cases compared to non-severe cases. Plasma fibrinogen levels exhibit rapid escalation in pathological states such as injury, infection, and inflammation, which are crucial in facilitating fibrinolysis, resulting in damage to vascular endothelial cells. In patients with COVID-19, inflammation can directly target vascular endothelial cells and initiate coagulation. Consequently, a salient hallmark of COVID-19 resides in its acute-phase procoagulant response, whereby acute-phase reactants are associated with an elevated risk of thrombosis and are intrinsically linked to increased fibrinogen levels.[20,24]

D-dimer, a product of fibrin breakdown triggered by endothelial damage, inflammation, or insufficient oxygen in the blood (hypoxemia), can increase owing to intensified inflammation as COVID-19 severity escalates, prompting increased fibrin degradation and, consequently, elevated D-dimer levels.[19] These elevated D-dimer levels are frequently associated with the severity of COVID-19 and are linked to unfavorable outcomes. Higher D-dimer concentrations can worsen conditions by promoting clot formation within the pulmonary veins, leading to venous thromboembolism.[24] Elevated D-dimer levels may indicate a severe viral infection. Viral infections progressing to sepsis can disturb coagulation, which is common in severe disease progression, especially for COVID-19. In addition, elevated D-dimer levels are indirectly associated with inflammatory reactions, as inflammatory cytokine responses can disrupt the coagulation-fibrinolysis balance in pulmonary alveoli, leading to activation of the fibrinolysis system and increased D-dimer levels.[25]

Prolonged PT is another coagulation factor contributing to elevated fibrinogen and D-dimer levels. In the present study, prolonged PT in both dependent groups was associated with COVID-19 severity. While previous research generally concurs about the significance of fibrinogen and D-dimer levels, studies on the relationship between PT and disease severity have yielded conflicting results. Di Minno et al[21] and Zhang et al[22] observed significant PT prolongation in patients with severe COVID-19 compared with non-severe cases. The viral presence in COVID-19 incites the extrinsic coagulation pathway via prothrombin-to-thrombin transformation, which is characterized

Table 3. Variables associated with survival

Variables	Survive (N = 522)	Non-survive (N = 73)	Bivariate analysis*		Multivariate analysis†	
			OR (95% CI)	*p*	OR (95% CI)	*p*
Sex, n (%)				**0.02**		0.55
Male	246 (47.1)	45 (61.6)	1.00		1.00	
Female	276 (52.9)	28 (38.4)	0.55 (0.33–0.91)		0.49 (0.24–1.01)	
Age (years), n (%)				**<0.001**		0.05
≤50	330 (63.2)	32 (43.8)	2.20 (1.34–3.61)		0.50 (0.25–1.01)	
>50	192 (36.8)	41 (56.2)	1.00		1.00	
Length of stay (days), mean (SD)	10.40 (6.30)	9.48 (7.36)				
>10, n (%)	210 (40.2)	25 (34.2)	0.77 (0.46–1.29)	0.32	-	-
Thrombocyte (/µl), mean (SD)	288,544.64 (118,862.11)	268,438.36 (137,435.74)				
<150,000, n (%)	43 (8.2)	14 (19.2)	2.64 (1.36–5.12)	**<0.001**	2.19 (0.82–5.85)	0.11
Fibrinogen (mg/dl), mean (SD)	351.96 (148.88)	422.52 (205.63)				
>375, n (%)	184 (35.2)	42 (57.5)	2.49 (1.51–4.09)	**<0.001**	1.99 (0.99–3.98)	0.05
D-dimer (µg/ml), mean (SD)	2.58 (7.61)	13.34 (22.43)				
≥0.5, n (%)	279 (53.4)	69 (94.5)	15.02 (5.40–41.77)	**<0.001**	1.76 (0.50–6.24)	0.37
PT (sec), mean (SD)	11.04 (1.34)	12.62 (2.68)				
≥14, n (%)	17 (3.3)	14 (19.2)	7.05 (3.30–15.02)	**<0.001**	4.02 (1.35–12.00)	**0.01**
COVID-19 severity, n (%)			87.81 (34.22–225.35)	**<0.001**	92.08 (33.86–250.43)	**<0.001**
Severe	70 (13.4)	68 (93.2)				
Non-severe	452 (86.6)	5 (6.8)				

CI=confidence interval; COVID-19=coronavirus disease 2019; OR=odds ratio; PT=prothrombin time; SD=standard deviation
*Chi-square test, significant if $p<0.05$; †binary logistic regression test, significant if $p<0.05$

by prolonged PT. Prolonged PT signifies inflammation-induced coagulation in infection-driven conditions and is associated with increased disease severity.

In patients with COVID-19, the mechanism underlying thrombocytopenia is likely multifactorial. The combination of viral infection and mechanical ventilation causes endothelial damage that triggers platelet activation, aggregation, and microthrombi formation to overcome the damage in the lung, leading to excessive platelet consumption and decreased platelets in the blood.[26] Coronavirus can also directly infect bone marrow cells, resulting in abnormal hematopoiesis or triggering an autoimmune response to blood cells.[13] High values of fibrinogen and D-dimer levels accompanied by prolonged PT and decreased platelet levels indicate a high coagulopathy process in patients with severe COVID-19, which is one of the factors often associated with disease prognosis.[9,14,27] However, in the present study, thrombocytopenia did not significantly influence the severity of COVID-19 or patient survival. Therefore, thrombocytopenia was not a primary contributing factor to COVID-19 progression, although this condition persisted in some patients.

Several studies have reported that patients with severe COVID-19 have higher mortality rates than those with less severe COVID-19. In addition, patients with non-severe COVID-19 showed a higher probability of recovery than those who died of COVID-19.[28–33] This is consistent with the results of our study. Wang et al[29] observed that individuals subjected to high-flow oxygen therapy and mechanical ventilation had decreased survival rates compared to those without mechanical ventilation who survived COVID-19. The utilization of high-flow oxygen therapy and mechanical ventilation was more prevalent in patients with severe COVID-19, thereby indirectly supporting the notion that higher degrees of severity are associated with a higher susceptibility to unfavorable outcomes. Consequently,

the present study also found an association between disease severity and duration of hospitalization. Severe cases were more associated with longer hospitalization than non-severe cases.

Low platelet levels were not significantly associated with coagulation factors and patient outcomes. The lack of statistical significance in the results of the present study could be due to significant differences in the number of survivors and non-survivors. Although the platelet counts tended to be lower in the non-survivor group owing to the difference in numbers between the two groups, the mean platelet counts were not statistically significant. A meta-analysis by Di Minno et al[21] showed a significant increase in D-dimer levels in 1,149 non-survivors compared with 4,407 survivors. In addition, 15 studies showed a significant prolongation of PT in 840 non-survivors compared to 3,287 COVID-19 survivors.[21] Furthermore, Zhang et al[22] found increased D-dimer levels and a significant prolongation of PT in the non-survivor group compared to the survivor group. In the present study, only prolonged PT was significantly associated with patient survival among the various coagulation factors. This lack of significance can be caused by comorbidities in patients with COVID-19, which may affect the severity and length of hospitalization. These findings deepen our understanding of the complex interactions among sex, age, length of hospitalization, and coagulation variables affecting patient outcomes in determining the survival dynamics of patients with COVID-19.

This study had several limitations. This investigation was conducted retrospectively over a short period to meet the essential requirements for short-term mortality predictors and to establish appropriate management methods. Using secondary data from medical records introduced potential biases, including selection, recall, and misclassification biases. Furthermore, the study design precluded the establishment of causal relationships. The cohort of examined patients underwent multidisciplinary care, which increased the potential bias when defining each comorbidity based on individual interpretations. Consequently, a comprehensive analysis of the comorbidities may have been more feasible.

In conclusion, coagulation factors such as elevated D-dimer and fibrinogen levels and prolonged PT predicted the severity of COVID-19 in patients, leading to death. These markers are promising predictors of disease severity and individual outcomes in patients with COVID-19. As a future direction, we suggest additional prospective clinical investigations that carefully explore the interaction between coagulation factors and patient outcomes to predict disease severity and mortality in critically ill patients with COVID-19.

Conflict of Interest

The authors affirm no conflict of interest in this study.

Acknowledgment

The author would like to thank all clinical colleagues at the Department of Pulmonology and Respiratory, Faculty of Medicine, Universitas Hasanuddin, Indonesia for their assistance and discussions throughout this work. Also, the authors would like to thank Muhammad Naufal Zuhair for his assistance in reviewing the statistical analysis, proofreading, and formatting this manuscript.

Funding Sources

None.

REFERENCES

1. Jones DS. History in a crisis - lessons for covid-19. N Engl J Med. 2020;382(18):1681–3.
2. World Health Organization (WHO). COVID-19 weekly epidemiological update, edition 94, 1 June 2022 [Internet]. World Health Organization (WHO); 2022 [cited 2023 Jan 29]. Available from: https://apps.who.int/iris/handle/10665/354776.
3. Wu Y, Kang L, Guo Z, Liu J, Liu M, Liang W. Incubation period of COVID-19 caused by unique SARS-CoV-2 strains: a systematic review and meta-analysis. JAMA Netw Open. 2022;5(8):e2228008. Erratum in: JAMA Netw Open. 2022;5(9):e2235424.
4. Chen N, Zhou M, Dong X, Qu J, Gong F, Han Y, et al. Epidemiological and clinical characteristics of 99 cases of 2019 novel coronavirus pneumonia in Wuhan, China: a descriptive study. Lancet. 2020;395(10223):507–13.
5. Rothe C, Schunk M, Sothmann P, Bretzel G, Froeschl G, Wallrauch C, et al. Transmission of 2019-nCoV infection from an asymptomatic contact in germany. N Engl J Med. 2020;382(10):970–1.
6. Ryu S, Chun BC; Korean Society of Epidemiology 2019-nCoV Task Force Team. An interim review of the epidemiological characteristics of 2019 novel coronavirus. Epidemiol Health. 2020;42:e2020006.
7. Connors JM, Levy JH. COVID-19 and its implications for thrombosis and anticoagulation. Blood. 2020;135(23):2033–40.
8. Mehta P, McAuley DF, Brown M, Sanchez E, Tattersall RS, Manson JJ, et al. COVID-19: consider cytokine storm syndromes and immunosuppression. Lancet. 2020 Mar 28;395(10229):1033–4.
9. Tang N, Bai H, Chen X, Gong J, Li D, Sun Z. Anticoagulant treatment is associated with decreased mortality in severe coronavirus disease 2019 patients with coagulopathy. J Thromb Haemost. 2020;18(5):1094–9.
10. Zhang L, Yan X, Fan Q, Liu H, Liu X, Liu Z, et al. D-dimer levels on admission to predict in-hospital mortality in patients with Covid-19. J Thromb Haemost. 2020;18(6):1324–9.
11. Huang C, Wang Y, Li X, Ren L, Zhao J, Hu Y, et al. Clinical features of patients infected with 2019 novel coronavirus in Wuhan, China. Lancet. 2020;395(10223):497–506.
12. Richardson S, Hirsch JS, Narasimhan M, Crawford JM, McGinn T, Davidson KW, et al. Presenting characteristics, comorbidities,

and outcomes among 5700 patients hospitalized with COVID-19 in the New York City area. JAMA. 2020;323(20):2052–9. Erratum in: JAMA. 2020;323(20):2098.
13. Lippi G, Plebani M, Henry BM. Thrombocytopenia is associated with severe coronavirus disease 2019 (COVID-19) infections: a meta-analysis. Clin Chim Acta. 2020;506:145–8.
14. Katneni UK, Alexaki A, Hunt RC, Schiller T, DiCuccio M, Buehler PW, et al. Coagulopathy and thrombosis as a result of severe COVID-19 infection: a microvascular focus. Thromb Haemost. 2020;120(12):1668–79.
15. Han H, Yang L, Liu R, Liu F, Wu KL, Li J, et al. Prominent changes in blood coagulation of patients with SARS-CoV-2 infection. Clin Chem Lab Med. 2020;58(7):1116–20.
16. Fogarty H, Townsend L, Ni Cheallaigh C, Bergin C, Martin-Loeches I, Browne P, et al. COVID19 coagulopathy in Caucasian patients. Br J Haematol. 2020;189(6):1044–9.
17. Ramasamy R, Milne K, Bell D, Stoneham S, Chevassut T. Molecular mechanisms for thrombosis risk in Black people: a role in excess mortality from COVID-19. Br J Haematol. 2020;190(2):e78–80.
18. Lucijanic M, Marelic D, Stojic J, Markovic I, Sedlic F, Kralj I, et al. Predictors of prolonged hospitalization of COVID-19 patients. Eur Geriatr Med. 2023;14(3):511–6.
19. Rostami M, Khoshnegah Z, Mansouritorghabeh H. Hemostatic system (fibrinogen level, D-dimer, and FDP) in severe and non-severe patients with COVID-19: a systematic review and meta-analysis. Clin Appl Thromb Hemost. 2021;27:10760296211010973.
20. Nugroho J, Wardhana A, Mulia EP, Maghfirah I, Rachmi DA, A'yun MQ, et al. Elevated fibrinogen and fibrin degradation product are associated with poor outcome in COVID-19 patients: a meta-analysis. Clin Hemorheol Microcirc. 2021;77(2):221–31.
21. Di Minno MND, Calcaterra I, Lupoli R, Storino A, Spedicato GA, Maniscalco M, et al. Hemostatic changes in patients with COVID-19: a meta-analysis with meta-regressions. J Clin Med. 2020;9(7):2244.
22. Zhang A, Leng Y, Zhang Y, Wu K, Ji Y, Lei S, et al. Meta-analysis of coagulation parameters associated with disease severity and poor prognosis of COVID-19. Int J Infect Dis. 2020;100:441–8.
23. Sui J, Noubouossie DF, Gandotra S, Cao L. Elevated plasma fibrinogen is associated with excessive inflammation and disease severity in COVID-19 patients. Front Cell Infect Microbiol. 2021;11:734005.
24. Gómez-Mesa JE, Galindo-Coral S, Montes MC, Muñoz Martin AJ. Thrombosis and coagulopathy in COVID-19. Curr Probl Cardiol. 2021;46(3):100742.
25. Zhan H, Chen H, Liu C, Cheng L, Yan S, Li H, et al. Diagnostic value of D-dimer in COVID-19: a meta-analysis and meta-regression. Clin Appl Thromb Hemost. 2021;27:10760296211010976.
26. Ghahramani S, Tabrizi R, Lankarani KB, Kashani SMA, Rezaei S, Zeidi N, et al. Laboratory features of severe vs. non-severe COVID-19 patients in Asian populations: a systematic review and meta-analysis. Eur J Med Res. 2020;25(1):30.
27. Xu P, Zhou Q, Xu J. Mechanism of thrombocytopenia in COVID-19 patients. Ann Hematol. 2020;99(6):1205–8.
28. Iba T, Levy JH, Levi M, Thachil J. Coagulopathy in COVID-19. J Thromb Haemost. 2020;18(9):2103–9.
29. Wang Y, Lu X, Li Y, Chen H, Chen T, Su N, et al. Clinical course and outcomes of 344 intensive care patients with COVID-19. Am J Respir Crit Care Med. 2020;201(11):1430–4.
30. Rees EM, Nightingale ES, Jafari Y, Waterlow NR, Clifford S, B Pearson CA, et al. COVID-19 length of hospital stay: a systematic review and data synthesis. BMC Med. 2020;18(1):270.
31. Chiam T, Subedi K, Chen D, Best E, Bianco FB, Dobler G, et al. Hospital length of stay among COVID-19-positive patients. J Clin Transl Res. 2021;7(3):377–85.
32. Cai Q, Huang D, Ou P, Yu H, Zhu Z, Xia Z, et al. COVID-19 in a designated infectious diseases hospital outside Hubei Province, China. Allergy. 2020;75(7):1742–52.
33. Wang D, Hu B, Hu C, Zhu F, Liu X, Zhang J, et al. Clinical characteristics of 138 hospitalized patients with 2019 novel coronavirus-infected pneumonia in Wuhan, China. JAMA. 2020;323(11):1061–9. Erratum in: JAMA. 2021;325(11):1113.

Editorial

Role of a journal for the publication of doctoral dissertations

Harrina Erlianti Rahardjo

"A research that is not published, might as well has not been done." (Stefan Ückert)

A doctoral program, a structured educational program with a doctoral degree, is the highest academic degree as the endpoint. Original research with specific scientific, professional, and ethical standards is the core curriculum of any doctoral program, embodied in a doctoral dissertation as the defining component.[1] A doctoral dissertation should contain novelty in its field, thus advancing a body of knowledge, making it a perfect candidate for publication material in a peer-reviewed scientific journal. Published dissertation also increases citation index[2] and prevents unnecessary study replication efforts and systematic reviews/meta-analyses biases, which usually exclude unpublished thesis or dissertation.[3] However, unpublished doctoral dissertations still exist, commonly due to negative and nonsignificant results, leading to the "file drawer" dissertation phenomenon.[4]

Since 2016, the publication of doctoral dissertations in reputable international journals has been mandatory for all doctoral candidates in Universitas Indonesia, including in the Doctoral Programme in Medical Sciences. A letter of acceptance for the manuscript is a prerequisite for the doctoral final exam. The manuscript's content must cover all or part of the dissertation results. Adapting a lengthy dissertation into a single or multiple-publication manuscript can be a challenge of its own, especially within the time constraint of the 3-year doctoral study period. It requires a special skill acquired through multiple practices and experiences. Some doctoral students have already had several publications on their resumes before the doctoral study; however, some have not.

The Doctoral Programme of Medical Sciences Universitas Indonesia has addressed this need by initiating a collaboration with Medical Journal of Indonesia (MJI), the official journal of the Faculty of Medicine, Universitas Indonesia, and one of the reputable international journals indexed in Scopus. The role of MJI starts early in the first semester through a plenary lecture given by MJI's Chief Editor on publishing a scientific article in an international journal. The lecture covers manuscript preparation, authorship criteria, submission, and peer-review process. As doctoral candidates prepare for the commencement of their doctoral research, they should, in parallel, develop a strategic plan to conceive the manuscript(s) for publication together with the supervisors from the very beginning. This includes the content and authorship of the manuscript(s) since doctoral research project commonly involves many parties.

After research completion, both the doctoral dissertation and manuscript for publication should be drafted immediately. During this process, MJI offers a hands-on coaching method, where one of its editorial board members will be assigned to coach one doctoral candidate to adapt the dissertation into a manuscript suitable for publication in a reputable international journal. With this timeline and valuable mentorship, a feasible dissertation and publication could be finalized in due time (3 years or less). Meanwhile, submissions to MJI will be regarded as standard submissions, which require approval from the publication ethics before submission and undergo the peer-review process.

On the other side of the coin, the publication of a doctoral dissertation, which should have met a certain standard and quality in MJI, could contribute to the journal's benefit. The most recent publication from a doctoral dissertation in MJI by Yuliarti et al[5] contained part of the main study aiming to learn the profile of human milk oligosaccharides and *FUT2* genotype in Indonesian mother-infant dyads, which have not been investigated before.

The knowledge, skills, and experiences during the years of doctoral study should be the backbone and

inspiration of continuous research and publications beyond the doctoral degree as a contribution to the academic community. MJI has taken an important part in this journey, and therefore, the Doctoral Programme in Medical Sciences would like to express its utmost appreciation.

From Medical Journal of Indonesia; Department of Urology, Faculty of Medicine, Universitas Indonesia, Cipto Mangunkusumo Hospital, Jakarta, Indonesia
pISSN: 0853-1773 • eISSN: 2252-8083
https://doi.org/10.13181/mji.ed.237163
Med J Indones. 2023;32:65–6
Published online: October 10, 2023

Corresponding author:
Harrina Erlianti Rahardjo
E-mail: harrinaerlianti@gmail.com

REFERENCES

1. Evans SC, Amaro CM, Herbert R, Blossom JB, Roberts MC. "Are you gonna publish that?" Peer-reviewed publication outcomes of doctoral dissertations in psychology. PLoS One. 2018;13(2):e0192219.
2. Larivière V, Zuccala A, Archambault É. The declining scientific impact of theses: implications for electronic thesis and dissertation repositories and graduate studies. Scientometrics. 2008;74:109–21.
3. Open Science Collaboration. Estimating the reproducibility of psychological science. Science. 2015;349(6251):aac4716-1–8.
4. Pautasso M. Worsening file-drawer problem in the abstracts of natural, medical and social science databases. Scientometrics. 2010;85:193–202.
5. Yuliarti K, Mansyur M, Timan IS, Ariani Y, Ernawati, Sidhiarta IGL, et al. DNA quality from buccal swabs in neonates: comparison of different storage time. Med J Indones. 2023;32(1):7–12.